A NUTRIENT NETWORK REGULATING CELLULAR CHOLESTEROL and

GLUCOSE METABOLISM

Guruprasad R. Pattar

Accepted by the Faculty of Indiana University, in partial
fulfillment of the requirements for the degree of Doctor of Philosophy.

_____
Jeffrey S. Elmendorf, Ph.D., Chair

_____
Robert V. Considine, Ph.D.

Doctoral Committee

_____
Mark A. Deeg, M.D., Ph.D.

September 3, 2009

_____
B. Paul Herring, Ph.D.

_____
Stephen A. Kempson, Ph.D.

Dedication

I dedicate this thesis to all those that have paved the way for and have subsequently given me every opportunity to pursue my dreams. First and foremost, I would like to dedicate this to my parents. Your constant support, guidance, and most importantly love has always and will always push me to become the greatest person I can be. You have taught me to do it the correct way and I will always cherish the words that you have said to me time and again, "There is no such thing as a shortcut." I hope that I can touch and help a quarter of the lives that you both have. You have given so much without expecting anything back in return. To my sister Kala and brother Rishi, I will always cherish both your "cheerleading" and wisdom that you have imparted on me. I am extremely proud to have a sister and brother who are not only so strong in character but are extremely kind, caring, and humble people. Whether you know it or not, you have set examples for me of how to be persistent and never let anything stand in the way of your dream. I also would like to dedicate this thesis to my family in India that I do not get to see often enough. But I always feel the support and love even across the ocean. I would particularly like to dedicate this to my Ajja who played an important role in my education.

Finally, I dedicate this to my love, Kiley. Without your support and encouragement through both the fun times and the hard times, I would be lost.

Your constant enthusiasm, willingness to help, and open mind has helped me in

achieving my dreams. I wish that someday I could give you the same in return.

Acknowledgements

I owe a great deal of gratitude to my mentor, Dr. Jeffrey Elmendorf. Your direction, both professionally and personally, is almost immeasurable. You have been an incredible teacher and I hope that I can help shape someone's life the way you have mine.

To my graduate committee: Dr. Bob Considine, Dr. Mark Deeg, Dr. Paul Herring, and Dr. Steve Kempson. I appreciate the guidance and constant challenges that you have always placed before me. It has made me understand the scientific process just a bit better.

To all the members of the Elmendorf lab that I have had the pleasure to work with over these years, I feel as if I have worked with some of the brightest and most talented individuals there are. Most importantly, the environment that was fostered in the lab was one that was enjoyable day after day. I will always cherish the times that I had in the laboratory because of all the comraderie and relationships that have developed.

To my closest friends and colleagues, Kirk and Jason, thank you both for all the advice you have given me over the years. The laughter, conversations, and ideas we have shared have not only taught me how to be a researcher but more importantly, a good person.

Abstract

Guruprasad R. Pattar

A NUTRIENT NETWORK REGULATING CELLULAR CHOLESTEROL and
GLUCOSE METABOLISM

Insulin resistance, a hallmark of type 2 diabetes (T2D), is associated with accompanying derangements such as hyperinsulinemia that promote the progression of insulin resistance, yet a mechanism(s) is imperfectly understood. Data have demonstrated that hyperinsulinemia promotes insulin resistance as evidenced by diminished ability of insulin to mobilize glucose transporter GLUT4 to the plasma membrane (PM). We found that loss of PM phosphatidylinositol 4,5-bisphosphate (PIP_2)-regulated filamentous actin (F-actin) structure contributes to hyperinsulinemia-induced insulin resistance. We tested if increased glucose flux through hexosamine biosynthesis pathway (HBP) causes dysregulation of PM components necessary for GLUT4 translocation. Increased HBP activity was detected in 3T3-L1 adipocytes cultured in hyperinsulinemia (5 nM Ins; 12 h) and also 2 mM glucosamine (GlcN), a distal HBP activator, inducing losses of PM PIP_2 and F-actin. In accordance with HBP flux directly weakening PIP_2/F-actin structure, inhibition of the rate-limiting HBP enzyme (glutamine:fructose-6-phosphate amidotransferase) restored F-actin and insulin responsiveness. Furthermore, less invasive challenges with glucose led to

PIP$_2$/F-actin dysregulation. New findings support a negative correlation between PM cholesterol accrual, PIP$_2$/F-actin structure and GLUT4 regulation. These data stemmed from parallel study aimed at understanding the antidiabetic mechanism of the nutrient chromium (Cr^{3+}). We found that chromium picolinate (CrPic) enhanced insulin-stimulated GLUT4 trafficking via reduction in PM cholesterol. In line with glucose/cholesterol toxicity findings, we demonstrated that therapeutic effects of CrPic occurred solely in adipocytes with increased HBP activity and a concomitant elevation in PM cholesterol. Mechanistically, data are consistent with a role of AMP-activated protein kinase (AMPK) in CrPic action. These data show that CrPic increases AMPK activity and perhaps suppresses cholesterol synthesis via distal phosphorylation and inactivation of 3-hydroxy-3-methylglutaryl CoA reductase (HMGR), a rate-limiting enzyme in cholesterol synthesis. Continued study of the consequence of increased HBP activity revealed alterations in cholesterogenic transcription factors – Sp1, SREBP-1, and NFY – with Sp1 showing a significant increase in *O*-linked glycosylation. Consistent with Sp1 modification eliciting maximal transcriptional activation of SREBP-1, *Hmgr* mRNA was significantly enhanced. In conclusion, these data are consistent with a central role of PM cholesterol in glucose transport and suggest perturbations in this lipid have a contributory role in developing insulin resistance.

Jeffrey S. Elmendorf, Ph.D., Chair

Table of Contents

List of Figures

Abbreviations

2-DG   2-deoxyglucose

ABC   ATP binding cassette transporter

AMP   Adenosine monophosphate

AMPK   5' AMP-activated protein kinase

ATP   Adenosine triphosphate

AS160   Akt substrate of 160 kDa

βCD   Methyl-β-cyclodextrin

βCD:Chol   Methyl-β-cyclodextrin pre-loaded with cholesterol

BCS   Bovine calf serum

BMI   Body mass index

BSA   Bovine serum albumin

Cav-1   Caveolin 1

Cr   Chromium

Cr^{3+} Trivalent chromium

CrPic   Chromium picolinate

DAG   Diacylglycerol

DMEM   Dulbecco's modified Eagle's medium

DON   6-Diazo-5-Oxo-Norleucine

ER   Endoplasmic reticulum

F-actin   Cortical filamentous actin

FBS   Fetal bovine serum

FITC	Fluorescein isothiocyanate
G-6-Pase	Glucose-6-Phosphatase
G-actin	Monomeric globular actin
GFP	Green fluorescent protein
GLUT	Glucose transporter
HDL	High density lipoprotein cholesterol
HMG-CoA	3-hydroxymethyl-3-glutaryl coenzyme A
HMGR	HMG-CoA reductase
HBP	Hexosamine biosynthesis pathway
INSIG	Insulin-induced gene
IP3	Inositol-3 phosphate
IR	Insulin receptor
IRS	Insulin receptor substrate
N-WASP	Neural Wiscott-Aldrich syndrome protein
O-GlcNAc	O-linked-N-acetylglucosamine
OGT	O-linked-N-acetylglucosamine transferase
PA	Phosphatidic acid
PBS	Phosphate buffered saline
PDK	Phosphoinositol dependent kinase
PEPCK	Phosphoenolpyruvate carboxykinase
PGC-1α	Peroxisome proliferative activated receptor γ co-activator 1
PH	Pleckstrin homology
PI	Phosphoinositol

PI3K	Phosphatidylinositol-3-kinase
PIP_2	Phosphatidylinositol 4,5 bisphosphate
PIP_3	Phosphatidylinositol 3,4,5 trisphosphate
PLD	Phospholipase D
PM	Plasma membrane
PTB	Phosphotyrosine binding
PTP	Protein tyrosine phosphatase
PUGNAc	*O*-(2-acetamido-2-deoxy-D-glucopyranosylidene)-amino-*N*-phenylcarbamate
RRX	Rhodamine Red-X
SCAP	SREBP cleavage activating protein
SDS-PAGE	Sodium dodecyl sulfate-polyacrylamide gel electrophoresis
SH	Src homology
SNARE	soluble *N*-ethylmaleimide-sensitive fusion factor attachment receptor
Sp1	Specificity protein 1
SREBP	Sterol response element binding protein
T2D	Type 2 diabetes
TBS	Tris buffered saline
UDP	Uridine diphosphate
UDP-GlcNAc	UDP-*N*-acetylglucosamine

Chapter I

Introduction

Diabetes is currently reaching epidemic proportions worldwide. Incidence of this disease is growing at a staggering rate. It is now appreciated that there are multiple avenues and chronic metabolic insults involved in the development of type 2 diabetes (T2D) including the hallmark characteristic, insulin resistance. Insulin resistance is a state whereby peripheral tissues (adipose, skeletal muscle, and liver) become unresponsive to the actions of insulin. This resistance occurs at the cellular level and is associated with diminished glucose transport in skeletal muscle and adipose tissue. Ironically, compensatory hyperinsulinemia is considered a key derangement that promotes the progression and worsening of insulin resistance, yet a mechanism(s) is imperfectly understood. Elucidating how insulin resistance develops and eventually results in T2D remains a fundamental challenge in biology and a significant issue in medicine. Now, pharmacologic therapies are primarily designed to minimize accompanying defects associated with conditions of T2D and only a few medications present are designed to slow the progression of insulin resistance. None of these therapies have been proven to reverse the critical factor of glucose intolerance in these patients without significant surgical or lifestyle intervention. However, it can be speculated that early therapeutic intervention, during the pre-diabetic state, may essentially reverse this defect and protect an individual from the development of T2D.

Nutritional supplementation, especially that of chromium (Cr^{3+}), is thought to perhaps alleviate glucose intolerance yet the mechanism is unclear.

Recent evidence from our laboratory as well as others have appreciated that cellular disturbances found at the level of the plasma membrane (PM) is a key contributing factor to diminished glucose transport in both fat and muscle cells by conditions of the diabetic milieu [1]. Namely, PM cholesterol and its role in determining membrane fluidity is an important mediator of glucose transport in these cells. In addition, modifications in PM cholesterol levels concomitantly occur alongside changes in PM phosphatidylinositol-4,5-bisphosphate (PIP_2) amount and cortical F-actin (F-actin) structure that regulate glucose transporter 4 (GLUT4) translocation necessary for cellular glucose uptake.

This introduction reviews evidence about what is currently known about the fundamentals of insulin action. Specifically, evidence will be presented regarding the role of PM cholesterol in regulating glucose transport. A brief overview of insulin-regulated glucose transport will be highlighted before outlining the cellular components necessary for insulin responsiveness and these cellular defects contributing to insulin resistance. Next, several sections are devoted to presenting research on mechanisms of PM cholesterol regulation of insulin-stimulated glucose transport. Within the same context, mechanisms involved in the regulation of cellular cholesterol homeostasis are also outlined. Finally, recent data highlighting the benefits of Cr^{3+} supplementation will be detailed.

1. Insulin-mediated glucose regulation

Insulin action is important in regulating many metabolic processes in the body. Insulin is a hormone that is produced and stored in the β-cells of the pancreas. In the post-prandial state, elevated plasma glucose levels stimulate secretion of insulin from the pancreas into the blood. The circulation of insulin allows for it to bind peripheral tissues that are important in regulating whole body glucose homeostasis, namely adipose tissue, skeletal muscle, and the liver. The cellular action of insulin, which will be detailed below, stimulates the uptake of glucose into adipocytes and skeletal muscle myotubes, allowing for critical cellular processes of energy regulation to occur. In the liver, insulin's main responsibility is to inhibit hepatic glucose production or gluconeogenesis thus representing a shift from the fasted state to the fed state in the body. This intricate balance of glucose by insulin accounts for maintenance of plasma glucose concentrations in healthy individuals within very strict limitations, generally not falling below 70 mg/dL or straying upwards from 99 mg/dL. The action of insulin at the level of the whole body actually begins at cell membranes where the insulin receptor (IR) is localized. The focus of this thesis was GLUT4 regulation by insulin in skeletal muscle and fat.

2. Cellular Insulin Action/Glucose Transport

On a cellular level, insulin is able to regulate changes in plasma glucose concentrations via the regulation of subcellular trafficking of GLUT4 in adipose tissue and skeletal muscle. This process is the main mediator of glucose

disposal, which accounts for greater than 80% of post-prandial glucose disposal. In the basal state, GLUT4 cycles continuously between the PM and intracellular membranes, with the majority of transporters being bound and residing intracellularly [2-5]. Insulin stimulation causes a large increase in the rate of exocytosis of GLUT4 vesicles and a relatively smaller decrease in the rate of endocytic internalization resulting in a net increase of GLUT4 present at the PM allowing for cellular glucose transport [6-8]. In a simplistic fashion, this seems like a straightforward process. However, research has shown that the regulation of GLUT4 trafficking by insulin is well-regulated and incredibly complex and that defects in GLUT4 translocation contribute to insulin resistance.

In addition, insulin plays a substantial role in the regulation of glucose homeostasis within the liver. As will be detailed below, insulin action of hepatocytes involves 'classic' proteins involved in insulin signal transduction. In hepatocytes, the main purpose of insulin is to inhibit and suppress glucose production or gluconeogenesis. Two components that play an important role in regulating gluconeogenesis in the liver include the forkhead transcription factor, FOXO1, and peroxisome proliferative activated receptor-γ co-activator 1 (PGC-1α) which is another transcriptional co-activator necessary for inducing gluconeogenic enzymes, phosphoenolpyruvate carboxykinase (PEPCK) and glucose-6-phosphatase (G-6-Pase). FOXO1 is a transcription factor that can bind directly to the promoters of these gluconeogenic genes thus causing enzymatic increases in regulators of glucose production in the 'starved' state in the absence

of insulin. Insulin signaling in hepatocytes results in phosphorylation of FOXO1 and subsequently disrupts its ability to localize to the nucleus thus silencing the transcription of gluconeogenic enzymes [9]. The aforementioned transcriptional coactivator, PGC-1α, is also under the regulation of insulin. PGC-1α is able to bind FOXO1 and enhance its transcriptional activity [9]. Insulin is able to disrupt the interaction between FOXO1 and PGC-1α thus inhibiting the production of gluconeogenic enzymes. In addition to PGC-1α, insulin may also target other coactivators of transcriptional activity of the p300/CREBP family. Evidence has suggested that phosphorylation of p300 by the insulin signaling cascade shuts down transcription of PEPCK and G-6-Pase [10]. This effect of insulin on inhibiting gluconeogenic processes is important in regulating glucose concentrations in the blood because perturbations in insulin sensitivity can be associated with unregulated hepatic glucose production. The uptake of glucose into adipocytes and myotubes, as well as the inhibition of glucose production in hepatocytes, requires an extensive signal transduction cascade that is still incompletely understood.

2.1. Insulin Signal Transduction

The mechanism by which insulin action can influence GLUT4 translocation or inhibition of gluconeogenesis requires an extensive, and still somewhat incomplete, network of signaling molecules which will be detailed here. The beginning of the insulin signal and its translation to cellular processes begins at the level of the PM. After this peptide hormone's journey through the

5

bloodstream, it is able to bind to the insulin receptor (IR), which is localized at the PM. The IR is composed of two disulphide-linked heterodimers, each of which has an α and β subunit. The action of insulin binding to its receptor induces a conformational change in the receptor allowing for stimulation of intrinsic tyrosine kinase activity and autophosphorylation of its β-subunit on specific tyrosine residues [11, 12]. This stimulatory activity of tyrosine phosphorylation by the β subunits can lead to downstream signal transduction, including phosphorylation of a host of proteins. In particular, proteins that are phosphorylated by the IR include all the members of the insulin receptor substrate family (IRS-1, -2, -3, -4, -5, and -6), Gab-1, Shc, p62[dok], signal regulatory protein (SIRP) family members, APS (adapter protein containing a pleckstrin homology and Src-homology 2 domain).

Insulin receptor substrates (IRS) are docking proteins that associate with the IR in order to regulate its signal by differentiating the insulin signal into its various metabolic and gene regulatory functions. Of the six IRS proteins identified, only the specific isoforms IRS-1 and IRS-2 have been firmly placed as a mediator of glucose homeostasis. Animal models have been useful in determining the importance of IRS molecules. In genetically-manipulated mouse models, the knockout of IRS-1 has been demonstrated to be associated with severe growth retardation and mild peripheral insulin resistance [13, 14]. Conversely, ablation of IRS-2 in knockout mice develop frank diabetes simulataneous with impaired growth of pancreatic β-cells, β-cell failure, and

insulin resistance at the liver [15]. Cell culture studies utilizing L6 myotubes displayed that siRNA knockdown of IRS-1 significantly diminished insulin-stimulated GLUT4 translocation and glucose uptake whereas IRS-2 knockdown in these same cells resulted in no diminishment of glucose transport [16]. Taken together, these studies suggest that both molecules are important in the action of insulin where IRS-1 is critical in peripheral adipose and skeletal muscle insulin action while IRS-2 seems to be important in the liver and β-cell sensitivity. Additionally, compensatory mechanisms occur due to molecular redundancy found in this family of proteins. For example, in IRS-1 knockout mice, IRS-3 was identified as the principal mediator of insulin signaling and became the key substrate of IR tyrosine phosphorylation events. However, studies performed in humans displayed a lack of functional IRS-3 protein or gene in adipose tissue [11]. In regards to IRS-4, -5, and -6 family members, they seem to play a minor role in glucose homeostasis. IRS-4 knockout studies have demonstrated mild defects in growth and glucose homeostasis, along with reproductive abnormalities. However, the actual importance of IRS-4 on normal insulin action is debatable since skeletal muscle (the insulin-sensitive tissue responsible for ~80% of whole body glucose uptake) has not been shown to express IRS-4 [17]. Conversely, IRS-5 and IRS-6 are substrates that may be phosphorylated by insulin; however, they do not activate the downstream signaling component phosphatidylinositol 3-kinase (PI3K) [17]. Therefore, the roles of IRS-1 and -2 as mediators of the metabolic effects of insulin action are fairly well established whereas the role of these newly discovered members on insulin action is still

somewhat speculative. Regardless, IRS proteins are key intermediates in propagating the insulin signal from outside the cell to the inside resulting in key cellular metabolic actions.

After rapid insulin-induced tyrosine phosphorylation of IRS-1 and/or IRS-2, docking sites are now created allowing for the recruitment of signaling molecules with Src homology 2 (SH2) domains, which includes Class IA PI3K [18]. PI3K is a heterodimer, made up of the SH2-containing regulatory subunit, p85, and also the p110 catalytic subunit. The binding of the p85 regulatory subunit to IRS proteins is able to both activate the catalytic subunit p110 while also localizing the kinase near the PM. This PM localization of PI3K places the enzyme near its substrate phosphatidylinositol 4,5-bisphosphate (PIP_2) allowing for the phosphorylation of this PM lipid on the 3 position of the inostiol ring, forming phosphatidylinositiol 3,4,5-trisphosphate (PIP_3). The formation of PIP_3 is necessary for the translocation of two pleckstrin homology (PH) domain-containing proteins, Akt (protein kinase B, PKB) and phosphoinositide-dependent-kinase-1 (PDK1) which can further propagate the insulin signal to stimulate GLUT4 translocation.

Upon membrane recruitment, the 60 kDa serine/threonine kinase Akt can be phosphorylated at two key sites, serine 473 (Ser473) occurring first by PDK2 [19] and threonine 308 (Thr308) which occurs after Ser473 phosphorylation that stabilizes interaction with PDK1 [20, 21]. Currently, there are three identified Akt

isoforms. In Akt1-deficient mice, there was no diminished effect of glucose homeostasis observed, although their growth was severly compromised [22]. However the deleted isoform, Akt2, in mice caused a reduction in insulin sensitivity [23]. This then allowed for the identification that Akt2 was the predominant isoform found in insulin-sensitive tissues, adipose and skeletal muscle suggesting that this isoform is necessary for normal glucose homeostasis. In cell culture studies utilizing siRNA gene silencing of Akt1 and Akt2 revealed that Akt2 plays a predominant role in the translocation of GLUT4 upon insulin stimulation [24, 25] whereas Akt1 is only a minor contributor. Intracellular localization analyses lend further credence to Akt2 as the primary mediator of insulin-stimulated GLUT4 translocation. Utilizing cultured adipocytes, it was demonstrated that Akt1 was found primarily in cytosolic fractions whereas Akt2 can be found in both cytosolic and membrane fractions. Using 3T3-L1 adipocytes, it was discovered that Akt2 was associated with GLUT4-containing vesicles and that insulin increases Akt2-GLUT4 association while concomitantly phosphorylating various GSV component proteins [26, 27]. The role of Akt3 in physiology is currently unknown. Although Akt is an important signaling mediator, a distal component of the insulin signaling cascade involved in GLUT4 translocation has been recently identified.

The importance of Akt on glucose transport was enhanced by the discovery of Akt substrate of 160 kDa (AS160) which provided a downstream signaling effector between IR and GLUT4 transolcation [28]. Interestingly, AS160

was originally named TBC1D4 before its function was known [29]. A close relative of this protein is TBC1D1, a protein that contains similarities yet interesting differences to AS160/TBC1D4. While both of these proteins are phosphorylated on Ser/Thr residues similarly, TBC1D1 exhibits Thr596 and Ser507 phosphorylation sites whereas AS160 demonstrates Thr642 and Ser570 phosphorylation sites [29]. AS160 contains a GTPase-activating (GAP) domain for Rab proteins or small G proteins involved in the trafficking of vesicles. This was demonstrated in a study of 3T3-L1 adipocytes that contain mutated phosphorylation sites on AS160 which then markedly inhibited insulin-stimulated GLUT4 transolcation [30]. Since that time, knockdown studies of AS160 have demonstrated increased basal PM GLUT4 due to increased exocytosis in 3T3-L1 adipocytes. This can then be rescued via transfection of wild-type human AS160. However, when the GAP domain is mutated in these transfected human AS160 proteins, no rescue of this increase in basal GLUT4 is experienced. This suggests that in basal condition, AS160 is unphosphorylated and associated with GLUT4 vesicles with its intrinsic GAP activity consistently inactivating Rab proteins, due to it being bound to GDP. Conversely, when stimulated with insulin, AS160 can then be phosphorylated causing an inhibitory effect on GAP activity, allowing for Rab proteins to be bound to GTP and thus active for proper GLUT4 translocation. [31-33]. As mentioned, substrates of AS160 are Rab proteins. Specific isoforms of Rab proteins that are heavily associated with AS160 and GLUT4 containing vesicles are Rabs 2A, 8A, 10, and 14 [31, 34, 35]. Since then, Sano *et al.* has demonstrated through knockdown studies that Rab10 is the main

participant in GLUT4 translocation in 3T3-L1 adipocytes [36]. In skeletal muscle and cultured myotube anaylses, the specific Rab protein(s) associated with GLUT4 translocation are still unknown [29].

In addition to the activation of Akt, PIP_3 along with PDK1 have been demonstrated to activate atypical protein kinase C (aPKC, PKC ζ/λ). Both of these isoforms have regulatory roles in glucose transport [37]. Overexpresion of PKCζ stably increased glucose uptake in fibroblasts, adipocytes, and L6 myotubes. Whereas, a dominant-negative form of this protein exhibited decreased glucose transport basally and upon insulin stimulation [37]. In accordance, data now exist that expression of a constitutively active aPKC mimics insulin's action on GLUT4 translocation and glucose transport. Despite the importance of propagation of the insulin signal, evidence for insulin signaling-independent translocation of GLUT4 has now been offered. Importantly, there is evidence from our laboratory and others that demonstrate cellular dynamics associated with PM lipids and its effects on the underlying cortical filamentous actin (F-actin) play an important role in insulin-stimulated glucose transport.

2.2 PM Lipid and Cytoskeletal Regulation of GLUT4 Translocation

It has recently been appreciated that cellular cytoskeletal rearrangements play an important role in GLUT4 translocation. Specifically, the role of cortical actin is essential in the translocation of GLUT4 [38-43]. Cellular cortical actin exists in two forms: monomeric globular actin (G-actin) and filamentous actin (F-

11

actin). Polymerization of monomeric actin into filamentous actin requires ATP

hydrolysis. Evidence exists that insulin promotes the formation of F-actin

structure [44, 45] and that disruption of this structure, with such agents as

latrunculin B or the actin depolymerizing agent cytochalasin D, causes an

inhibition of insulin-stimulated GLUT4 translocation [38, 46, 47]. It should be

noted that in these situations, the disruption of actin filaments by pharmacological

means does not appear to induce changes in proximal insulin signaling, such as

insulin's ability to activate PI3K and Akt [43, 44, 48]. Intriguingly, utilizing

jasplakinolide, an F-actin stabilizing compound, an inhibition of GLUT4

translocation is witnessed, suggesting that a dynamic reorganization of actin is

required for the insulin to be effective [43]. Interestingly, regulation of this cortical

actin structure occurs via actin-binding proteins and membrane lipids. Previous

data from our laboratory have explored the regulatory nature of a particular PM

phosphoinositide on cortical F-actin structure. The coordination of

rearrangements of the actin cytoskeleton is thought to occur through signals

transmitted by this membrane phosphoinositide, PI 4,5-P_2 (PIP$_2$). PIP$_2$ is

generated from phosphorylation of PIP by PI4P 5-kinase and is present in

relative abundance at the PM, representing around 1% of all PM phospholipids

[49]. Multiple studies have shown that the sequestration or hydrolysis of PI 4,5-P_2

downregulates the interaction between the PM and underlying cytoskeletal

structures, resulting in a depletion of cortical F-actin [50-54]. As mentioned, this

role of PM PIP$_2$ is critical in optimizing the reorganization of cortical F-actin

structure necessary for GLUT4 translocation. Furthermore, our laboratory has

identified another important membrane component that interacts with PM PIP_2/F-actin regulation of GLUT4 translocation. An essential lipid in the context of membrane integrity, the role of PM cholesterol has been established in modulating membrane dynamics. In the context of GLUT4 translocation, we have shown that manipulations in PM cholesterol amount are sufficient in altering the cell's ability to regulate glucose transport.

Work from our laboratory and others has illustrated the potential role of membrane cholesterol content in the regulation of GLUT4 mobilization to the PM. It is generally well accepted that PM cholesterol is an important determinant of membrane fluidity as relative increases in cholesterol causes a highly ordered, gel-like state. Kanzaki *et al.* utilized PIP5K overexpression to generate elevated levels of PIP_2 in 3T3-L1 fibroblasts and adipocytes. These authors demonstrated that cholesterol loading of fibroblasts expressing PIP5K increased formation of membrane vacuoles coated with F-actin, cortactin, dynamin, and the actin regulatory protein N-WASP, which inhibited the endocytosis of GLUT4. This led the authors to hypothesize that cholesterol has an effect on trafficking events such as GLUT4 endocytosis by altering membrane thickness and curvature or through its influence on PIP_2 level and distribution [55]. Nonetheless, it is apparent that there is a delicate balance of PM cholesterol amount for optimal GLUT4 translocation. This idea was evident in studies from our group exhibiting that lowering of PM cholesterol by sphingomyelinase- an enzyme that degrades the cholesterol-associated phospholipid sphingomyelin- stimulated GLUT4

translocation [56]. Additional use of a moderate concentration of methyl-β-cyclodextrin (βCD) (2.5 mM) that was demonstrated to remove 44% of PM cholesterol resulted in an increase in GLUT4 translocation independent of enhancing any insulin signaling properties. We have also witnessed similar results utilizing other cholesterol lowering agents, such as nystatin and filipin [56]. New evidence from our laboratory has documented that the essential nutrient, chromium (Cr), has the ability to enhance insulin action on 3T3-L1 adipocytes through PM cholesterol reduction. As will be discussed later and is the focus of these studies, the balance of PM cholesterol is an important determinant in the influence of cellular glucose transport. We have found that key components of the diabetic milieu, including hyperinsulinemia, hyperlipidemia, and hyperglycemia, are all associated with increases in PM cholesterol and a concomitant dysregulation of the underlying cortical F-actin structure. Lending further evidence for the importance of PM cholesterol on GLUT4 translocation is the ability of insulin-sensitizing agents (*i.e.* CrPic and known AMPK activators) to enhance cellular insulin action and glucose transport along with PM cholesterol lowering events [57, 58].

2.3 Hyperinsulinemia and Insulin Resistance

A continuous component of insulin resistance is hyperinsulinemia [59, 60]. This compensatory increase in insulin during the insulin-resistant state initially offsets the reduced ability of insulin to stimulate GLUT4 translocation and glucose uptake, which is essential for the maintenance of blood glucose

homeostasis. However, *in vivo* and *in vitro* studies demonstrate that the hyperinsulinemic state has a negative effect on insulin action. The temporal sequence in the pathogenesis of type 2 diabetes resulting in compensatory elevations of blood insulin and blood glucose is unknown and is the topic of a review by the late J Dennis McGarry [61]. In this review, the possibility that hyperinsulinemia and insulin resistance may arise simultaneously or by a preexisting defect in leptin signaling is raised. A possibility in the temporal sequence of the development of insulin resistance that McGarry favored is that hyperinsulinemia may beget insulin resistance, possibly as a necessary adaptation to prevent hypoglycemia. The breakdown of glucose homeostasis is actually secondary to disturbances in lipid breakdown. Interestingly, the cause of hyperinsulinemia may be in response to dyslipidemic conditions present in the blood whereby plasma free fatty acid concentrations are significantly increased. This elevation in fatty acids may inhibit glucose transport in skeletal muscle rendering a state of insulin resistance. However, an intriguing possibility raised by McGarry is that the elevation of fatty acids, in itself, may provide a stimulus for insulin secretion, leading to hyperinsulinemic conditions.

Plasma insulin concentrations have been measured in multiple population-based studies. For example, as reviewed by Ferrannini [62] in the San Antonio Heart Study, a survey involving ~3,000 subjects stratified by age and socioeconomic condition, fasting insulin typically ranged between 1 and 50 µU/ml (6 and 300 pM), while 2 h post-glucose plasma insulin concentrations ranged

between 1 and 700 µU/ml (6 and 4,200 pM). Hyperinsulinemia was defined as a value 2 standard deviations above the mean (or the top 2.5%) of the healthy (non-obese, non-diabetic) group, the low end value being 31 µU/ml (186 pM). In the population screened, 8% had fasting insulin values exceeding this level. Clearly, the prevalence of hyperinsulinemia may vary in different populations depending on environmental and genetic factors. Nevertheless, in the San Antonio Heart Study, the clinical impact of hyperinsulinemia was large. Obesity, impaired glucose tolerance, T2D, hypertension, and hypertriglyceridemia were found to be two to three times more prevalent in the 239 individuals with fasting insulin levels greater than 31 µU/ml (186 pM) than in the 2,700 subjects with fasting insulin concentrations below that level. This quantitative definition of hyperinsulinemia is useful to the extent that a clinically relevant endpoint is identified. Cell culture studies have attempted to decipher a mechanism by which hyperinsulinemia may be contributing to this decrement of insulin sensitivity.

To date, extensive study has built a good understanding of how insulin itself can be involved in the staging of diabetes. For example, chronic exposure to pharmacological doses of insulin (≥100 nM) have been shown by several laboratories [63-65] to markedly attenuate expression levels and/or activity states of the IR, IRS-1, PI3K, At, and GLUT4 proteins in 3T3-L1 adipocytes and, thus, produce a defect in the ability of the cell to respond to subsequent acute insulin stimulation with an increase in GLUT4 translocation and glucose transport. On the other hand, similar defects in the ability of insulin to acutely regulate the

glucose transport system can be induced by physiological doses of insulin (≤ 5 nM) that are not associated with disturbances in early insulin signaling [66, 67]. Therefore, defects positioned more distal in the insulin signaling pathway may contribute to the insulin-mediated cellular insulin resistance. Within this thesis, a study conducted by our laboratory provided evidence that sutained exposure of 3T3-L1 adipocytes to a physiological dose of insulin results in a marked loss of cortical F-actin and PM PIP_2. These studies will be presented in Chapter II supporting a new membrane/cytoskeletal model of insulin resistance.

2.4 Hexosamine Biosynthesis Pathway Involvment in Glucose Intolerance

Marshall *et al.* [68], using primary adipocytes, first proposed that excess glucose flux through the heoxsamine biosynthesis pathway (HBP) may contribute to insulin resistance. In normal healthy conditions, HBP is a relatively minor pathway in the utilization of glucose representing only ~2-5% of total intracellular glucose [69]. Glucose entry into the HBP is catalyzed by the first and rate-limiting enzyme, glutamine:fructose-6-phosphate (F-6-*P*) amidotransferase (GFAT), which converts F-6-*P* and glutamine into glucosamine 6-phosphate (GlcN-6-*P*) and glutamate. GlcN-6-*P* is metabolized to UDP-*N*-acetylglucosamine (UDP-GlcNAc), the major product of the pathway [68]. UDP-GlcNAc and other amino sugars generated by the pathway provide building blocks of glycosyl side chains for proteins and lipids. UDP-GlcNAc is also the obligatory substrate of *O*-linked *N*-acetylglucosamine (*O*-GlcNAc) transferase (OGT), a cytosolic and nuclear enzyme that modifies Ser/Thr residues of proteins by attaching single GlcNAc

moieties in *O*-linkage [70, 71]. *O*-GlcNAcylation frequently occurs on transcription factors and often involves known phosphorylation sites, suggesting a regulatory role for this post-translational modification [72]. Beginning in the 1950s, multiple *in vitro* and *in vivo* studies in rodent models have demonstrated that chronic elevated flux through the HBP may represent a possible mechanism by which changes in cellular glucose handling can lead to insulin resistance. GFAT levels are markedly elevated in skeletal muscle of diabetic patients [73]. In order to place the HBP as a central player in the development of insulin resistance, there are a few routine experimental procedures that have been utilized. The first is a chronic incubation of cells to a state of hyperglycemia, inevitably increasing intracellular glucose flux through this pathway. Second, treatments with glucosamine, a compound that directly enters the HBP distal to the rate-limiting enzyme GFAT, also subsequently increases cellular UDP-GlcNAc levels and thus *O*-linked glycosylation modifications of proteins. Finally, changes in expression and activity of GFAT have been undertaken to further analyze HBP activity on insulin resistance. Interestingly, incubation of adipocytes with a potent inhibitor of GFAT, 6-Diazo-5-Oxo-L-Norleucine (DON), was able to reverse this state of insulin resistance in adipocytes [68]. Modest overexpression (approximately 20%) of OGT in fat, skeletal and cardiac muscle of transgenic mice was sufficient to induce insulin resistance as assessed by diminished glucose disposal and hyperinsulinemia [74]. It was also noted in this study that the *ob* gene and its product, leptin, is influenced by hexosamines. Evidence from these OGT overexpressing mice displayed hyperleptinemia due to an observed

18

70% increase in leptin mRNA [75]. However, a direct relationship between elevated O-linked glycosylation and the development of insulin resistance is still imperfectly understood. However, GlcN-induced insulin resistance results in tremendous cellular accumulation of GlcN-6-PO_4 whereas this compound is nearly undetectable in cells exposed to glucose alone. Importantly, GlcN-6-PO_4 accumulation depletes intracellular ATP which was clearly demonstrated by Hresko $et\ al.$ in 3T3-L1 adipocytes incubated with high concentrations of GlcN, in the presence of insulin and no glucose. However, under milder conditions lacking insulin and/or addition of an energy source, ATP depletion due to GlcN treatment becomes trivial or tyrosine phosphorylation-based abnormalities do not occur, yet GlcN-induced insulin resistance still occurs. Additional evidence for O-linked glycosylation in mediating insulin resistance is offered by treating 3T3-L1 adipocytes with O-(2-acetamido-2-deoxy-D-glucopyranosylidene)-amino-N-phenylcarbamate (PUGNAc), an inhibitor of O-GlcNAcase (OGA) protein. OGA is a protein that is able to dynamically remove glycosylation modifications from proteins. PUGNAc inhibition of OGA has been demonstrated to cause a substantial increase in O-GlcNAc levels and the eventual development of insulin resistance [76]. Utilizing these experimental manipulations of proteins present in the HBP, an association between the development of insulin resistance and increased HBP activity is quite strong. Research from our laboratory has suggested a role of HBP in induction of defective glucose transport into 3T3-L1 adipocytes. Additional data in rat epitrochlearis muscle incubated with PUGNAc for 19 h was sufficient in the induction of insulin resistance as assessed by

diminished insulin-stimulated glucose uptake [77]. In this same study, no change

was seen in the activity of insulin signaling molecules, including phosphorylation

of AS160. The authors concluded in this study that PUGNAc was an effective

inhibitor of O-GlcNAcase significantly increasing O-linked glycosylation on

cellular proteins that then diminished skeletal muscle insulin sensitivity

independent of attenuated insulin signaling effects [77]. As mentioned earlier,

previous work from our group has suggested a new molecular framework for

insulin-induced insulin resistance involving defects in PM PIP_2-regulated cortical

F-actin [1, 41]. One key focus of my thesis work was to determine whether a

connection between these hyperinsulinemia-induced PM disturbances and

increased HBP activity played a contributory role in insulin resistance. Since it

has been previously shown that basal transcription factors involved in multiple

cellular processes are frequently the target of O-linked glycosylation

modifications [78], the findings outlined in Chapter II supported future study to

determine whether the basis of PM cholesterol accrual in response to

hyperinsulinemia is mediated via changes in key cholesterol regulatory

transcription factors such as the sterol regulatory element-binding protein

(SREBP).

3. Cellular Cholesterol Homeostasis

　　　　Sterol regulatory element-binding protein (SREBP), a transcription factor

that activates genes involved in fatty acid and cholesterol biosynthesis, maintains

tight control of cellular cholesterol as first identified by the works of Brown and

Goldstein [79]. The SREBP family consists of three members, SREBP-1a, SREBP-1c, and SREBP-2 proteins. SREBP-1a and SREBP-2 are constitutively expressed in most tissues. These factors reside in an immature, 125 kDa form, localized to the ER/Golgi with SREBP cleavage-activating protein (SCAP). In addition, the insulin-inducible genes (Insig) interact with SCAP and 3-hydroxy-3-methylglutaryl coenzyme-A (HMG-CoA) reductase (HMGR), the rate-limiting enzyme of cholesterol biosynthesis, in a manner dependent on levels of sterols. When intracellular sterol levels are high, sterols then bind SCAP and HMGR changing their conformation to favorably associate with Insig. Insig proteins are then able to either retain the SCAP/SREBP complex in the ER and also downregulate the levels of HMGR by promoting its ubiquitation and degradation. Conversely when intracellular sterol levels are low and cholesterol synthesis needs to be induced, this results in the 125 kDa form of SREBP being cleaved into a mature 68 kDa form that then can redistribute to the nucleus where it upregulates the transcription resulting in increased expression of proteins regulating cholesterol synthesis [80]. Additionally, intracellular cholesterol transport is essential for the maintenance of cholesterol homeostasis. The fundamental pathways in cholesterol metabolism (synthesis, uptake, gene regulation) all rely on its proper intracellular distribution among membranes and subcellular organelles [81].

As mentioned above, our laboratory has extensive research interests in understanding cellular cholesterol homeostasis and how components of the

metabolic syndrome, including dyslipidemia, hyperinsulinemia, and even hyperglycemia, perturb this finely-tuned system. Work performed by Nadeau *et al.* demonstrated the ability of insulin to alter lipid content through alterations on SREBP-1 protein expression in both 3T3-L1 adipocytes and L6 myotubes. Incubating either 3T3-L1 adipocytes or L6 myotubes with physiological doses of insulin, 1-10 nM, for 24 hours was sufficient to enhance SREBP-1 protein expression [82]. Total cellular protein levels of SREBP-1 were increased under these conditions and inhibitors of downstream insulin signaling molecules could subsequently inhibit this. Specifically, it was demonstrated that the insulin-induced upregulation of SREBP-1 in adipocytes could be blocked by various PI3K inhibitors, wortmannin (WT) and LY294002. Interestingly, the MAPK inhibitor, PD98059 (PD), was only effective in blocking insulin's ability to induce SREBP-1 upregulation in L6 myotubes. Unlike in the adipocyte model, the aforementioned PI3K inhibitors did not display any effect in diminishing the role of insulin on SREBP-1 transcription. This suggests that insulin has dual functions, potentially occurring through different signaling mechanisms, that differ in L6 myotubes and 3T3-L1 adipocytes [82]. In light of this work, our laboratory has demonstrated that incubation of adipocytes or L6 myotubes with a physiological (5 nM) dose of insulin did not cause a significant defect in insulin signal propagation compared to control; however, significant decreases in glucose transport were observed along with increases in lipogenic mechanisms as demonstrated through PM cholesterol accrual [1, 41]. Studies demonstrating

the exact mechanism by which hyperinsulinemic conditions may induce cellular lipogenesis and PM cholesterol accrual are currently being undertaken.

3.1 Role of HBP Flux & Transcription of Cholesterogenic Enzymes

Our data has identified the HBP as a mediator of diminished glucose transport thereby playing a role in the development of insulin resistance. The HBP has also been shown to mediate the glycosylation of an important transcription factor involved in regulating cholesterol synthesis, Sp1. This basal transcription factor with effects on many different cellular properties was first identified to be glycosylated by Han *et al.* [83]. It was demonstrated that the increased glycosylation status of Sp1 resulted in increased protein stability and enhanced its ability to bind DNA [83]. Conversely, it has been demonstrated by a number of investigators that phosphorylation of Sp1 targets the protein for degradation [84]. This is due to the phosphorylation occurring on PEST sequences or protein regions that are enriched in Pro, Glu, Ser, and Thr residues used as signals for the rapid degradation of proteins [85]. Many investigators have also shown that protein sequences modified by *O*-GlcNAc have high PEST sequences and therefore it has been proposed that this enhanced glycosylation can prevent phosphorylation of these PEST sequences and inhibit degradation [84]. In the context of affecting cholesterol synthesis, new studies have identified a novel mechanism by which maximal activation of the rat SREBP-1c gene by insulin requires Sp1 [86, 87]. Additionally, the presence of Sp1-binding motifs adjacent to an SRE (Sterol Regulatory Element) has been observed in the

promoters of a number of SREBP-responsive genes [88, 89]. Additional cis-acting elements (*e.g.* SREBP, LXR, NF-Y) have been documented to play a role in insulin-activated SREBP-1c promoter through combinatorial actions [86]. In these thesis studies, I have focused on HBP-induced Sp1 glycosylation and its regulation on modulating transcription of cholesterol synthetic enzymes and PM cholesterol accrual in the development of insulin resistance.

The focus of my thesis work revolves around cellular and membrane changes in cholesterol amount in regards to cellular insulin action on glucose transport. As I have previously mentioned, there is a significant amount of work from our group demonstrating that insulin resistance conditions are a response to PM cholesterol accrual in both fat and skeletal muscle. We have also demonstrated that cholesterol-lowering can be a therapeutic target for slowing and possibly ceasing the progression from insulin resistance to type 2 diabetes. The cellular energy sensor, 5' AMP-activated protein kinase (AMPK), is a target of one of the first-line anti-diabetic medications, metformin, that has been demonstrated to enhance glucose transport. Interesingly, AMPK is responsible for many other cellular actions including the inhibition of glycogenic and lipogenic processes.

4. 5'-AMP Protein Kinase (AMPK) Cellular Actions

Classically, AMPK is a multimeric protein known as a cellular fuel gauge. Physiological activation of AMPK occurs when there is a rise in cellular AMP

concentration and a decrease in ATP concentration. Additionally, upstream activators of AMPK include a serine/threonine kinase, LKB1, as well as the Ca^{2+}/Calmodulin-Dependent Kinase II (CaMKII) [90]. These proteins have been demonstrated to phosphorylate and activate AMPK on its Thr172 residue. Once activated AMPK has been demonstrated to affect a myriad of cellular activities including glucose transport, inhibition of fatty acid synthesis, and promoting fatty acid oxidation. Interestingly, AMPK activation is also associated with inhibition of cholesterol synthesis via phosphorylation of the rate-limiting enzyme in cholesterol biosynthesis, HMGR. AMPK has recently become a pharmacological target for patients with T2D. However, most of what is currently known on the importance of AMPK in peripheral insulin sensitivity was performed in skeletal muscle. The role of AMPK in adipose tissue is controversial with conflicting reports, some demonstrating that activation of the protein inhibits GLUT4 translocation and glucose uptake [91] while other reports maintain that AMPK activity is beneficial to glucose transport [92] in this same cell type.

4.1. AMPK Involvement in Anti-Diabetic Interventions

As mentioned earlier, an important result of cellular AMPK activation is the inhibition of energy-consuming processes such as lipid/cholesterol synthesis. Therefore, one could speculate the activation of this energy regulator could be used as a benefit for diabetic individuals through the decrease of detrimental cellular metabolic actions. It has been identified that a number of activators of AMPK have displayed benefits on correcting insulin resistance and enhancing

glucose transport. Although a mechanism is not fully understood, a widely held view is that AMPK increases insulin sensitivity. For example, several agents that normalize blood glucose concentrations and/or improve insulin action including the adipokines adiponection [93] and leptin [94], creatine [95], rosiglitazone [96], troglitazone [97], chromium picolinate (CrPic) [57], and alpha-lipoic acid [98] have been demonstrated to be the result of the activation of AMPK. Additionally, other identified activators of AMPK that display insulin-sensitizing actions have included exercise [99], newly identified nutritional supplements including berberine [100], and prescribed diabetic medications such as metformin [101]. Metformin has become one of the most popular and commonly prescribed medications for diabetic individuals. The actions of this drug have corrective benefits on hyperglycemia without stimulating insulin secretion, inducing weight gain, and causing hypoglycemia. Additionally, the actions of metformin have been far-reaching in that a decrease in circulating lipids associated with cardiovascular disease is witnessed with metformin treatment. Utilizing this background information and the ability of metformin to stimulate AMPK, it has been demonstrated that metformin is able to enhance glucose transport in L6 myotubes in an insulin-independent fashion [102-104].

Additional work from our laboratory [58] has tested the mechanism whereby exercise-induced glucose transport is mediated. This work placed AMPK as a central player in the benefits observed in a cell culture model of exercise. Using AICAR (an AMP analog) and 2,4-dinitrophenol (DNP, a

mitochondrial uncoupler that prevents cellular production of ATP) on L6 myotubes, a significant enhancement of both basal and insulin-stimulated GLUT4 translocation occurred concomitant with increased phosphorylation of AMPK. An unappreciated effect with the use of these AMPK activators that was also witnessed was a ~25% reduction in PM cholesterol. In several pilot studies, siRNA knockdown of the α-catalytic subunit of AMPK ablated the DNP-induced decrease in PM cholesterol compared to that of DNP treatment in siScramble myotubes. Taken together, these new findings regarding the AMPK activators, metformin and exercise-mimetic agents, support our hypothesis that a distal target/event of AMPK activation is PM cholesterol lowering.

Interestingly, work from our laboratory has demonstrated that the beneficial actions of a common nutritional supplement on glucose metabolism, chromium, are mediated by PM cholesterol lowering. Utilizing 3T3-L1 adipocytes, we have seen that this reduction of PM cholesterol is sufficient to enhance insulin-stimulated glucose transport by a pharmacologically relevant dose of chromium picolinate (CrPic). However, the mechanism by which CrPic-mediated reduction of PM cholesterol was still not understood allowing us to hypothesize that CrPic action may be a result of AMPK activation and its downstream inhibition of HMGR, the rate-limiting enzyme in cholesterol synthesis.

5. Chromium Supplementation in Health & Disease

In the late 1950s, chromium (Cr) was recognized in animals to be an essential nutrient required for normal glucose and lipid metabolism. Nutritional or trivalent chromium (Cr^{3+}) is an essential mineral found in a multitude of foods, especially that of brewer's yeast, meats, and whole-grain products. Additionally, health supplements are a significant and popular source of Cr^{3+} as evidenced by CrPic being the second highest-selling overall health supplement, only behind the sales of calcium supplements [105]. Its essentiality comes from the inability of humans to produce this mineral; therefore, the body must obtain Cr^{3+} through dietary sources. Unlike hexavalent chromium (Cr^{6+}), a byproduct of stainless steel and pigment processing and classified as a human carcinogen, Cr^{3+} has been revealed to be stable and relatively non-toxic [106]. Ingestible Cr^{3+} can be found in a variety of forms, namely chromium yeast (CrY), chromium chloride (CrCl), and as the most stable and bioavailable supplement, chromium picolinate (CrPic).

Recent studies performed on the effects of Cr^{3+} have also designed and tested different pharmacologic compounds and complexes of Cr^{3+} such as chromium nicotinate (niacin, CrN), chromium (D-phenylalanine)$_3$ (Cr(D-phe)$_3$) and chromium citrate (CrC). Interestingly, all these complexes have been shown to have positive metabolic effects in the body and seem to be specific for Cr^{3+} compared to other minerals such as magnesium (Mg^{2+}), manganese (Mn^{3+}), and iron (Fe^{2+}). The identification of Cr^{3+} as an essential nutrient was pioneered in

work by Schwarz and Mertz [107] where evidence was presented that an unidentified substance in brewer's yeast protected rats from an age-related decline in glucose tolerance in 1957. The term coined for this substance was "glucose tolerance factor" or GTF. Shortly thereafter, GTF was actually recognized to be the nutrient, Cr^{3+}. In 1977, it was observed that a 40 year old white female receiving total parenteral nutrition (TPN) for 5 years developed peripheral neuropathy, unexpected weight loss, and glucose intolerance as analyzed by an intravenous glucose tolerance test (IVGTT). She was given regular insulin and glucose infusions to restore her weight loss; however, her IVGTT remained remarkably unaffected. It was determined in this patient that her blood Cr^{3+} levels were extremely low (0.55 ng/ml) compared to a normal defined range between 4.9 and 9.5 ng/ml. Also, the patient's hair Cr^{3+} levels were quite low (154 to 175 ng/g) compared to normal levels exceeding 500 ng/g. It was then recognized that her TPN was devoid of Cr^{3+} and after discontinuing her regular insulin infusions, the patient's daily infusate was supplemented with 250 μg of Cr^{3+} for 2 weeks. Surprisingly, her glucose tolerance normalized. Subsequently in the next 5 months, regular insulin infusions were not needed and glucose infusions had to be dramatically reduced to avoid becoming overweight. During this 5-month period, her nerve conduction vastly improved suggesting that her peripheral neuropathy had subsided. Following regular maintenance of Cr^{3+} (20 μg/day) levels, the patient remained well for 18 months [108]. Following this clinical observation, additional support for the essentiality of Cr^{3+} was offered when similar effects were witnessed in other hyperglycemic patients

supplemented with Cr^{3+} [109, 110]. Also, documentation exists that Cr^{3+} deficiency can result in defects associated with cardiovascular disease such as elevated serum cholesterol and triglycerides, and decreased high density lipoprotein cholesterol (HDL) [111, 112]. These clinical studies demonstrating pathologies associated with a Cr^{3+} deficiency prompted research pursuits into the mechanism of Cr^{3+} action on glucose and lipid metabolism. Although a precise mechanism(s) of Cr^{3+} action is still not known, *in vitro* and *in vivo* investigations highlight that Cr^{3+} indeed engages key cellular and molecular mechanisms that are regulatory for normal glucose and lipid metabolism.

5.1. Chromium & Glucose/Lipid Disorders

Much like the case study presented above, encouraging findings in animal and human studies [113-115] have led many investigators to hypothesize that dietary Cr^{3+} supplementation may help to control T2D. Cr supplements are available as trivalent Cr in the chloride ($CrCl_3$) or picolinate (CrPic) salt forms. Animal studies have shown that a deficiency in dietary Cr^{3+} can result in an inability to remove glucose efficiently from the bloodstream [116]. Evidence also suggests that diet-induced insulin resistance in experimental animals can be improved by Cr^{3+} supplementation [117]. In humans, there also seems to be an association between insulin resistance and Cr^{3+} status [118].

The exact mechanism whereby Cr^{3+} participates in the functions of insulin has not been elucidated, but theories range from direct interaction of Cr^{3+} with

insulin [119] to a role of Cr^{3+} in increasing IR number [120], as well as increasing IR tyrosine kinase activity already engaged by insulin [121]. It has been demonstrated that a naturally occurring oligopeptide, low-molecular weight Cr-binding substance (termed "chromodulin") binds chromic ions in response to an insulin-stimulated IR, activating the receptor's tyrosine kinase activity as much as 8-fold in the presence of insulin [121, 122]. The chromodulin-mediated autoamplification of the IR's tyrosine kinase activity would be expected to enhance the regulated movement of GLUT4 and, subsequently, enhance glucose disposal. This anticipated biological outcome has been observed [115], but signaling molecules responsible for the translocation have not yet been evaluated.

Another aspect of Cr^{3+} action that may explain, at least in part, its enhancement of insulin sensitivity is its effect on increasing membrane fluidity and the rate of insulin internalization [123]. Although insulin-stimulated GLUT4 translocation does not appear dependent upon insulin first being transported into the cell [124], studies suggest that IR internalization may compartmentalize and efficiently promote interaction with its substrate(s) associated with internal membranes [125-127]. In agreement with membrane fluidity changes as a basis for the effect of Cr^{3+}, moderate increases in PM fluidity have been documented to increase glucose transport [128, 129]. Furthermore, it has been shown that basal glucose transport is not fully active in fat cells and that it can be increased further by augmenting membrane fluidity [128]. Consistent with membrane fluidity

influencing insulin responsiveness, insulin-stimulated glucose transport is decreased when fluidity diminishes [129]. Interestingly, recent data suggest that the antidiabetic drug metformin enhances insulin action by increasing membrane fluidity [130, 131]. As has been observed after Cr^{3+} treatment [115], metformin treatment has been reported to increase GLUT4 translocation [65, 103, 132]. Work presented in this thesis demonstrated that the beneficial effects of Cr^{3+} on insulin action resulted from changes in PM properties. These data demonstrated that PM cholesterol content was diminished in cells exposed to Cr^{3+} and that exogenous cholesterol replenishment rendered the enhancement of insulin action by Cr^{3+} ineffective.
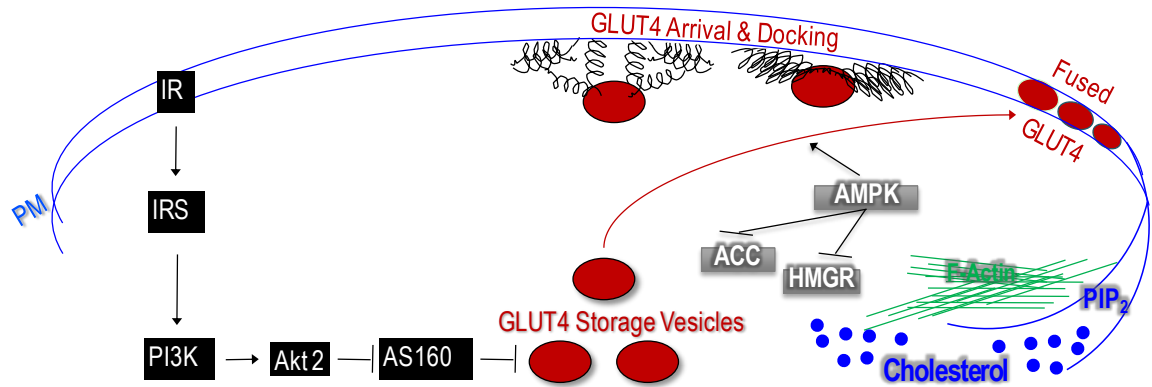
Overview of Proposed Mechanism(s) of Cellular GLUT4 Translocation.

Above figure depicts insulin signaling proteins (*black*) involved in the translocation of intracellular GLUT4 storage vesicles to the plasma membrane. Depicted on the right hand side of the figure is the result of work from our laboratory demonstrating the interconnection between cholesterol, PIP_2, and cortical F-actin in insulin-stimulated GLUT4 translocation. An insulin-independent mechanism involving AMPK is also shown (*grey boxes*) and its downstream effects such as inhibition of ACC and HMGR as well as stimulation of GLUT4 translocation to the PM.

Hypothesis/Summary of Proposed Mechanism

Throughout my thesis studies, the main hypothesis tested was that perturbations in the PM was a contributory factor to the development of insulin resistance and pharmacologic and nutritional agents designed to correct these PM defects would then result in normalized insulin sensitivity and GLUT4 translocation. As outlined in Chapter II, the testing of this hypothesis resulted in three main parts. My studies began with hyperinsulinemia-induced disturbances of GLUT4 translocation through changes in PIP_2 and cortical F-actin which was tested in Chapter IIA. Subsequently, Chapter IIB outlines the results of testing demonstrating that chromium action was a result of PM cholesterol lowering and enhancement of GLUT4 translocation. Finally, the results presented in Chapter IIC exhibited that increased HBP activity, as a result of hyperinsulinemia or hyperglycemia, contributed to the alterations in the PM PIP_2 and cortical F-actin. Interestingly, preliminary studies that were undertaken throughout suggested that increased HBP activity resulted in PM cholesterol accrual via alterations in the transcriptional activity of cholesterol synthetic enzymes.

Chapter II

Results

II. A

Protective Effect of Phosphatidylinositol 4,5-Bisphosphate Against Cortical Filamentous Actin Loss and Insulin Resistance Induced by Sustained Exposure of 3T3-L1 Adipocytes to Insulin

1. Summary

Muscle and fat cells develop insulin resistance when cultured under hyperinsulinemic conditions for sustained periods. Recent data indicate that early insulin signaling defects do not fully account for the loss of insulin action. Given then cortical filamentous actin (F-actin) represents an essential aspect of insulin regulated glucose transport, we tested to see whether cortical F-actin structure was compromised during chronic insulin treatment. The acute effect of insulin on GLUT4 translocation and glucose uptake was diminished in 3T3-L1 adipocytes exposed to a physiological level of insulin (5 nM) for 12 h. This insulin-induced loss of insulin responsiveness was apparent under both low (5.5 mM) and high (25 mM) glucose concentrations. Microscopic and biochemical analyses revealed that the hyperinsulinemic state caused a marked loss of cortical F-actin. Since recent data link phosphatidylinositol 4,5-bisphosphate (PIP_2) to actin cytoskeletal mechanics, we tested to see whether the insulin-resistant conditions affected

PIP$_2$ and found a noticeable loss of this lipid from the plasma membrane. Using a PIP$_2$ delivery system, we replenished plasma membrane PIP$_2$ in cells following the sustained insulin treatment and observed a restoration in cortical F-actin and insulin responsiveness. These data reveal a novel molecular aspect of insulin-induced insulin ressistance involving defects in PIP$_2$/actin regulation.


2. Results

Insulin-stimulated GLUT4 translocation is impaired by chronic insulin treatment

The generation of insulin resistance by exposure of 3T3-L1 adipocytes to a medium containing a high concentration of glucose and insulin has been well documented [66, 67, 133]. In our initial experiments, 3T3-L1 adipocytes preincubated in control medium (25 mM glucose) exhibited a marked response to an acute maximal dose of insulin (30' Ins) as assessed by GLUT4 immunofluorescence of highly purified PM sheets (**Fig. 1A**, compare panels 1 and 3). On the other hand, the presence of a physiological dose of insulin (5 nM) for 12 h was associated with an elevation of PM GLUT4 in the basal state and a clear loss in the acute maximal insulin-stimulated GLUT4 translocation (**Fig. 1A**, compare panels 2 and 4). To confirm the accumulation of GLUT4 in the PM sheets, we used differential centrifugation to isolate PM fractions. Fractions prepared from control 3T3-L1 adipocytes displayed a characteristic insulin-stimulated increase in GLUT4 compared with PM fractions prepared from

untreated cells (**Fig. 1B**, compare lanes 1 and 2). Consistent with microscopic analyses, the immunoblots showed that chronic insulin treatment was associated with an elevation of the basal stae PM GLUT4 level and a loss in the insulin stimulated increment above the basal (**Fig. 1B**, compare lanes 1-4). Densitometry analysis of four separate experiments shows that sustained insulin exposure tended to increase (p=0.08) the basal state PM level of GLUT4 and attenuate insulin-stimulated GLUT4 translocation by 42% ($p < 0.05$).
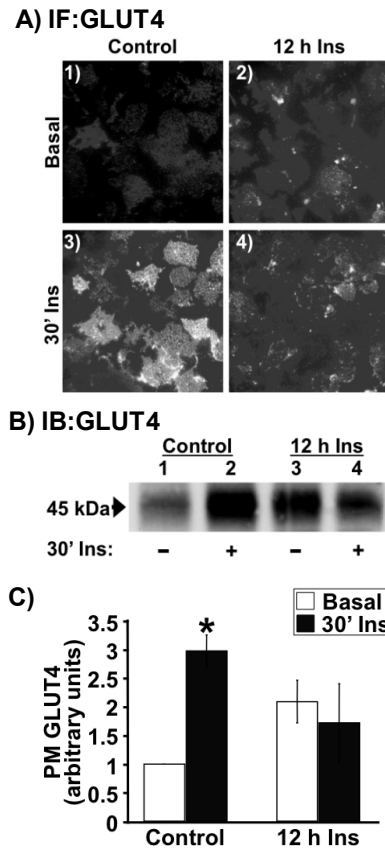
Fig. 1 Chronic Insulin Treatment Impairs Subsequent Acute Insulin Stimulated GLUT4 Translocation. Adipocytes were treated for 12 h in the absence (*Control*) or presence of 5 nM insulin (*12 h Ins*). Following this incubation period, cells were washed and stimulated with 100 nM insulin for 30 min (*30' Ins)* or left in the basal state (*Basal*). **(A)** PM sheets were prepared and subjected to immunofluorescent GLUT4 labeling. All microscopic and camera settings were identical between groups, and representative images from five to eight independent experimnts are shown. **(B)** plasma membrane fractions were prepared, resolved on a 10% polyacrylamide gel, and subjected to Western blotting with GLUT4 antibody. **(C)** densitometric quantification (±S.E., *, $p<0.05$) of the three independent Western blotting analyses.

Prolonged Insulin Treatment Reduces Cell Surface PIP$_2$ and Actin Levels

There are several possible mechanisms that could account for the decreased insulin-stimulated GLUT4 translocation by the hyperinsulinemia. However, consistent with previous work [134, 135], known proximal insulin signal transduction events including the IR autophosphorylation, IRS-1, and Akt phosphorylation were not significantly different between 3T3-L1 adipocytes maintained in control medium with or without 5 nM insulin (data not shown). Because the proximal insulin signaling cascades appeared to be fully functional, we next examined the effect of high glucose/insulin on cortical F-actin. Chronic insulin led to a marked reduction in cortical F-actin as assessed with phalloidin staining of fixed whole cells (**Fig. 2A**, compare panels 1 & 2). Red fluorescent co-staining of nucleic acids with propidium iodide was employed to verify the presence of cells (**Fig. 2A**, compare panels 1-3). Actin staining was verified in cells with latrunculin B (Lat B, an actin monomer binding toxin) treatment (**Fig. 2A**, panel 3). In addition, F-actin to G-actin ratio determination by Western immunoblot analysis confirmed that cells incubated overnight in 5 nM insulin undergo a marked reduction in F-actin and an increase in G-actin, consistent with an induced depolymerization of cortical F-actin (**Fig. 2B**). Since recent data link PIP$_2$ to actin cytoskeletal regulation [136], we next tested whether this insulin-resistant condition affected PIP$_2$. The level of plasma membrane PIP$_2$ was markedly reduced by 5 nM insulin treatment as assessed by anti-PIP$_2$ immunofluorescent labeling of plasma membrane sheets (**Fig. 2C**, panels 1 & 2).

The immunoreactivity of the anti-PIP$_2$ antibody was confirmed in cells in which

PIP$_2$ levels were reduced by LiCl treatment (**Fig. 2C**, panel 3).

A) Actin

B) F-/G-Actin

C) PIP$_2$
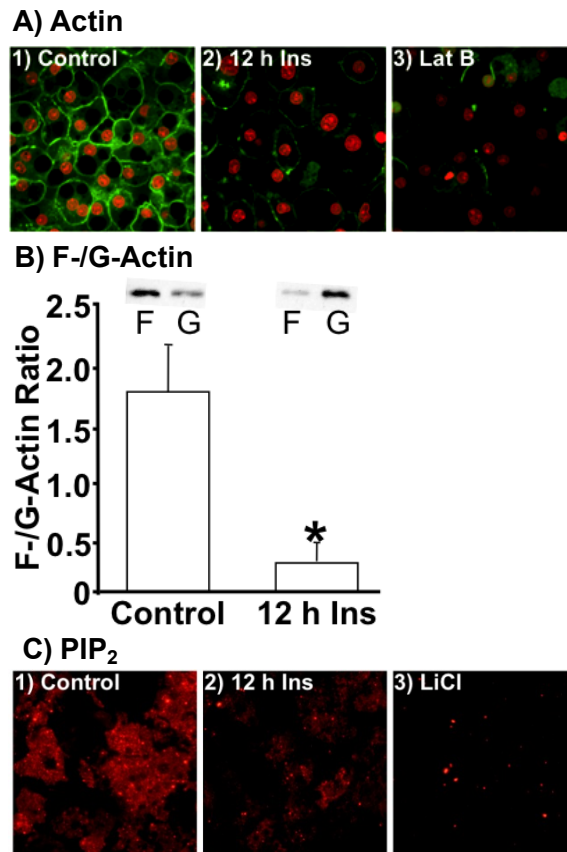
Fig. 2 Cellular Cortical F-actin and PM PIP$_2$ Levels are Diminished in Cells Treated with Insulin for 12 h. Adipocytes were treated as described in the legend to Fig.1. **(A)** nucleic acids and actin in whole cells were co-stained with propidium iodide (*red*) and phalloidin (*green*), respectively. A subset of cells co-labeled the same way presented in *panel 3* were treated with latrunculin B. Representative images from four independent experiments are shown. **(B)** F- and G-actin fractions were prepared, resolved on a 12% polyacrylamide gel, and subjected to Western blotting with actin antibody. Densitometric quantification (±S.E., *, $p<0.05$) derived from three independent experiments are shown. **(C)** membrane sheets were labeled for PIP$_2$. Sheets, derived from cells treated with 10 mM LiCl, are presented in *panel 3*. Representative images from five independent experiments are shown.

**The Loss of PIP$_2$, Actin, and Insulin Sensitivity is Restored with PIP$_2$
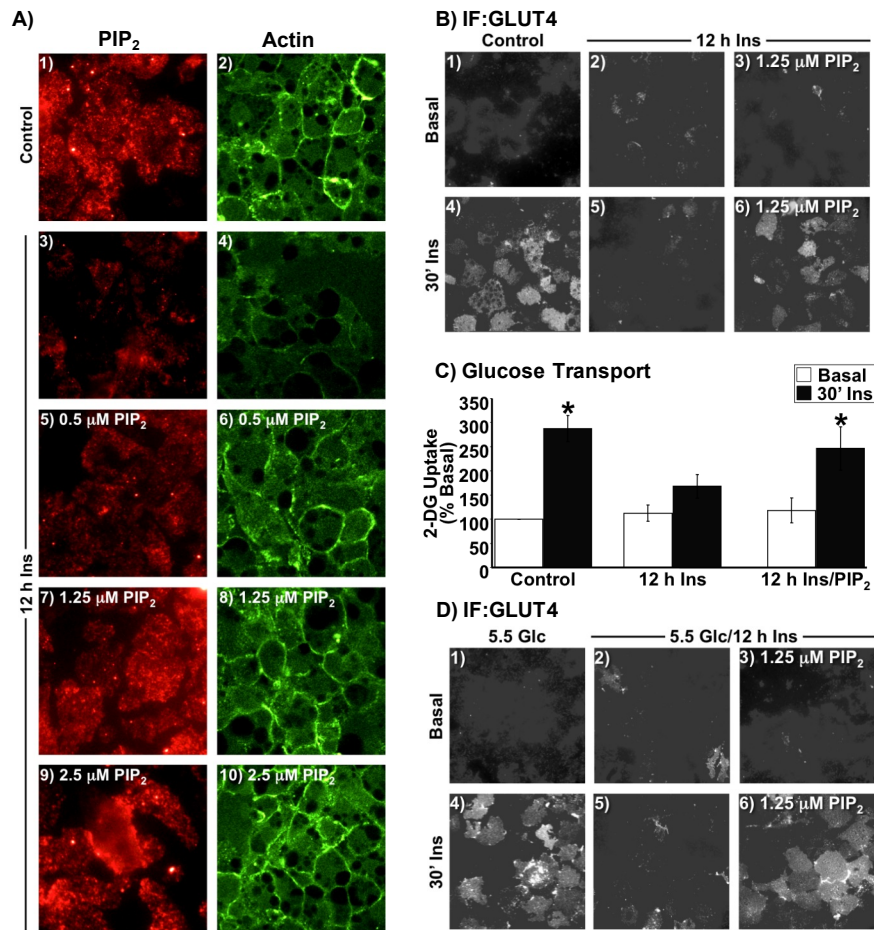Replenishment**

Carrier delivery of PIP$_2$ into insulin-resistant adipocytes led to a dose-dependent replenishment of PIP$_2$ (**Fig. 3A**, panels 1, 3, 5, 7, and 9) and cortical F-actin (**Fig. 3A**, panels 2, 4, 6, 8, and 10). Complete restoration of both PIP$_2$ and cortical F-actin was apparent with a PIP$_2$ addback concentration of 1.25 µM. Thus, we used this concentration to directly test whether the impairment in insulin action occurred as a result of the chronic insulin-induced losses of PIP$_2$ and cortical F-actin. A characteristic increase in insulin-stimulated GLUT4 translocation as assessed by the sheet assay was observed in cells incubated with carrier alone (**Fig. 3B**, panels 1 and 4). Carrier alone did not change the negative consequence of overnight insulin treatment on acute insulin-stimulated GLUT4 translocation (**Fig. 3B**, panels 2 and 5). Remarkably, acute insulin-stimulated GLUT4 translocation in adipocytes rendered insulin resistant was concomitantly restored by 1.25 µM PIP$_2$ replenishment (**Fig. 3B**, panels 3 and 6). In concert with our findings presented in Fig. 1, we also observed a slight increase in the basal state PM level of GLUT4 under hyperinsulinemic conditions (**Fig. 3B**, compare panels 1 and 2). Interestingly, we consistently observed that this increase in transporter was reduced by PIP$_2$ replenishment (**Fig. 3B**, compare panels 1-3). Parallel examination of 2-deoxyglucose uptake showed a concomitant loss of insulin-stimulated glucose transport in cells preincubated in the presence of insulin compared with cells that were not (**Fig. 3C**). In line with previously published work [66, 67, 137], the hyperinsulinemic condition was not

associated with a statistically significant increase in basal glucose transport. Consistent with PIP_2 correction of insulin action, the reduced insulin-stimulated glucose transport was restored with PIP_2 replenishment (**Fig. 3C**). Given that our control medium contained 25 mM glucose and the combination of high glucose with insulin has been suggested to be the cause of the insulin resistant state [66, 67], we also examined the effect of hyperinsulinemia on cells incubated in a low glucose medium (5.5 mM Glc). Insulin acutely increased GLUT4 translocation in cells cultured in low glucose medium (**Fig. 3D**, compare panels 1 and 4), and the extent of PM-associated GLUT4 was qualitatitively equivalent with that induced acutely by insulin in cells cultured in high glucose media (**Fig. 3B**, compare panels 1 and 4), as reported previously [67]. Cells cultured in low glucose in the presence of 5 nM insulin for 12 h displayed an increase in the basal state PM level of GLUT4 and a marked reduction in the ability of insulin to acutely stimulate GLUT4 translocation (**Fig. 3D**, compare panels 2 and 5). The effect of chronic insulin on insulin sensitivity in cells cultured in low glucose was strikingly similar to that in cells cultured in high glucose medium and further analyses also revealed a chronic insulin-induced loss of PM PIP_2 in these cells (data not shown). Accordingly, acute insulin-stimulated GLUT4 translocation in adipocytes cultured in low glucose medium rendered insulin resistant by chronic insulin was concomitantly restored by 1.25 µM PIP_2 replenishment (**Fig. 3D**, panels 3 and 6). As observed in cells cultured in high glucose, the chronic insulin-induced augmentation of PM GLUT4 was reduced upon PIP_2 addback (**Fig. 3D**, panel 3).

Taken together, these data suggest that the PIP_2-dependent insulin resistant state was independent of glucose load.

Interestingly, the work presented in this section offered an interesting observation to our laboratory in that increasing cellular glucose flux was a key mediator of insulin resistance. In parallel, my research interests lied in the mechanism by which anti-diabetic therapies may enhance glucose transport in these tissues. In accord with these research interests, our laboratory was beginning to study the mechanism by which the essential nutrient chromium was beneficial in diabetic patients. Much like the development of insulin resistance as an effect of changes in glucose flux, work that will be presented below demonstrated that chromium action was dependent on PM cholesterol lowering in adipocytes that were only cultured in high glucose medium.

Fig. 3 Diminished Cortical F-actin and Insulin-Stimulated GLUT4 Translocation in Cells Treated with Chronic Insulin are Corrected by PIP$_2$ Replenishment. (A-C) cells were treated overnight in the absence (*Control*) or presence of 5 nM insulin for 12 h. **(A)** during the last 60 min of the 12 h period, the medium was replaced with the same medium enriched with either histone H1 (*panels 1-4*) or indicated concentrations of PIP$_2$/histone H1 (*panels 5-10*). PM sheets (*panels 1, 3, 5, 7, and 9*) or whole cells (*panels 2, 4, 6, 8, and 10*) were labeled for PIP$_2$ (*red*) and actin (*green*), respectively. **(B)** histone H1 (*panels 1, 2, 4, and 5*) or 1.25 µM PIP$_2$ (*panels 3 and 6*) addback incubations were performed as described. **(C)** 2-[^{3}H]deoxyglucose (2-DG) uptake was determined as described. **(D)** cells cultured in 5.5 mM glucose were treated overnight in the absence (*5.5 Glc*) or presence of 5 nM insulin (*5.5 Glc/12 h Ins*) for 12 h.

45

II. B

Chromium Activates GLUT4 Trafficking and Enhances Insulin-Stimulated Glucose Transport in 3T3-L1 Adipocytes Cultured Under Hyperglycemic Diabetic Conditions via a Cholesterol-Dependent Mechanism

1. Summary

Evidence suggests that chromium supplementation may alleviate symptoms associated with diabetes, such as high blood glucose and lipid abnormalities, yet a molecular mechanism remains unclear. We have found that exposure of 3T3-L1 adipocytes to a pharmacologically-relevant dose (10 nM) of chromium picolinate (CrPic) or chromium chloride ($CrCl_3$) mobilizes the glucose transporter, GLUT4, to the plasma membrane (PM). Since CrPic is the most popular supplemental form of Cr^{3+}, my thesis studies focused on the actions of CrPic rather than the less bioavailable and less popular $CrCl_3$. Accumulation of intracellularly sequestered GLUT4 at the PM by CrPic was dependent on PM cholesterol reduction consistent with a previously published report demonstrating that chromium increases membrane fluidity. Concomitant with an increase in GLUT4 at the PM, insulin-stimulated glucose transport was enhanced by Cr^{3+} treatment. Regulation of GLUT4 translocation by CrPic did not involve known insulin signaling proteins such as the IR, IRS-1, PI3K, and Akt.

Although CrPic supplementation has been shown to be preventative in the development of diabetes in otherwise healthy individuals, the actual benefits of CrPic supplementation on glucose metabolism solely occur in hyperglycemic, insulin-resistant individuals. Using our 3T3-L1 cell culture system, we tested whether the CrPic effect on cells was glucose-dependent. We found that GLUT4 redistribution in adipocytes treated with CrPic occurred only in cells cultured under 25 mM glucose conditions (HG; high glucose), which resemble a poorly-controlled diabetic individual, and not in cells cultured under non-diabetic 5.5 mM glucose conditions (LG; low glucose). As previously mentioned, this GLUT4 translocation event by CrPic occurred as a result of PM cholesterol reduction in HG adipocytes alone. Examination of the effect of CrPic on proteins involved in cholesterol homeostasis revealed that the activity of SREBP, a membrane-bound transcription factor ultimately responsible for controlling cellular cholesterol balance, was upregulated by CrPic. In addition, ATP-binding cassette A1 (ABCA1), a major player in mediating cholesterol efflux was decreased. Although the exact mechanism of CrPic-induced cholesterol loss remains to be determined, these cellular responses highlight a novel and significant effect of Cr^{3+} on cholesterol homeostasis.

2. Results

Cr^{3+} triggers the redistribution of GLUT4 to the plasma membrane in adipocytes

Our preliminary treatment parameters were selected based on *in vitro* data showing trivalent Cr in the chloride and picolinate salt formulations, ranging from 1 mM to 20 mM, enhanced glucose uptake and membrane fluidity in cultured mouse and rat skeletal muscle cells [123, 138]. Incubation of 3T3-L1 adipocytes with 10 µM CrCl$_3$ or 10 µM CrPic for 16 h increased the basal and insulin-stimulated level of GLUT4 in the plasma membrane as assessed by GLUT4 immunofluorescence of highly purified plasma membrane sheets (**Fig. 4A**). Digital image processing showed the basal-state plasma membrane levels of GLUT4 following CrCl$_3$ and CrPic pretreatments were increased 44% ($p<0.001$) and 35% ($p<0.001$), respectively. The insulin-stimulated plasma membrane level of GLUT4 was increased 151% ($p<0.005$) and this stimulation was amplified by both CrCl$_3$ and CrPic pretreatments by 43% ($p<0.05$) and 39% ($p<0.05$), respectively. To confirm the effect of Cr^{3+} on the accumulation of GLUT4 in isolated plasma membrane sheets, we used differential centrifugation to isolate plasma membrane from 3T3-L1 adipocytes. Plasma membrane fractions prepared from cells treated with insulin displayed a characteristic increase in GLUT4 compared with plasma membrane fractions prepared from untreated cells (**Fig. 4B**, compare lanes 1 and 2). Consistent with the microscopic analysis, immunoblot analysis showed that Cr^{3+} treatment for 16 h increased the basal-

48

state level of GLUT4 in the plasma membrane (**Fig. 4B**, compare lanes 1, 3 and 5), and the insulin effect was enhanced in the presence of Cr^{3+} (**Fig. 4B**, compare lanes 2, 4 and 6). A constant finding with plasma membrane preparation via subcellular fractionation (**Fig. 4B**) was the chromium-induced increase in the basal-state plasma membrane level of GLUT4 was similar to that induced by insulin alone; whereas, this was not the case in isolated plasma membrane sheets where the chromium effect on the basal-state plasma membrane level of GLUT4 was less than that of insulin. In contrast to plasma membranes obtained with the "sheet" assay, which are highly purified, the fractions isolated by centrifugation are likely contaminated, to some extent, with cytosol and intracellular vesicles [139]. Therefore, although chromium appears to be mobilizing GLUT4 to the plasma membrane, the majority of it may not be physically incorporated into the cell surface. Nonetheless, these microscopic and biochemical data clearly show that chromium elicits an insulin-like accumulation of GLUT4 at the plasma membrane in 3T3-L1 adipocytes. As shown in Fig. 4C, this accumulation elicited by CrPic treatment occurs concomitant with a loss of GLUT4 protein in the low density microsome (LDM) fraction. Also, Cr^{3+} treatment did not affect total GLUT4 protein levels detected in crude total membrane (CM) fractions (**Fig. 4D**).

A) IF: GLUT4

B) PM Fraction
IB: GLUT4

C) LDM Fraction
IB: GLUT4

D) CM Fraction
IB: GLUT4
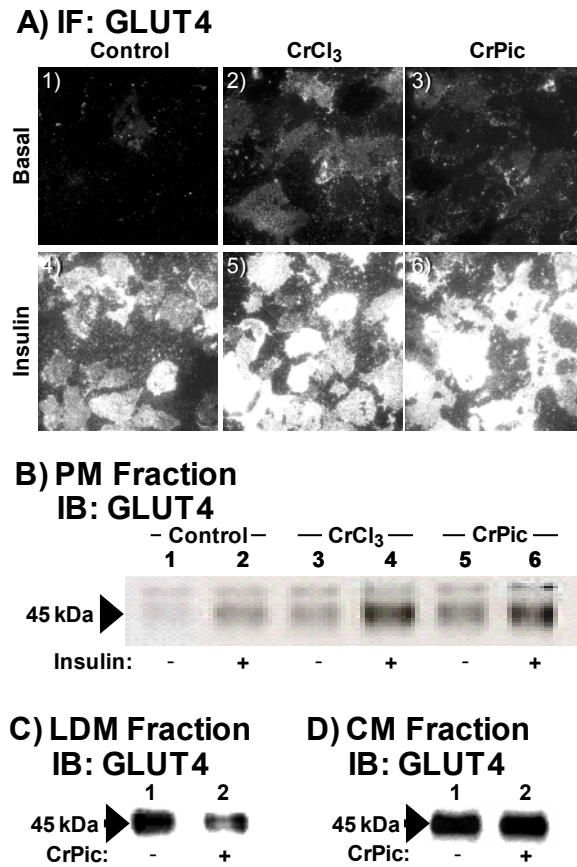
Fig. 4 Cr³⁺ stimulates GLUT4 translocation. 3T3-L1 adipocytes were treated with 10 µM CrCl$_3$ or 10 µM CrPic in serum-free DMEM for 16 hours. During the last 30 min of incubation, the cells were either left unstimulated (Basal) or stimulated with 1 nM insulin. **(A)** Representative plasma membrane (PM) sheet GLUT4 images are shown from 5-8 experiments. **(B)** PM, **(C)** low density microsome (LDM), and **(D)** crude membrane (CM) fractions immunoblotted (IB) for GLUT4. These are representative immunoblots (IB) from 3-5 independent experiments.

Key insulin signal transduction events are not stimulated by Cr^{3+}

There are several possible mechanisms that could account for the increased GLUT4 translocation by Cr^{3+}. We first explored whether known proximal insulin signal transduction events including insulin receptor (IR) autophosphorylation, insulin receptor substrate-1 (IRS-1) and Cbl tyrosine phosphorylation, and Akt phosphorylation were involved. Given that the most popular form of chromium in dietary supplements is CrPic [140], here and most of the subsequent analyses aimed at understanding the molecular mechanism of Cr^{3+} action used CrPic. Insulin stimulation resulted in increased tyrosine phosphorylation of the IR β-subunit, IRS-1 and Cbl at 5 min (**Figs. 5A, 5B, and 5C**, compare lanes 1 and 3) or at 2-, 15-, 30-min treatment intervals (data not shown). In contrast to the effect of insulin, the overnight CrPic pretreatment associated with insulin-like activity had no effect on the phosphorylation of these proteins in the absence or presence of insulin (**Figs. 5A, 5B, and 5C**, compare lanes 1 and 2, and 3 and 4). Immunoblotting of those same membranes with anti IR β-subunit, IRS-1, and Cbl antibodies demonstrated the presence of equal amounts of IR β-subunit, IRS-1 and Cbl (**Figs. 5A, 5B, and 5C**, lanes 5-8). In addition to immunoblotting cell lysates, we immunoblotted IR, IRS-1, and Cbl immunoprecipitates and these data confirmed that insulin, but not CrPic, increased the extent of tyrosine phosphorylation of these proteins (data not shown).

Although the signaling events distal to the Cbl cascade remain unclear, recognized molecules of the IRS-1 cascade involved in GLUT4 translocation are

PI3K and the Akt serine/threonine kinase. Akt-1 phosphorylation, which is indicative of activation, was assessed by using an anti-phospho-Ser473 antibody that is specific for the serine phosphorylated Akt-1 isoform, whereas the phosphorylation of Akt-2 was determined by monitoring the mobility shift indicative of the phosphorylated and active enzyme [141]. Insulin stimulated the phosphorylation of both Akt-1 (**Fig. 5D**, left immunoblot, compare lanes 1 and 3) and Akt-2 (**Fig. 5D**, right immunoblot, compare lanes 5 and 7). In contrast, exposure of cells to CrPic did not result in phosphorylation of either Akt isoform (**Fig. 5D**, compare lanes 1 and 2, and 5 and 6) or increase insulin's effect on these kinases (**Fig. 5D**, compare lanes 3 and 4, and 7 and 8).

To further assure ourselves that the classical insulin signaling pathway was not a target of Cr^{3+} action we sought to test the effect of phosphatidylinositol 3-kinase (PI3K) inhibition on CrPic action. However, testing the role of PI3K with the PI3K inhibitors wortmannin or LY294002 was complicated by the 16 h CrPic treatment. Moreover, since PI3K regulates endocytosis, a wortmannin-induced loss of CrPic action may reflect a loss of the endocytic uptake of CrPic and not CrPic-stimulated PI3K signaling. To circumvent these issues and assess the effect of CrPic on PI3K activity we evaluated phosphatidylinositol 3,4,5-trisphosphate (PIP_3) generation as we have previously reported [142]. Using a specific PIP_3 antibody [143, 144], microscopic analyses revealed very little endogenous PIP_3 localized at the plasma membrane in the absence or presence of CrPic treatment (**Fig. 5E**, panels 1 and 2). Strong nuclear PIP_3 labeling was observed in all cells (**Fig. 5E**), as previously documented [145]. Consistent with

PI3K activation by insulin, an increase in plasma membrane PIP_3 was apparent in insulin-stimulated cells (**Fig. 5E**, panel 3), an amplification of this by CrPic exposure was not evident (**Fig. 5E**, compare panels 3 and 4).
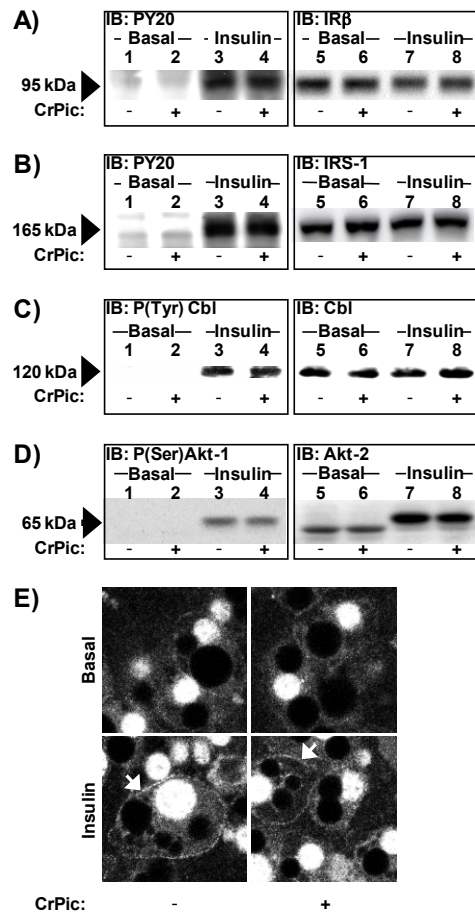
Fig. 5 Cr³⁺ treatment does not enhance basal or insulin-stimulated phosphorylation states of the insulin receptor β-subunit, IRS-1, Cbl, PI3K, or Akt. 3T3-L1 adipocytes were left untreated (lanes 1 and 3) or treated with 10 mM CrPic (lanes 2 and 4) in serum-free DMEM for 16 hours. During the last 5 min of incubation, the cells were either left unstimulated (Basal) or stimulated with 1 nM insulin. Whole-cell detergent lysates were generated and subjected to immunoblotting with antibodies to **(A and B)** phosphotyrosine (left immunoblots, lanes 1-4), **(A)** IRβ (right immunoblot, lanes 5-8), **(B)** IRS-1 (right immunoblot, lanes 5-8), **(C)** P(Tyr) c-Cbl (left immunoblot, lanes 1-4) and Cbl (right immunoblot, lanes 5-8), and **(D)** P$^{(Ser)}$Akt (left immunoblot, lanes 1-4) and Akt-2 (right immunoblot, lanes 5-8) as described in *Materials and Methods*. These are representative immunoblots from 3 separate experiments. **(E)** Shown are representative images of whole cell PIP$_3$ from 3 independent experiments.

Cr^{3+}-induced GLUT4 translocation is coupled to plasma membrane cholesterol loss

Recently, we reported that moderate cholesterol depletion from the plasma membrane increases the basal-state plasma membrane level of GLUT4 [141]. Given that Cr^{3+} has been demonstrated to influence membrane fluidity [146], we next evaluated whether the insulin mimetic action of Cr^{3+} may be coupled to changes in plasma membrane properties, in particular, cholesterol content. Exposure of the cells to CrPic for 16 h resulted in a 29% loss ($p<0.05$) of plasma membrane cholesterol (**Fig. 6A**). This loss of cholesterol from the plasma membrane prompted us to ask whether Cr^{3+}-induced GLUT4 translocation could be prevented by restoring the basal-state plasma membrane level of cholesterol. Here we used methyl-β-cyclodextrin (βCD) preloaded with cholesterol as we have previously reported [141] to replenish the depleted plasma membrane cholesterol. The reduction in plasma membrane cholesterol induced by CrPic treatment was prevented in cells incubated in medium enriched with βCD preloaded with cholesterol (βCD:Chol) (**Fig. 6A**). The effect of βCD:Chol did not significantly alter the basal-state level of cholesterol content in the plasma membrane (**Fig. 6A**). The ability of CrPic to mobilize GLUT4 to the plasma membrane was prevented in cells incubated in βCD:Chol (**Fig. 6B**, compare panels 2 and 4) and the effect of βCD:Chol did not alter the basal-state level of GLUT4 in the plasma membrane (**Fig. 6B**, compare panels 1 and 3). These findings are consistent with previous work by our group [141] showing that reduction in plasma membrane cholesterol activates GLUT4 translocation.

A) Membrane Cholesterol
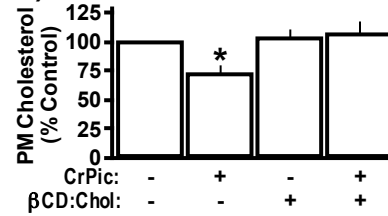
B) IF: GLUT4
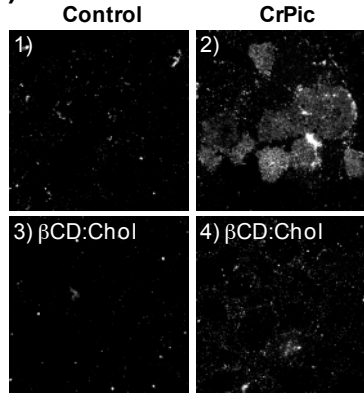
Fig. 6 Cr^{3+} diminishes plasma membrane cholesterol and cholesterol replenishment prevents Cr-induced GLUT4 translocation. 3T3-L1 adipocytes were left untreated (-CrPic, panels 1 and 3) or treated with 10 mM CrPic (+CrPic, panels 2 and 4) in serum-free DMEM for 16 hours, which did not (panels 1 and 2) or did contain (panels 3 and 4) 1 mM bCD preloaded with cholesterol. **(A)** Cells were harvested, plasma membrane fractions were prepared, and membrane cholesterol content was determined as described under *Materials and Methods*. Results are expressed as percent of control. They represent the mean (± SE, * *P<0.05*) from 3-4 independent experiments. **(B)** Representative plasma membrane (PM) sheet GLUT4 images are shown from 3 experiments.

To further explore this cholesterol-dependency of Cr^{3+} action, we next tested if the Cr^{3+} effect would be compromised in cells where membrane cholesterol was depleted by βCD pretreatment. As shown in **Fig. 7A**, exposure of 3T3-L1 adipocytes to 1.0 mM βCD for a total of 16.5 hr lowered plasma membrane cholesterol by 20% ($p<0.05$). Consistent with our previous findings, this βCD-induced loss of plasma membrane cholesterol was associated with an increase in basal (**Fig. 7B**, compare panels 1 and 2) and insulin-stimulated (**Fig. 7B**, compare panels 4 and 5) GLUT4 translocation. As shown in Fig. 6, CrPic treatment (16.5 hr) in this experiment lowered plasma membrane cholesterol and increased GLUT4 translocation to the same extent as 1.0 mM βCD (data not shown). Interestingly, no further reduction in plasma membrane cholesterol was observed in βCD -treated cells exposed to CrPic (**Fig. 7A**). Consistent with Cr^{3+} action being cholesterol-dependent, no further augmentation of plasma membrane GLUT4 was observed in cells co-treated with βCD and CrPic (**Fig. 7B**, panels 3 and 6).

A) Membrane Cholesterol
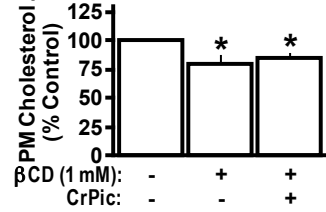
B) IF: GLUT4
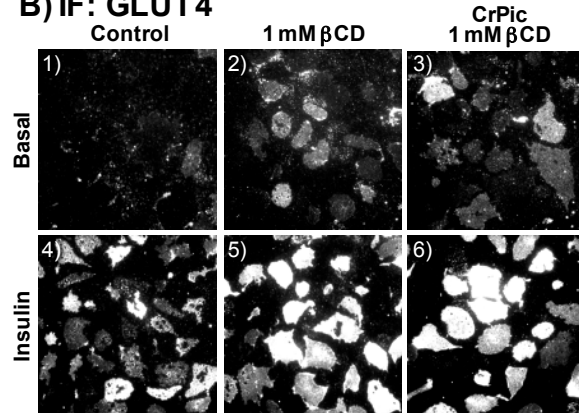
Fig. 7. Cells with a βCD-induced moderate cholesterol loss are unresponsive to Cr^{3+}. Cells were pretreated without or with 1 mM βCD for 30 min and then left untreated or treated with 10 mM CrPic in serum-free DMEM in the continual presence of βCD for 16 hours. Following this 16.5 hr period cells were either left untreated or treated with 1 nM insulin for 30 min. **(A)** Membrane cholesterol was determined and is presented as described in preceding legend. They represent the mean (± SE, * *P<0.05*) from 3 independent experiments. **(B)** Representative plasma membrane (PM) sheet GLUT4 images are shown from 3 experiments.

Finally, since CrPic treatment was not associated with an amplification of the insulin signal (**Fig. 5**), we assessed whether the augmented action of insulin to stimulate glucose transport in the presence of a pharmacologic dose of CrPic (10 nM) was due to the cholesterol-dependent increase in GLUT4 at the cell surface. Fig. 8 shows that this pharmacological dose of CrPic significantly decreased the basal-state plasma membrane level of cholesterol. The reduction in plasma membrane cholesterol induced by CrPic treatment was prevented in cells incubated in medium enriched with βCD:Chol (**Fig. 8A**). The effect of βCD:Chol did not significantly alter the basal-state plasma membrane level of cholesterol (**Fig. 8A**). Consistent with the beneficial effect of CrPic on insulin action being due to the cholesterol-dependent mobilized pool of GLUT4, the ability of CrPic to enhance insulin-stimulated glucose transport was prevented in cells incubated in βCD:Chol (**Fig. 8B**). Also, βCD:Chol alone did not alter basal and insulin-stimulated glucose transport.

A) Membrane Cholesterol

B) Glucose Transport
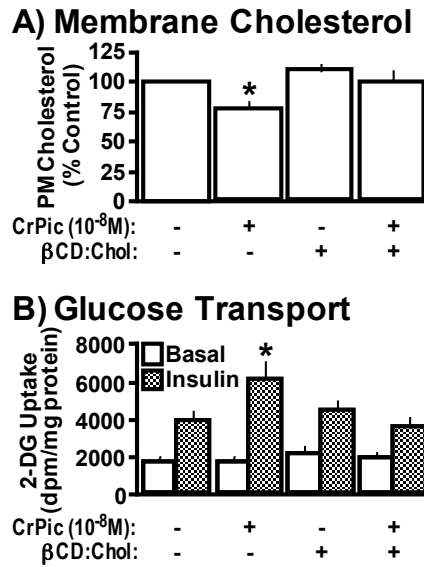
Fig. 8 Cr^{3+}-enhanced insulin-stimulated glucose transport is cholesterol-dependent. 3T3-L1 adipocytes were pretreated in the absence (-) or presence (+) of 10^{-8} M CrPic for 16 hr in serum free media which did not (-) or did contain (+) 1 mM βCD preloaded with cholesterol. **(A)** Cells were harvested, plasma membrane fractions were prepared, and membrane cholesterol content was determined as described under *Materials and Methods*. Results are expressed as percent of control. They represent the mean (± SE, * $p<0.05$) from three independent experiments. **(B)** Glucose transport was determined by specific uptake of 2-[^{3}H]deoxyglucose as described under *Materials and Methods*. All insulin-stimulated uptakes were significantly ($p<0.001$) elevated over their respective controls. (*$p<0.05$ versus all other groups).

Insulin Mimetic Activity of CrPic is Cholesterol-Dependent

In the work presented above, it was discovered that both CrPic and $CrCl_3$ at concentrations as low as 10 nM stimulated the mobilization of GLUT4 to the plasma membrane of 3T3-L1 adipocytes [57]. A novel observation was that this redistribution of GLUT4 was dependent on a Cr^{3+}-induced loss of plasma membrane cholesterol. Although these data are consistent with Cr^{3+} exerting a positive effect on the glucose transport system and lowering elevated blood glucose in type 2 diabetic individuals, a confounding issue is that non-diabetic individuals do not experience a change in blood glucose following CrPic treatment. Since the standard medium used to culture 3T3-L1 adipocytes contains 25 mM glucose, a concentration of glucose akin to that in a poorly controlled diabetic individual, we tested if the cellular response to Cr^{3+} treatment would be diminished in cells cultured in a normal level of glucose (5.5 mM).

Consistent with an enhancing effect of CrPic on GLUT4 translocation in cells cultured in 25 mM glucose, plasma membrane fractions from these cells displayed an increase in GLUT4 compared with plasma membrane fractions prepared from untreated cells (**Fig. 9**, compare lanes 1 and 2). Interestingly, the same treatment parameters did not increase the basal-state plasma membrane level of GLUT4 in cells cultured in medium containing 5.5 mM glucose (**Fig. 9**, compare lanes 3 and 4). With our previous observations that CrPic action requires changes in plasma membrane cholesterol, we next compared the

plasma membrane cholesterol levels in the high glucose (CrPic-sensitive) and low glucose (CrPic-resistant cells).

Fig. 9B shows that plasma membrane fractions prepared from cells cultured in 25 mM glucose were more cholesterol enriched by 13% ($p<0.05$) than membranes prepared from cells cultured in 5.5 mM glucose, and CrPic selectively lowered this excess cholesterol only in the "high glucose" cells by 18% ($p<0.05$). Notably, cells cultured in 5.5 mM glucose contain a similar level of plasma membrane cholesterol to those cultured in 25 mM glucose/10 nM CrPic, and treatment of the low-glucose cultured cells tended to increase plasma membrane cholesterol, but this was not statistically significant. Therefore, we next confirmed if addition of exogenous cholesterol in the culture medium prevented CrPic action. As previously reported [56, 57], this experimental manipulation that replenished the reduced cholesterol effectively prevented the translocation of GLUT4 to the plasma membrane elicited by CrPic (**Fig. 9C**).
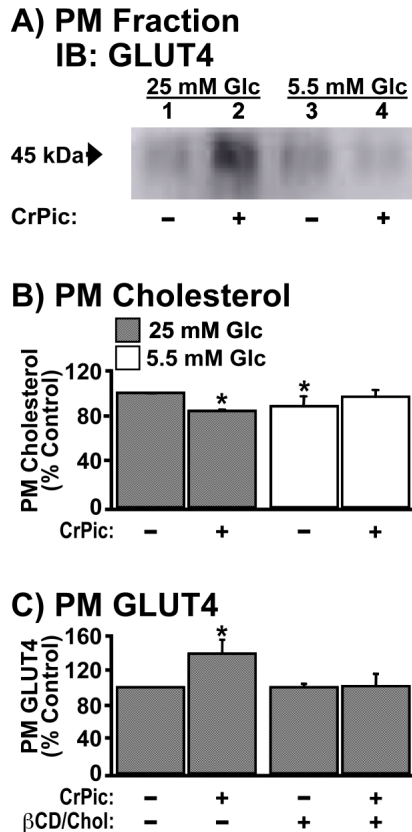
Fig. 9 GLUT4 translocation and cholesterol loss stimulated by CrPic in cells cultured in high, but not low, glucose containing medium. 3T3-L1 adipocytes were left untreated or treated with 10 nM CrPic in serum-free DMEM containing 25 mM glucose (Glc) or 5.5 mM Glc for 16 hours. Shown are **(A)** GLUT4 immunoblot (IB) and **(B)** cholesterol content of plasma membrane (PM) fractions prepared by ultracentrifugation as described in Material and Methods. **(C)** Quantitated GLUT4 content in PM fragments prepared by sonication as described in Material and methods from cells left untreated or treated with 10 nM CrPic in serum-free DMEM containing 25 mM Glc for 16 hours. **(A)** Representative IB from three independent experiments and **(B, C)** results, expressed as percent of 25 mM glucose control, representing the mean (± SE, * $P<0.05$) from 3-4 independent experiments.

CrPic Induces a Reciprocal Response in SREBP and ABCA1

In order to confirm the CrPic-induced change in cellular cholesterol, we next studied whether the activity of SREBP-1, a predominantly expressed SREBP in 3T3-L1 adipocytes that can stimulate all SREBP-responsive genes including those involved in cholesterol homeostasis, was affected in cells treated with CrPic. In contrast to our initial thoughts that CrPic may decrease plasma membrane cholesterol by repressing the cleavage of the ER/Golgi-localized 125 kDa precursor SREBP-1, CrPic exposure was associated with a clear loss of this precursor from the intracellular membrane fraction (**Fig. 10A**). At the same time, immunoblot analyses of nuclear extracts revealed an increased abundance of the 68 kDa mature SREBP-1 (**Fig. 10B**). In parallel, we tested if the increased nuclear localization of SREBP-1 induced the predicted shutdown of expression of ABCA1, a major player in mediating the cellular efflux of cholesterol. As shown in Fig. 10C, plasma membrane fractions prepared from cells treated with CrPic displayed a decrease in the basal-state plasma membrane level of ABCA1.

Interestingly, the work presented in this section demonstrated a novel membrane-based mechanism for the effects of a commonly used supplement, chromium, on the regulation of the glucose transport system in 3T3-L1 adipocytes. To our knowledge, this was the first time that a mechanism had been proposed regarding chromium's beneficial effects on the glucose transport system that did not involve direct enhancement of the insulin signaling pathway. The work presented in this section further supported a model of membrane-associated changes that affected glucose transport in adipocytes. This stimulated

work dissecting cellular and molecular alterations PM changes that then

influences GLUT4 translocation and glucose transport.
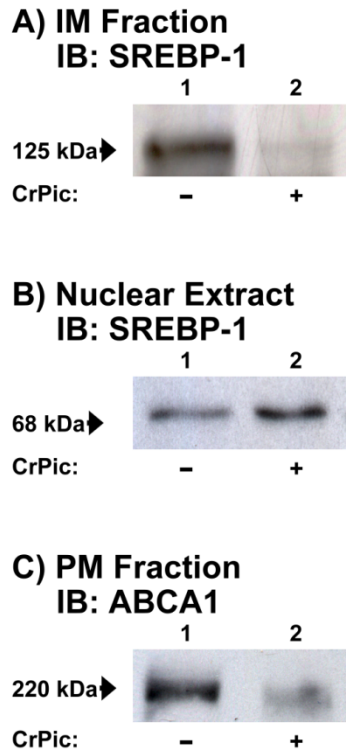
Fig. 10 SREBP-1 and ABCA1 protein response in cells exposed to CrPic.
PM, intracellular membrane (IM) and nuclear extracts (NE) were prepared as described in Material and methods from 3T3-L1 adipocytes treated with 10 nM CrPic in serum-free DMEM containing 25 mM Glc for 16 hours. Shown are representative IBs for **(A)** SREBP-1 in the IM fraction, **(B)** SREBP-1 in the NE fraction and **(C)** ABCA1 in the PM fraction.

II. C

Hexosamine Biosynthesis Pathway Flux Contributes to Insulin Resistance via Altering Membrane PIP$_2$ and Cortical F-Actin

1. Summary

We recently found that plasma membrane (PM) phosphatidylinositol 4,5 bisphosphate (PIP$_2$)-regulated filamentous actin (F-actin) polymerization was diminished in hyperinsulinemic cell culture models of insulin resistance. Here we delineated if increased glucose flux through the hexosamine biosynthesis pathway (HBP) causes the PIP$_2$/F-actin dysregulation and insulin resistance induced by hyperinsulinemia. Increased HBP activity was detected in 3T3-L1 adipocytes cultured under conditions closely resembling physiologic hyperinsulinemia (5 nM Ins for 12 h) and in cells where HBP activity was amiplified by 2 mM glucosamine (GlcN), an experimental substance entering the HBP distal to the rate-limiting enzyme (GFAT, glutamine:fructose-6-phosphate amidotransferase). Both the 5 nM Ins and experimental GlcN challenge induced comparable losses of PIP$_2$ and F-actin. In addition to protecting against the insulin-induced membrane/cytoskeletal abnormality and insulin-resistant state, exogenous PIP$_2$ corrected the GlcN-induced insult on these parameters. Moreover, in accordance with HBP flux directly weakening PIP$_2$/F-actin structrure, inhibition of GFAT restored PIP$_2$-regulated F-actin structure and insulin responsiveness. Conversely, overexpression of GFAT was associated

with a loss of detectable PM PIP_2 and insulin sensitivity. A slight decrease in intracellular ATP resulted from amplifying HBP by hyperinsulinemia and GlcN. However, experimental maintenance of the intracellular ATP pool under both conditions with inosine did not reverse the PIP_2/F-actin-based insulin resistant state. Furthermore, less invasive challenges with increased glucose concentrations in the absence of insulin, also led to PIP_2/F-actin dysregulation. Accordingly, we suggest that the functionality of cell systems dependent on PIP_2 and/or F-actin status, such as the glucose transport system, can be critically compromised by excessive HBP activity.

2. Results

Hyperinsulinemia- and Glucosamine-Induced Defects in Glucose Transport

Previous study by our laboratory has examined insulin- and GlcN-induced insulin resistance. The former studies revealed novel PIP_2/F-actin defects contributing to the insulin-induced insulin resistance. In addition, the later GlcN studies showed cell surface *O*-linked glycosylation in the insulin-resistant cells. As a start to probing whether the insulin-induced PIP_2/F-actin loss was coupled to inappropriate HBP activity, we visualized *O*-linked glycosylation to ensure replication of earlier GlcN findings. Consistent with other reports, strong nuclear membrane labeling resulting from nuclear pore complex protein *O*-linked glycosylation was detected in all cells. Concomitant with this strong nuclear signal, 3T3-L1 adipocytes exposed to 2 mM GlcN for 12 h displayed a marked

increase in cell surface membrane immunoreactivity to an *O*-GlcNAc-specific

antibody. A qualitatively detectable increase in PM localized *O*-linked

glycosylation was also present in cells treated with 5 nM insulin for 12 h (**Fig.**

11A). Inhibition of GFAT with DON reduced the cell surface *O*-GlcNAc signal

visualized in the cells exposed to the 12 h insulin treatment, lending support to

the involvement of the HBP in the insulin-induced increase in *O*-linked

glycosylation. Fig. 11B shows the quantitative results of digitally analyzing the *O*-

GlcNAc signal in multiple boxed regions of the cell surface area in several

images collected for each group from three to five independent experiments.

A) IF: *O*-GlcNAc

1) Control
2) 12h GlcN
3) 12h Ins.
4) 12h Ins. + DON

B)

PM *O*-GlcNAc/Area (arbitrary units)
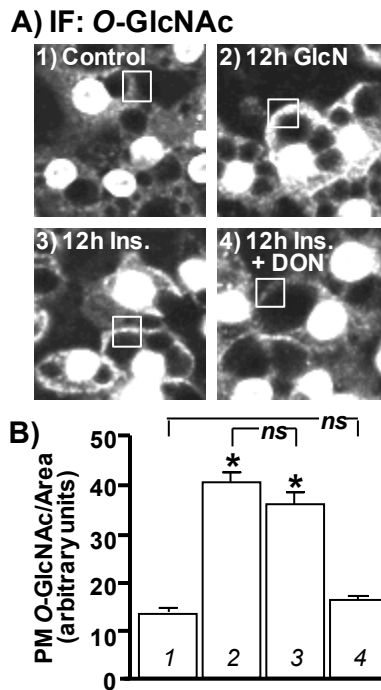
Fig. 11 Insulin and GlcN induce similar changes in cellular *O*-linked glycosylation. Following 36 h of incubation in DMEM containing 5.5 mM glucose, cells were left untreated *(Control)* or treated overnight (12 h) with 5 nM insulin in the presence *(12h Ins, +DON)* or absence *(12h Ins)* of DON. A subset of cells was treated with 2 mM glucosamine in the absence of insulin *(12h GlcN)* for 12 h. Representative images of cells subjected to immunofluorescence microscopy with RL2 antibody **(A)** and quantitation **(B)** are shown. *(*, P < 0.05 vs. Control; bar 1).*

Consistent with the negative effect of increased HBP activity on insulin-regulated GLUT4 translocation observed in these models, this acute insulin-regulated process was impaired for the 12 h Ins- and 12 h GlcN-treated cells, respectively (**Fig. 12A**). Quantitation of these data entailed normalizing the GLUT4 signal to wheat-germ agglutinin (WGA)-labeling of the same PM sheets (**Fig. 12B**). These analyses revealed that the chronic insulin and GlcN treatments decreased the ability of an acute insulin challenge to stimulate GLUT4 translocation by 21% and 24%, respectively. DON treatment completely restored both insulin-regulated GLUT4 translocation to control levels. Basal and acute insulin-stimulated GLUT4 translocations in control cells were not affected by DON.
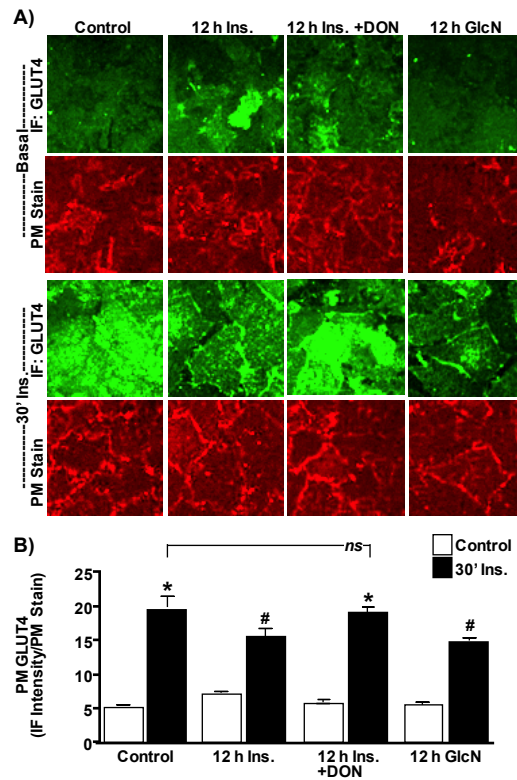
Fig. 12 Acute insulin responsiveness is impaired similarly by hyperinsulinemia and GlcN. Cells were treated exactly as described in Fig. 1. Following treatments, cells were washed, either left untreated (*Basal*) or acutely (30 min) challenged with 100 nM insulin *(30' Ins),* and GLUT4 translocation and glucose transport were determined. Representative images of PM sheets subjected to immunofluorescence microscopy with GLUT4 antibody **(A, Panels 1-4 and 9-12)** and WGA **(A, Panels 2-8 and 13-16)**, and signal quantitation (means ±S.E.) from three to five experiments **(B)** are shown. All microscopic and camera settings were identical between groups. *(*, P < 0.05 vs. Control; #, P < 0.05 vs. Control 30' Ins)*.

Plasma Membrane and Cytoskeletal Defects

We recently documented that this failed insulin response induced by the 12 h Ins treatment reflected a defect in PIP_2-regulated cortical F-actin. To test if the PIP_2/F-actin disturbance resulted from increased glucose flux through HBP, we first examined if inhibition of GFAT with DON protected against the insulin-induced decrease in detectable PM PIP_2 and F-actin. For these studies, we used a commercially available PIP_2 antibody (Assay Designs Inc, Ann Arbor, Michigan) that we have previously documented to be specific for $PI(4,5)P_2$. PM sheets prepared from 12 h Ins cells displayed a loss in detectable PM PIP_2 compared to control cells (**Fig. 13**, compare panels 1 and 2). In contrast, DON pretreatment completely prevented this decrease (**Fig. 13**, panel 3). As visualized in panels 4 and 5, DON treatment did not appear to affect the control level of PM PIP_2, but the overnight GlcN treatment was associated with a clear reduction in detectable PM PIP_2, similar to that induced by the chronic insulin conditions. Shown are representative images captured from 8-10 separate experiments and again, to ensure that this qualitative measure was performed in an unbiased manner, fields of sheets were selected based solely on their staining with rhodamine-conjugated WGA (**Fig. 13**, panels 6-10).
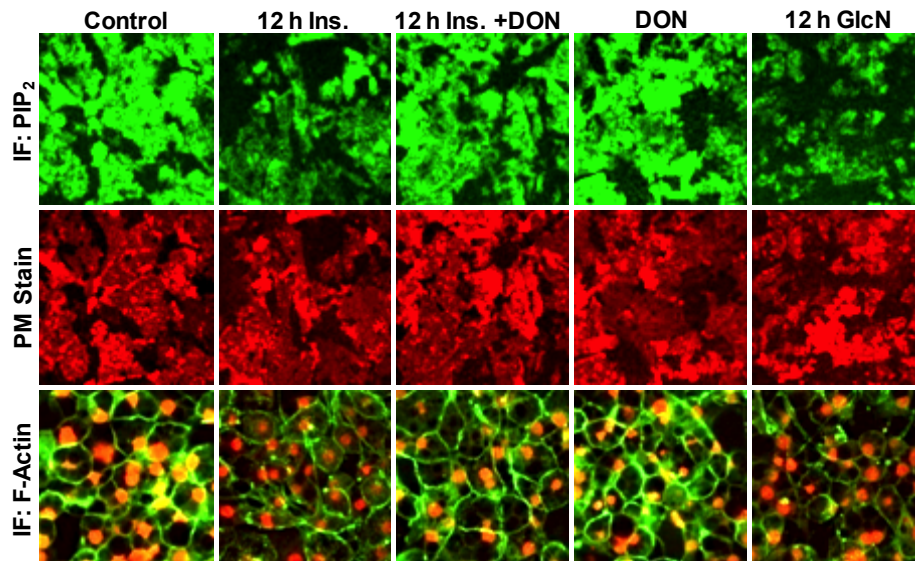
Fig. 13 Hyperinsulinemic- and GlcN-states induce a loss in PM PIP$_2$ detection and cortical F-actin. Representative immunofluorescent images of PIP$_2$ **(Panels 1-5)** and WGA **(Panels 6-10)** detected in PM sheets treated as described in preceding Figs., are shown. Phalloidin stained F-actin and propidium iodide labeled nuclei in these cells **(Panels 11-16)** are shown. Images are representative from three to five independent experiments.

In addition to these qualitative measure of signal intensity from 60x magnification fields, we also performed three separate population-based assays where the PM PIP_2 immunofluorescent signal was quantitated on an entire 35-mm cell culture plate well using the LI-COR Odyssey imaging system as we have previously described. As shown in Fig. 4A, PM PIP_2 detection in the entire 35-mm well area was reduced by 25% by both the chronic insulin exposure and the GlcN treatment and DON treatment prevented the insulin-induced PIP_2 loss.

Concomitant changes in the cortical F-actin immunofluorescent intensity were also detected by confocal imaging (**Fig. 13**, panels 11-15). In particular, microscopic analyses qualitatively revealed that cells treated overnight with 5 nM insulin or 2 mM GlcN displayed a reduction in F-actin (**Fig. 13**, panels 12 and 15). Also, in the presence of DON, this insulin-induced visualized loss of F-actin appeared to be reversed. To ensure the imaging of a comparable number of cells we co-stained nuclei with propidium iodine. As performed for the PIP_2 analyses, we also conducted three separate population-based assays where the F-actin immunofluorescent signal was quantitated on an entire 35-mm well area and normalized to nuclei. As shown in Fig. 14B, F-actin/nuclei detection was reduced by 15-25% by both overnight incubations (bars 1 and 4) and DON treatment prevented the insulin-induced F-actin loss (bar 2).
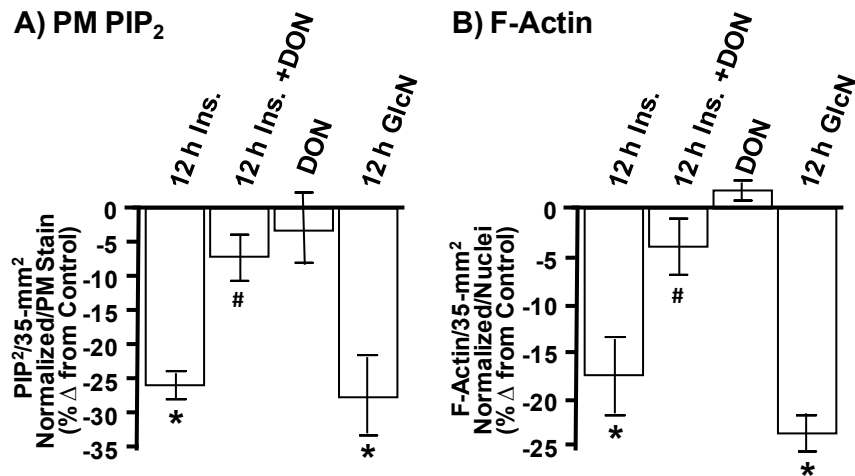
Fig. 14 Population-based LI-COR Odyssey analyses quantitate a loss in PM PIP$_2$ detection and cortical F-actin. For these analyses, PM sheets or cells on an entire 35-mm cell culture well were labeled as in Fig. 3 and the fluorescent signals in the entire well were quantitated using the LI-COR Odyssey system as described in Methods. PM PIP$_2$ **(A)** and F-actin **(B)** means ±S.E. from three independent experiments are shown. *(*, P < 0.05 vs. Control; #, P < 0.05 vs. 12 h Ins)*.

76

Both these microscopic field (**Fig. 13**) and separate 35-mm entire cell-well population-based (**Fig. 14**) analyses suggest the analogous changes in O-linked glycosylation (**Fig. 11**) and impairments in GLUT4 translocation/2-DG uptake (**Fig. 12**) induced by either 5 nM insulin or 2 mM GlcN result from a similar unappreciated HBP-coupled PIP_2/F-actin mechanism. Nevertheless work of Hresko *et al*. [147] underscores the importance of measuring intracellular ATP, because the use of GlcN can, under certain conditions, result in intracellular ATP depletion greater than that induced by insulin, and likely result in non-specific defects.

Consistent with our deliberate choice of a low concentration of GlcN with the omission of insulin in the medium, we found the loss of intracellular ATP in the GlcN treated cells (14.0±5.6%; *p*=0.042) to be similar to that induced by 5 nM insulin (10.4±3.4%; *p*=0.019) (**Fig. 15**, bars 1 and 2). Interestingly, although inosine prevented this loss of intracellular ATP (**Fig. 15A**, bars 3 and 4), it did not reverse the changes in O-linked glycosylation (*data not shown*), acute, insulin-stimulated PM GLUT4 (**Fig. 15B**)/WGA PM stain (*data not shown*), PIP_2/PM stain (*data not shown*), and F-actin/nuclei (*data not shown*) induced by these models.
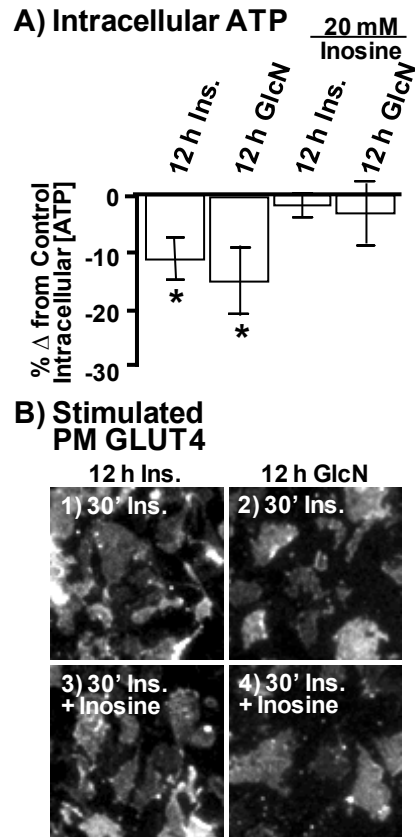
Fig. 15 Insulin and GlcN slightly deplete intracellular ATP to similar extents.
Following 36 h of incubation in DMEM containing 5.5 mM glucose, cells were left
untreated *(Control)* or treated overnight (12 h) with 5 nM insulin or 2 mM
glucosamine in the presence or absence of inosine. The percent changes of
intracellular ATP from control from three to eight separate experiments are
shown **(A)**. Values are means ± S.E. (*, P < 0.05*). Representative images of PM
sheet GLUT4 immunofluorescence from insulin-stimulated, insulin-resistant cells
from three separate experiments are shown **(B)**.

Exogenous PIP$_2$ Protects Against GlcN-Induced Loss of Cortical F-Actin and Insulin Action

It is of interest that experimental replenishment of PIP$_2$, as we previously reported [1, 41] or inhibition of GFAT with DON as we report here protects against insulin-induced insulin resistance. We reasoned that protection against GlcN-induced insulin resistance by PIP$_2$ replenishment would lend credence to a coupling between increased HBP activity and PIP$_2$/F-actin dysfunction. As we have established in several other studies [1, 41, 142, 148] histone-mediated delivery of 1.25 μM exogenous PIP$_2$ into cells displaying a 20-30% loss of immunodetectable PIP$_2$ effectively restores this lipid's PM content to that witnessed in control cells (**Figs. 16A and 16B**).
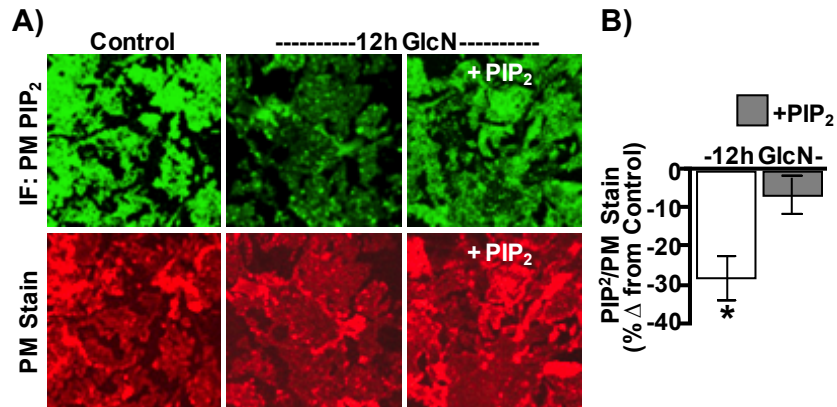
Fig. 16 PIP$_2$ addback restores GlcN-induced PIP$_2$ decrease. During the final 60 min of control or GlcN incubation, the medium was replaced with the same medium enriched with either histone H1 **(A, Panels 1, 2, 4, and 5)** or PIP$_2$/histone H1 **(A, Panels 3 and 6)**. Representative immunofluorescent images of PM PIP$_2$ **(A, Panels 1-3)** and WGA-stained PM **(A, Panels 4-6)**, and quantitation of PM PIP$_2$ **(B)** are shown. Images and means ± S.E. are from three to four independent experiments *(*, P < 0.05 vs. Control).*

This tactic concomitantly restored cortical F-actin structure (**Fig. 17A**) and insulin-stimulated GLUT4 translocation (**Figs. 17B and 17C**) in GlcN-induced insulin-resistant 3T3-L1 adipocytes [Note, WGA-labeling was performed but images are not shown. As performed above, the GLUT4 signal was normalized to the WGA PM stain, **Fig. 17C**]. To the best of our knowledge, this is the first time the negative effect of GlcN on insulin sensitivity has been experimentally eliminated.
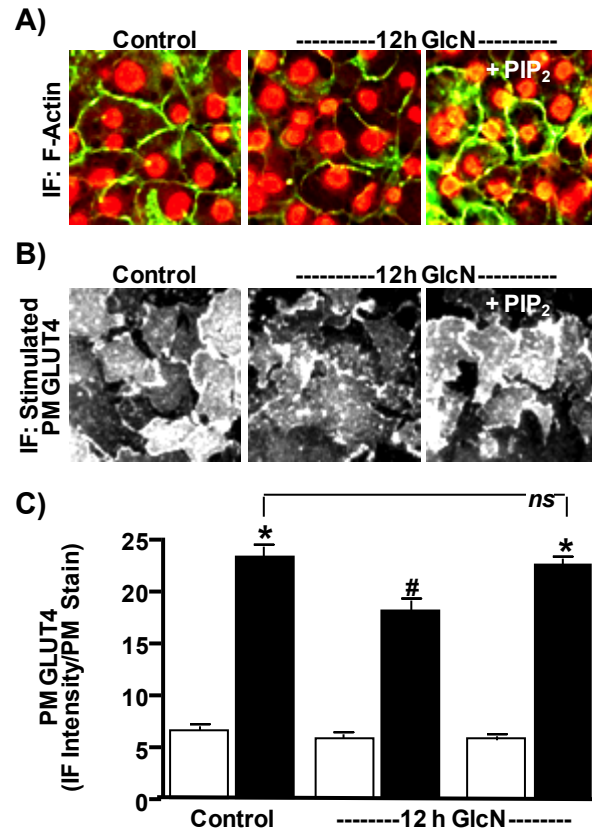
Fig. 17 PIP$_2$ replenishment protects against GlcN-induced F-actin loss and insulin resistance. Control and GlcN cells were treated with either histone H1 or PIP$_2$/histone H1 as described in Fig. 16. Phalloidin stained F-actin and propidium iodide stained nuclei in these cells **(A)**, insulin-stimulated PM GLUT4 images **(B)** and GLUT4 quantitation **(C)** are shown. All microscope and camera settings were identical between groups and representative images from three independent experiments are shown. Values are means ± S.E. from three to five independent experiments *(*, P < 0.05 vs. Control; #, P < 0.008 vs. 30' Ins).*

In line with these DON and GlcN data, GLUT4-eGFP expressing 3T3-L1 adipocytes co-overexpressing GFAT displayed a loss of plasma membrane PIP_2 compared to non-expressing neighboring cells (**Fig. 18**, panel 2). Co-expression of control empty vector had no effect on plasma membrane PIP_2 (**Fig. 18**, panel 1). Also, detected in these basal cells is the perinuclear localization of the eGFP-tagged transporter (**Fig. 18**, panels 1 and 2). Insulin-stimulated GLUT4-eGFP translocation to the plasma membrane was evident in empty vector expressing cells (**Fig. 18**, panel 3), but not in cells overexpressing GFAT (**Fig. 18**, panel 4). As we previously reported [142], acute insulin stimulation in control cells was associated with a slight, yet noticeable loss of PM PIP_2, reflecting the PI3K-induced conversion of that lipid substrate to phosphatidylinositol 3,4,5-trisphosphate (PIP_3).
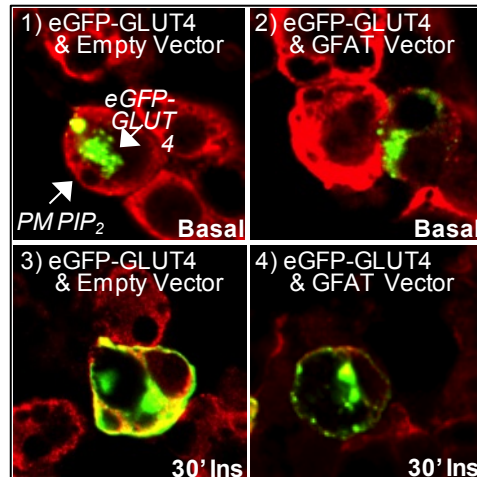
Fig. 18 Overexpression of GFAT reduces detectable cell-surface PIP$_2$ concomitant with a reduction in insulin-stimulated GLUT4–eGFP translocation. Differentiated 3T3-L1 adipocytes were electroporated with 50 µg GLUT4-eGFP cDNA and 200 µg GFAT cDNA empty vector or GFAT cDNA. The cells were allowed to recover for 16 h. Cells were subsequently incubated in serum-free medium for 2 h and then left untreated (Basal, Panels 1 and 2) or treated (30' Ins., Panels 3 and 4) with 100 nM insulin for 30 min. Cells were fixed, labeled for PIP$_2$, and subjected to confocal fluorescence microscopy. Representative images from 3 independent experiments are shown.

Glucose Challenge in the Absence of Insulin Negatively Impacts PM PIP$_2$/F-Actin Structure

Adipocyte studies presented up to this point utilized the conventional 3T3-L1 adipocyte differentiation protocol. This protocol calls for 25 mM glucose to be present at all stages of differentiation and culturing. As described in the *Materials and Methods* section, our 12 h Ins treatment took place during the last 12 h of a 48 h low glucose (5.5 mM) incubation. Work by Lin *et al*. [149] demonstrated that it is possible to propagate and differentiate 3T3-L1 cells at 5.5 mM glucose. An advantage to be understood further is that these "euglycemic" cultured cells are more insulin responsive. In accord, we observed that these cells displayed a robust labeling of PM PIP$_2$ that was decreased with exposure to 25 mM glucose medium for 16 h alone (**Fig. 19A**, compare panels 1 and 2). The same was true for cortical F-actin (**Fig. 19B**, compare panels 1 and 2). Also, we found that the 25 mM glucose challenge alone decreased insulin-regulated GLUT4 translocation (**Fig. 19C**, compare panels 1 and 2). A striking observation was the complete lack of cytoplasmic and PM *O*-GlcNAc immunofluoresence in the cells propagated, differentiated, and kept in 5.5 mM glucose (**Fig. 19D**, panel 1); whereas, cells cultured under the standard protocol (see **Fig. 11**, panel 1) or under euglycemic conditions and then exposed to 25 mM glucose overnight (**Fig. 19D**, panel 2) revealed comparable *O*-GlcNAc labeling. The effect of high glucose on PIP$_2$, F-actin, GLUT4, and *O*-GlcNAc were all inhibited by DON (Figs. **19A-D**, panel 3), supporting the negative contribution of flux through the HBP.

These data were normalized to WGA PM stain (PM PIP$_2$ and GLUT4) or area (F-actin and O-GlcNAc) and quantitated (**Fig. 19E**).
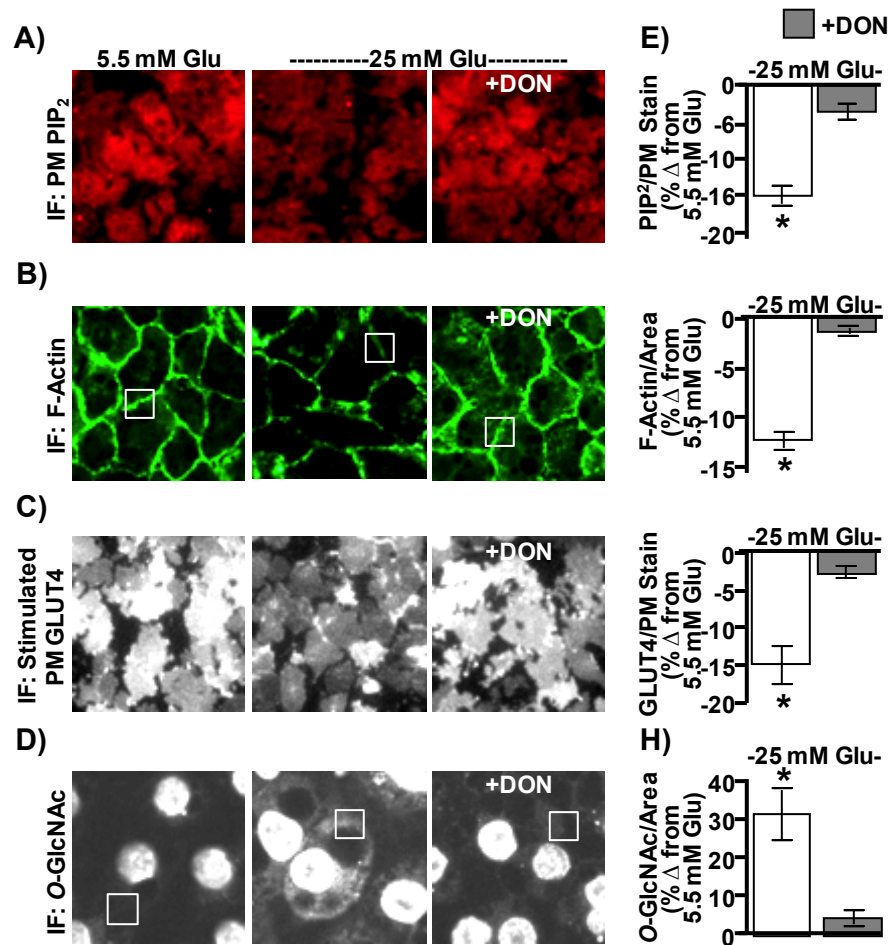
Fig. 19 High glucose alone induces PIP₂/F-actin loss and insulin resistance in 3T3-L1 adipocytes that were cultured and differentiated in 5.5 mM glucose. Murine 3T3-L1 preadipocytes cultured and differentiated in DMEM containing 5.5 mM glucose were left untreated (5.5mM Glu, Panel 1) or treated overnight (16 h) with 25 mM glucose (25 mM Glu, Panels 2 and 3) in the absence or presence of DON (Panel 3). PM PIP₂ **(A)**, F-actin **(B)**, insulin-stimulated PM GLUT4 **(C)**, and *O*-linked glycosylation **(D)** were determined and quantitated **(E)** as described in preceding Figs. All microscope and camera settings were identical between groups and representative images from three independent experiments are shown. Values are means ± S.E. from three independent experiments *(*, P < 0.05 vs. Control)*.

Chapter III

Perspectives
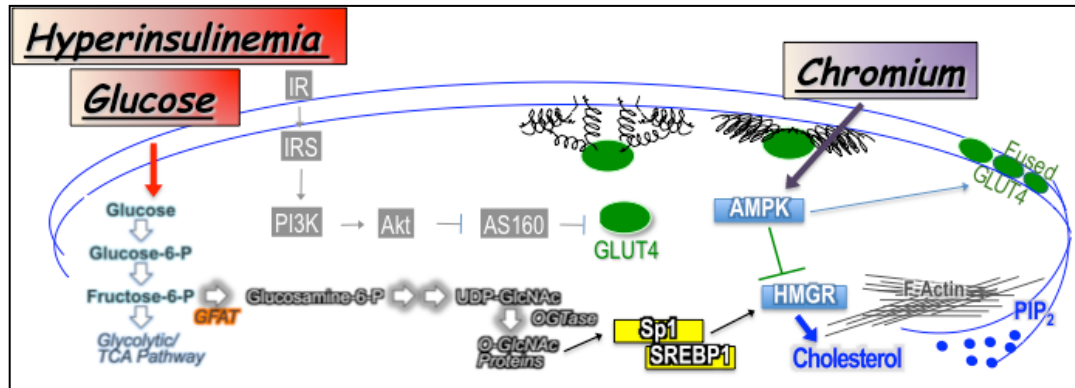
Mechanism(s) of Cholesterol-Based PM Architectural Changes in Insulin-Regulated GLUT4 Translocation

---

The studies presented in Chapter II exhibit the importance of membrane dynamics on glucose transport in both fat and skeletal muscle. Importantly, the previous studies highlight the essentiality of optimal PM cholesterol regulation on the cortical F-actin structure required for GLUT4 translocation. Perturbations in PM cholesterol amount, such as seen in states of hyperinsulinemia, disrupt insulin responsiveness without disturbing the propagation of intrinsic insulin signaling properties. Rather, we have observed that diabetogenic insults such as hyperinsulinemia and hyperlipidemia [150] redirect the utilization of intracellular glucose to the HBP. The notion of glucose toxicity as a mediator of insulin resistance stemmed from the studies designed to test the effects of CrPic on glucose transport. Interestingly, the evidence gleaned from that study

demonstrated that CrPic action was dependent on PM cholesterol accrual induced by conditions of excess glucose (hyperglycemia). This led to a set of studies which was presented in Chapter IIC distinctively placing the HBP as a mediator of insulin resistance in both adipocytes and skeletal muscle myotubes. A new joint project undertaken by Kirk Habegger, a recent graduate student in the laboratory, and myself focused on testing whether a mechanism existed in the development of membrane defects by HBP activation by either hyperinsulinemia or hyperlipidemia, particularly PM cholesterol accrual and F-actin loss. Preliminary data presented here place the HBP as a mediator of PM cholesterol accrual through transcriptional changes in cholesterogenic enzymes. In direct support of HBP activity and PM lipid coupling, PM prepared from treated 3T3-L1 adipocytes or L6 myotubes displayed an HBP-dependent increase in cholesterol content and impaired GLUT4 function (**Fig. 20**).
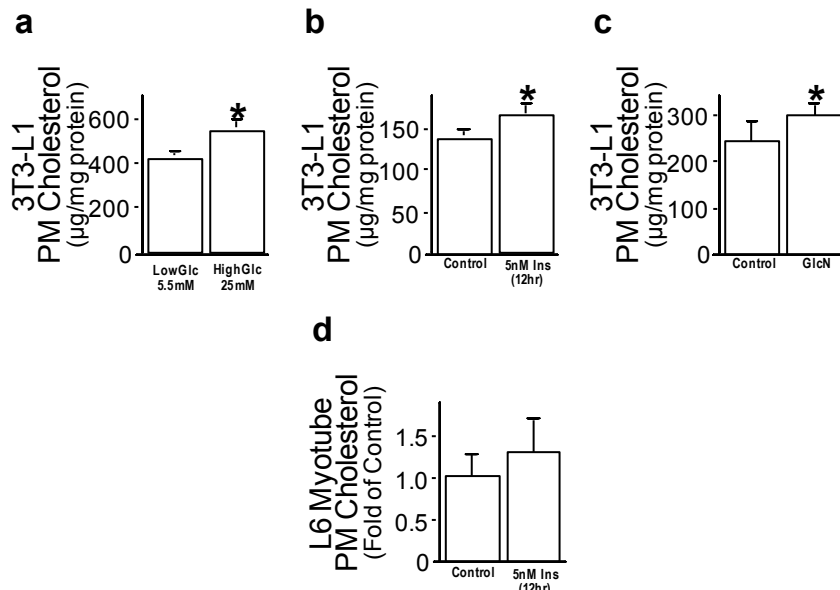
Fig. 20 Excess glucose flux results in PM cholesterol accrual. Plasma membrane fractions from hyperglycemia-, hyperinsulinemia-, and glucosamine-treated adipocytes as well as hyperinsulinemia- treated L6-GLUT4myc myotubes, exhibit increased cholesterol content. Values are means ± SE of membrane cholesterol. *(*, P < 0.05 vs. Control)*.

Furthermore, skeletal muscle removed from streptozotocin (STZ)-induced hyperglycemic C57Bl/6J mice showed an increase in PM cholesterol content (**Fig. 21A**). In both the cell culture and whole animal models, an HBP- and cholesterol-dependent loss of F-actin was evident (**Fig. 21B**).
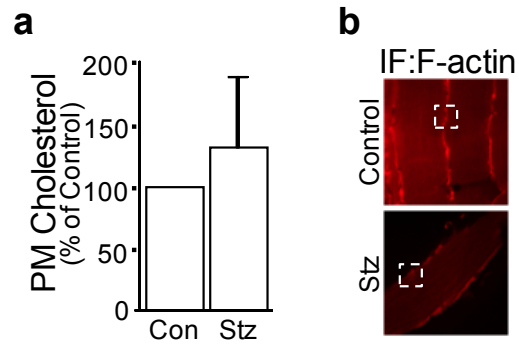
Fig. 21 Streptozotocin-induced hyperglycemic mice display increased membrane-associated defects. Skeletal muscle from STZ-treated mice demonstrated **(A)** increased PM cholesterol and **(B)** cortical F-actin loss.

As shown in Fig. 22, cells displaying HBP-induced PM cholesterol accrual, loss of actin filaments, and insulin resistance also demonstrated increased nuclear abundance of specificity protein, Sp1; sterol regulatory element binding protein (SREBP)-1; and NFY, transcription factors that regulate genes involved in cholesterol synthesis. Consistent with *O*-linked glycosylation of Sp1 participating in the maximal transcriptional activation of SREBP-1, this HBP-induced modification of Sp1 and upregulation of SREBP-1 gene products and rate-limiting enzyme in cholesterol synthesis, 3-hydroxy-3-methylglutaryl CoA reductase (*Hmgr*) was detected (**Fig. 22C**). These findings seem to causally link increased HBP activity to PM cholesterol accrual and cortical F-actin loss that compromises the efficient regulation of GLUT4 by insulin.

a. 3T3-L1
IB: Sp1

90 kDa

Control   12 h Ins

IB: SREBP-1

68 kDa

Control   12 h Ins

IB: NFY

40 kDa

Control   12 h Ins

b. 3T3-L1
IP: Sp1
IB: RL2

90 kDa

5.5mM   25mM

IB: HMGR

90 kDa

5.5mM   25mM

c. 3T3-L1

Relative *Hmgr* Expression (fold of control)

4.0
3.0
2.0
1.0
0.0

Con   12 hr Ins
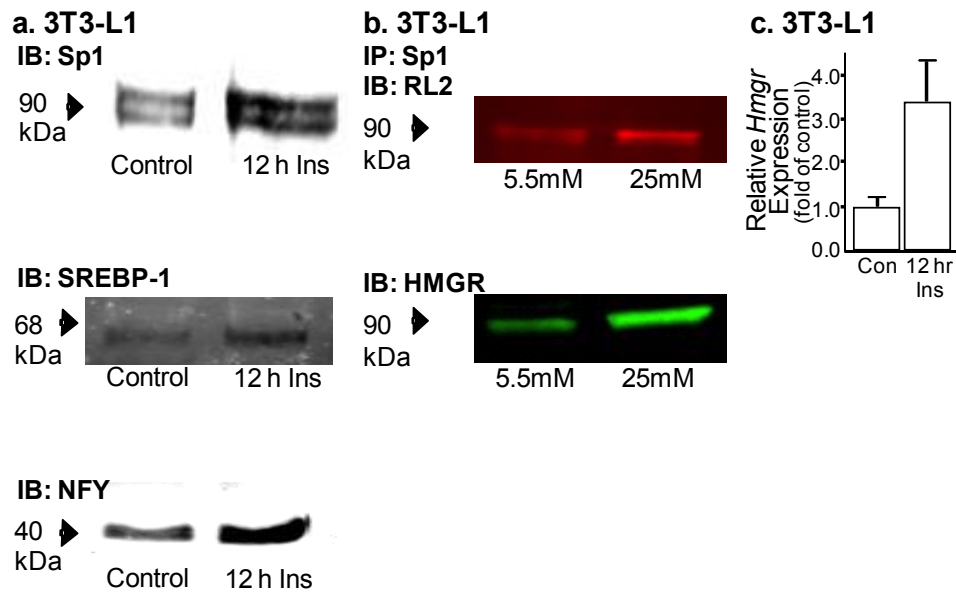
Fig. 22 Nuclear extracts from hyperinsulinemia- and hyperglycemia-treated adipocytes demonstrate a cholesterogenic response. (A) Nuclear fractions reveal an increase in Sp1, SREBP-1, and NFY in 3T3-L1 adipocytes cultured in hyperinsulinemic conditions. **(B)** O-linked glycosylation of Sp1 is elevated in 3T3-L1 adipocytes cultured in hyperglycemic conditions and this corresponds to an increase in HMGR protein. **(C)** Hyperinsulinemic 3T3-L1 adipocytes display elevated *Hmgr* expression. Values are means ± SE of fold *Hmgr* expression from control. *(*, P < 0.05 vs. Control).*

In order to firmly place the HBP at the crux of accumulating PM cholesterol and development of insulin resistance, we utilized the well-characterized L6-GLUT4myc cell culture system, that has been previously shown to develop insulin resistance by hyperinsulinemia [1], to genetically manipulate a component of the HBP. Utilizing siRNA technology, we were successfully able to knockdown OGT ~95% (**Fig. 23,** A and B). As shown in Fig. 23C, the knockdown of this protein led to a global decrease in *O*-linked glycosylation of these myotubes. Preliminarily, stimulators such as hyperinsulinemia and palmitate were ineffective in further increasing RL2 labeling. Further parameters important in GLUT4 translocation were tested which included PM cholesterol, F-actin structure, and *Hmgr* mRNA expression. Preliminary data with siOGT myotubes demonstrated that PM cholesterol accrual was sufficiently prevented in hyperinsulinemic cells that were lacking OGT (**Fig. 23E**). An interesting observation that we noted was that siOGT controls exhibited increased PM cholesterol compared to siScramble cells. However, more replicates will be needed to confirm this. Concomitant with this prevention of accumulation of PM cholesterol due to hyperinsulinemia, expression of *Hmgr* mRNA was unchanged in siOGT myotubes treated with hyperinsulinemia compared to its relative control (**Fig. 23G**). This was in direct contrast to hyperinsulinemia-treated siScramble myotubes with increased *Hmgr* expression compared to its relative control. Additionally, the distal F-actin disturbances were ablated in siOGT myotubes treated with hyperinsulinemia. Hyperlipidemia, which has been shown by many groups including ours [150, 151], to be a potent stimulator of HBP activity also caused PM cholesterol

accrual and defects in cortical F-actin structure necessary for GLUT4

translocation. Knocking down OGT in these cells also prevented the

dysregulation of PM cholesterol and cortical F-actin induced by palmitate

treatments (**Fig. 23**, D and F). Taken together, these preliminary data offer some

exciting evidence that these diabetogenic insults mediate insulin resistance

through disturbances seen at the PM via an HBP-mediated glycosylation events

that when inhibited protected the cell from developing insulin resistance and

glucose transport abnormalities.
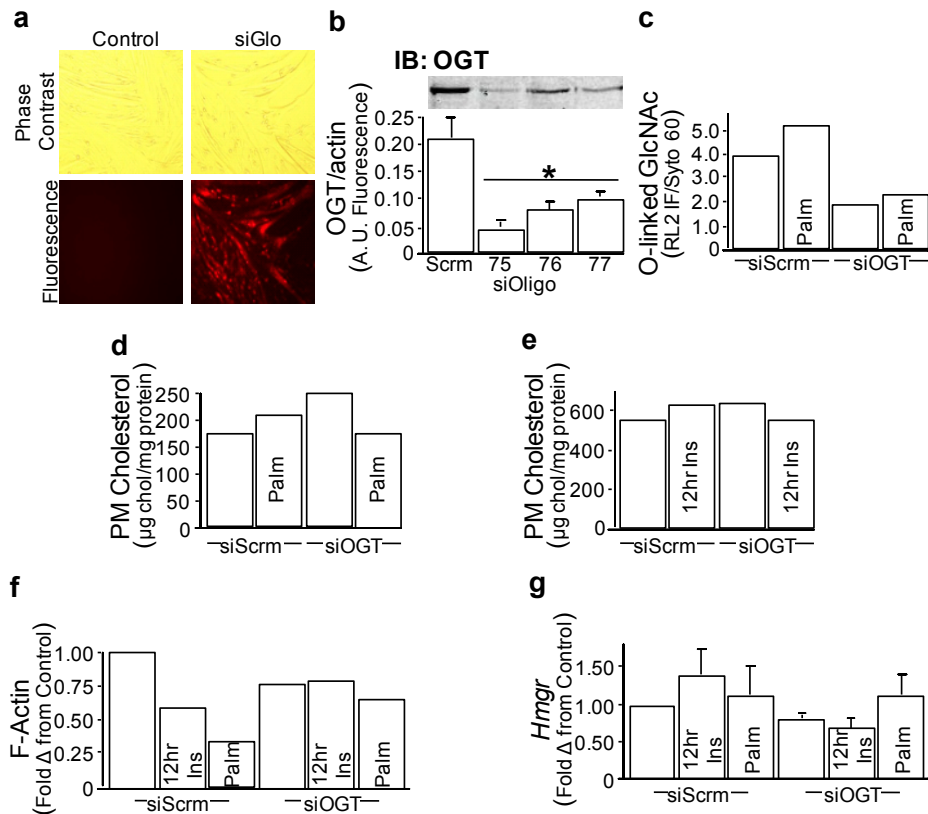
Fig. 23 siRNA-mediated knockdown of O-Glycosyltransferase (OGT) in L6-GLUT4myc myotubes. (A) Calcium-phosphate based transfection of L6-GLUT4myc myotubes with siGlo oligos revealed sufficient transfection efficiency. **(B)** siRNA-mediated knockdown of OGT revealed ~95% knockdown efficiency with oligo 75. **(C)** O-linked GlcNAc of palmitate-treated siOGT myotubes. **(D & E)** PM cholesterol in palmitate- and hyperinsulinemia-treated siOGT myotubes. **(F)** F-actin and **(G)** *Hmgr* expression in palmitate- and hyperinsulinemia-treated siOGT myotubes Values are means ± SE. *(*, P < 0.05 vs. Scramble [Scrm] Control)*.

Another interesting observation made during the course of these thesis studies is that CrPic action on reducing PM cholesterol may be attributed to a protein that is important in the energy regulation of a cell, 5'-AMP activated protein kinase (AMPK). When active, the responsibility of AMPK is to conserve energy for the cell by inhibiting energy-consuming reactions such as fatty acid/sterol synthesis via phosphorylation. Previous studies have demonstrated that AMPK activation occurs in response to physiologic exercise training [58] and the first-line antidiabetic medication, metformin [152]. Yet, its role in adipocytes was still controversial and undetermined [91]. As previously mentioned, AMPK is able to inhibit cellular cholesterol synthesis by phosphorylation of HMGR. Preliminary data presented here exhibit that CrPic activated AMPK as evidenced by phosphorylation of AMPK on its Threonine 172 residue (**Fig. 24A**), which has been implicated in the activation of the kinase. Consistent with AMPK activation occurring due to CrPic, we found increased phosphorylation on Acetyl-CoA carboxylase (ACC), a downstream substrate of AMPK (**Fig. 24C**). Using an antibody specific to a phosphorylation target of HMGR by AMPK, we observed that adipocytes, in response to CrPic, displayed increased phosphorylation on this serine residue targeted by AMPK. AICAR, an AMP analog that activates AMPK by directly interacting with its allosteric site [153], showed a similar increase in phosphorylation of HMGR (**Fig. 25**).

A) IB: P-AMPK-α (Thr172)

62 kDa ➡

    0   0.5   1.0   4.0   16.0

CrPic (hr)

B) IB: AMPK-α

62 kDa ➡

    0   0.5   1.0   4.0   16.0

C) IB: P-ACC (Ser79)

280 kDa ➡
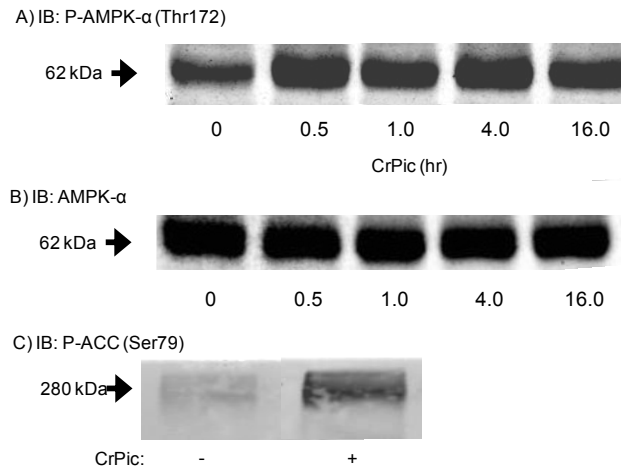
CrPic: -   +

Fig. 24 CrPic stimulates phosphorylation and activation of AMPK. (A) CrPic-treated adipocytes displayed early and sustained phosphorylation of AMPK. **(B)** CrPic had no effect on the level of total AMPK. **(C)** Treating adipocytes for 16 h with CrPic resulted in increased phosphorylation of a downstream target of AMPK, Acetyl-CoA Carboxlase.

A) IB: P-HMGR (Ser871)

90 kDa

CrPic: -   +   AICAR

B) IB: HMGR

90 kDa

CrPic: -   +   AICAR
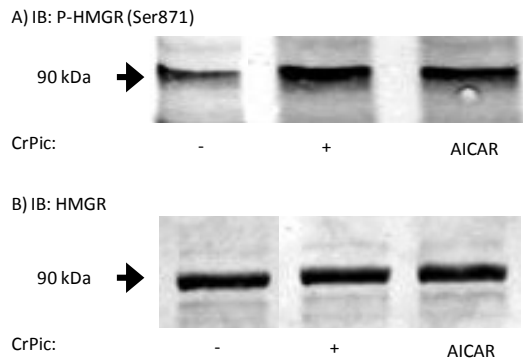
Fig. 25 CrPic induced phosphorylation of HMGR similar to that a known AMPK activator, AICAR. (A) Using a phospho-specific antibody to HMGR that recognized phosphorylation by AMPK, 16 h CrPic treatment stimulated HMGR phosphorylation. **(B)** AICAR, used as a positive control, caused a similar increase in HMGR phosphorylation. Total HMGR was unaffected by CrPic or AICAR.

Pilot studies examining the mechanism by which CrPic activates AMPK are currently being pursued. However, evidence from CrPic-treated 3T3-L1 adipocytes does not display a loss of ATP compared to that of control adipocytes suggesting that CrPic action is not dependent on an increase in the AMP:ATP ratio (**Fig. 26**). Other mechanisms by which CrPic may activate AMPK are being investigated. These mechanisms in question include LKB1, a upstream kinase known to phosphorylate AMPK on its Thr172 residue; Calcium (Ca^{2+})/Calmodulin-dependent Protein Kinase Kinase 2 (CaMKK2) protein, another protein that targets AMPK phosphorylation on its Thr172 residue; and decreased activity of Protein Phosphatase 2C (PP2C), a protein that dephosphorylates and inactivates AMPK. These three upstream activators/deactivators of AMPK regulation may play a key role in CrPic action on glucose transport and further explain the benefits of CrPic seen in hyperglycemic adipocytes. Taken together, these preliminary data offer a potentially exciting new stimulator of AMPK by an inexpensive, readily available supplement. Much like the mechanism responsible for exercise-induced benefits on glucose transport, activating AMPK via easy lifestyle modifications such as increased supplementation with CrPic may prove to be a worthwhile therapy for diabetic individuals.
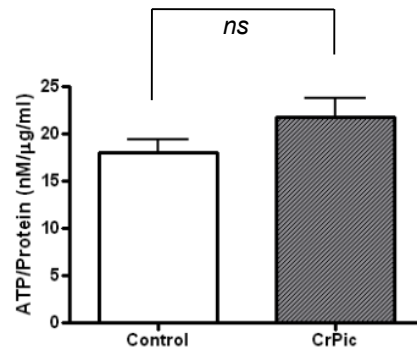
Fig. 26 ATP amount unchanged when adipocytes were treated with CrPic.
3T3-L1 adipocytes treated with 10 nM CrPic (16 h) demonstrated no change in ATP levels compared to control (*white bar*).

Although careful longitudinal study is required to test whether these membrane/cytoskeletal defects precede documented signaling defects *in vivo*, several cross-sectional studies from other groups demonstrate a clear association between excess glucose and membrane/cytoskeletal disorganization. For example, isolated neutrophils from patients with type 2 diabetes display decreased actin polymerization compared to neutrophils from non-diabetic control subjects [154, 155]. This impairment is associated with persistent expression of the endothelial adhering β_2 integrin CD11b/CD18, potentially exacerbating vascular dysfunction in diabetic patients. Also, diabetic retinal endothelial cells have a prominent reduction in F-actin integrity, a finding closely linked to vascular leakage [156]. Loss of rat mesangial cell F-actin has also been reported after exposure to early-diabetic state conditions [157, 158], possibly causing diabetic hyperfiltration. Further human support has been derived from collected erythrocytes from overweight insulin-resistant individuals showing marked changes in the phospholipid composition of the PM [159, 160], some of which may directly affect the actin cytoskeleton. Current animal studies are underway to test these findings *in vivo*. In direct support of our findings, we have observed that epitrochlearis skeletal muscle from insulin-resistant, hyperinsulinemic Zucker fatty rats display a loss of F-actin structure compared to that in muscle from lean insulin-sensitive littermates [1]. Together, these human and animal observations highlight that F-actin integrity is potentially influenced by the glycemic state.

In line with the preliminary data identifying glucose flux through the HBP as a stimulator of cholesterol accrual, Yang *et al*. recently observed that OGT overexpression increased hepatic cholesterol content [161]. It is important to note that those recent studies by Yang *et al*. show that OGT has a phosphoinositide-binding domain, and after insulin stimulation PIP_3 recruits OGT from the nucleus to the PM, where this enzyme catalyzes dynamic modification of the insulin signaling pathway by O-GlcNAc [161]. These signaling events target specific residues on the IRS-1 and Akt proteins (*e.g.,* phosphorylation of Akt on threonine 308, but not serine 473, is decreased). Although we have not witnessed changes in signaling, we have not specifically monitored phosphorylation of threonine 308. In another recent article Dentin *et al.* report that the transcriptional regulatory protein called transducer of regulated cAMP response element-binding protein 2 (TORC2, also known as CRTC2 [162]) is a target of *O*-linked glycosylation. The modification of CRTC2 activates glucose production in the liver and is an example of a mechanism by which glucose serves a signaling function in controlling a process, in this case, metabolism in the liver. Studies we are currently conducting are addressing the possibility that increased HBP activity negatively impacts PIP_2/F-actin structure essential for insulin-regulated GLUT4 translocation and glucose transport via increasing cellular cholesterol synthesis and PM cholesterol accrual.

Various nutritional components of the diabetic milieu - including excess insulin, glucose, and lipids - all resulted in an accumulation of PM cholesterol in

both 3T3-L1 adipocytes and L6 myotubes in this study. New work from our

laboratory also demonstrated that incubating L6 myotubes with a physiologic

dose of palmitate resulted in a substantial increase in cellular O-linked

glycosylation. Further, palmitate-treated myotubes exhibited increased PM

cholesterol, decreased cortical F-actin, and a loss of insulin responsiveness as

assessed by GLUT4 translocation and glucose transport [150]. These findings

are supported by preliminary data generated by Kirk Habegger where L6

myotubes simply overexpressing GFAT displayed a trend towards an increase in

O-linked glycosylation (31±17% p=0.21) while demonstrating a reciprocal loss of

cortical F-actin (48±25% p=0.20) (data not shown). Further evidence for the role

of HBP in the development of insulin resistance is offered by other groups. Arias

et al. concluded that increased O-linked glycosylation by inhibiting O-GlcNAcase,

an enzyme that catalyzes the removal of O-GlcNAc from proteins, induces insulin

resistance in rat epitrochlearis muscle. Interestingly and consistent with data

generated from our laboratory, this insulin resistance was independent of insulin

signaling defects as assessed by normal phosphorylation of Akt, GSK3α,

GSK3β, and AS160 [77]. Further evidence regarding the importance of HBP on

the progression of diabetes is present in that the intramuscular content of UDP-

GlcNAc is increased in diabetic mice [163, 164]. McClain *et al.* have

demonstrated that increased hexosamine flux in adipocytes from GFAT

overexpressing mice resulted in skeletal muscle insulin resistance and altered

regulation of leptin and adiponectin. Additionally, adipocytes overexpressing

GFAT from these transgenic mice were associated with an increase in total lipid

synthesis consistent with data that increased hexosamine flux is associated lipogenic processes [165]. Similarly, treating C2C12 myoblasts with glucosamine resulted in lipid accumulation due to transcriptional changes and mRNA expression levels, including an increase in SREBP-1c [166]. SREBP-1c is encoded from the SREBP-1 gene that also encodes an almost identical protein, SREBP-1a. Interestingly, preliminary data presented in this section are consistent with increased flux through the HBP stimulating lipogenic gene expression including an upregulation of *Hmgr* mRNA in both hyperinsulinemia- and palmitate-treated adipocytes and myotubes. SREBP-1 has been shown play an active role in transcriptional regulation of FA synthesis and albeit, to a lesser extent, regulation of cholesterol synthesis genes [79]. Our data in both 3T3-L1 adipocytes and L6 myotubes are consistent with a transcriptional increase in cholesterogenic genes in the development of insulin resistance.

Although this data is still preliminary, these findings highlight an importance of HBP-mediated membrane disturbances in the development of insulin resistance that may be reversible and offer exciting new therapies to slow the progression/worsening of insulin resistance. Future studies in the laboratory are directed at understanding the possible reversibility of this insulin resistance through PM cholesterol depletion as well as further understanding the molecular role of *O*-linked glycosylation modifications on gene transcription involved in lipogenesis and glucose transport.

As has been previously discussed, the beginning of these thesis studies had an interest in understanding the development of insulin resistance and progression to diabetes, I also was very interested in understanding a therapy that could benefit insulin action/glucose metabolism. Interestingly, recent work in the laboratory demonstrated the importance of the essential nutrient chromium on membrane properties, particularly depleting PM cholesterol, enhancing glucose transport in 3T3-L1 adipocytes [57]. In particular, our studies show that CrPic recruits intracellular GLUT4 to an area adjacent to the PM. In the presence of insulin, these juxtaposed transporters become functional by fusing into the PM and enhancing insulin-stimulated glucose transport. Recent clinical data is consistent with the theory that Cr^{3+} supplements, especially CrPic, enhance the metabolic action of insulin and lower certain risk factors for cardiovascular disease that are influenced by cellular cholesterol homeostasis. For example, several randomized, placebo-controlled, double blind clinical tirals, found supplementation with CrPic (200-1000 µg Cr/day) decreased total cholestrol and/or low density lipoprotein (LDL) cholesterol [167-169]. Interestingly, data from our laboratory has shown that the benefits experienced by CrPic treatments are dependent on the metabolic status of cells. In particular adipocytes that were in the presence of 25 mM glucose only benefited from CrPic whereas adipocytes that were in 5.5 mM glucose, a concentration akin to a euglycemic individual, did not experience an enhancement in glucose transport. Concomitant with this discrepancy in CrPic-mediated events on glucose transport between hyperglycemic and euglycemic cells, reduction of PM cholesterol by CrPic

occurred in adipocytes incubated in 25 mM glucose conditions only. Taken together, these data are consistent with CrPic action on glucose transport being dependent on PM cholesterol lowering. Further evidence for the necessary role of cholesterol reduction by CrPic in enhancing glucose transport was demonstrated by the addback of exogenous cholesterol in CrPic-treated cells preventing the beneficial effect of CrPic on both GLUT4 mobilization and insulin-stimulated glucose transport. An exciting prediction from these findings is that Cr^{3+} supplementation may lower blood glucose by altering the PM composition of cholesterol and F-actin, important in GLUT4 translocation, in fat and skeletal muscle cells. However, since Cr^{3+} supplementation has the greatest benefit in overweight, insulin-resistant individuals, a presumption also has to be that cells from these individuals possess cholesterol-laden plasma membranes. In contrast, the PM cholesterol content of cells from non-diabetic subjects with normal insulin sensitivity and glucose tolerance would be lower and not be affected by Cr^{3+}. Recent evidence from our laboratory is consistent with a cholesterol component of glucose intolerance clinically in that human skeletal muscle biopsies revealed an inverse correlation between membrane cholesterol and whole-body glucose disposal [150]. Taken together, these data demonstrate an importance for the role of PM cholesterol lowering in antidiabetic interventions, such as CrPic supplementation.

Studies were also undertaken to dissect a mechanistic basis for the PM modifications seen in the enhancement of glucose transport by CrPic. Although

the actions of AMPK are still imperfectly understood, the role of this protein in the enhancement of both basal and insulin-stimulated glucose transport has been well documented. Additionally, the ability of AMPK to inactivate energy consuming pathways (*i.e.* fatty acid and sterol synthesis) has been implicated in slowing down diabetes progression. In particular, the role of an activated AMPK on inhibiting cholesterol synthesis via phosphorylation of HMGR, the rate-limiting enzyme, was an attractive concept. Interestingly, data that we and others have now generated has firmly placed AMPK as a mediator of Cr^{3+}-containing supplements on glucose transport. Recent evidence from our laboratory has shown that direct AMPK activation with 5-aminoimidazole-4-carboxamide-1-beta-D-ribonucleoside (AICAR) or 2,4-dinitrophenol (DNP) in L6 myotubes [58] can acutely and chronically affect basal and insulin-regulated glucose transport, similar to that experienced by CrPic. Downstream targets of AMPK, including acetyl-CoA carboxylase (ACC) and HMGR, bears significant merit as both can affect glucose transport. ACC catalyzes the conversion of acetyl CoA to malonyl CoA, an inhibitor of translocation of long chain fatty acyl (LCFA) groups from the cytosol to the mitochondrial matrix for fatty acid oxidation. Inactivation of ACC by AMPK in insulin-resistant skeletal muscle would be predicted to decrease excess FAs and several metabolites including acyl-CoAs, ceramides, and diacylglycerol that activate kinases (*e.g. PKC, JNK, IKKβ*) that are detrimental to insulin action via increasing the inhibitory serine phosphorylation of insulin signaling cascade [170-172] perhaps providing an explanation to the beneficial effects of Cr^{3+} on insulin signaling. Study by Zhao *et al.* showed that activation of AMPK by Cr(D-

Phe)$_3$ in H9c2 myoblasts [173]. This activation of AMPK in this skeletal muscle cell line sufficiently stimulated glucose transport. Importantly, when AMPK activity was pharmacologically inhibited, the enhanced glucose uptake was blocked. Another study performed in 3T3-L1 adipocytes revealed that AMPK activation by Cr^{3+} decreased secretion of resistin, an adipokine associated with impaired glucose transport [174]. All these data taken together, the proposed mechanism that AMPK activity is being increased by Cr^{3+} may be a feasible explanation for the multiple actions in both relieving glucose and lipid disorders in metabolically challenged individuals.

Taken together, the published and preliminary work presented in these thesis studies have demonstrated that insulin resistance, as a result of HBP activation, impairs PIP$_2$ regulation of F-actin which when corrected protects against the insulin resistance. Consistent with these findings, we have also observed that the PIP$_2$/F-actin impairment is accompanied by a possible HBP-mediated increase in PM cholesterol. Correction of this increase in PM cholesterol with various cholesterol-lowering strategies, particularly the use of chromium, enhances insulin-stimulated glucose transport. In contrast to downregulation of insulin signal transduction observed in other studies, we have found that proximal insulin signaling is still intact yet these membrane-associated parameters account for alterations in insulin action.

Chapter IV

Experimental Procedures

1. Materials

Murine 3T3-L1 preadipocytes were purchased from American Type Culture Collection (Manassas, VA). Dulbecco's modified Eagle's medium (DMEM) was from Invitrogen. Fetal bovine serum and bovine calf serum were obtained from Hyclone Laboratories Inc. (Logan, UT). Polyclonal rabbit caveolin-1 and polyclonal goat GLUT4 antibodies were purchased from Santa Cruz Biotechnology Inc. (Santa Cruz, CA). Monoclonal mouse phosphatidylinositol 4,5-bisphosphate antibody and phosphatidylinositol 3,4,5-trisphosphate antibody were purchased from Assay Designs Inc. (Ann Arbor, MI). Anti-phospho-AMPK (Thr172), anti-phospho-ACC (Ser79), and anti-AMPK was from Cell Signaling (Danvers, MA). Anti-HMGR and anti-ACC were from Millipore (Temecula, CA). Anti-phospho-HMGR (Ser 879) was from Kinasource (Scotland, UK). Anti-ABCA1 antibody was from Novus Biologicals (Littleton, CO). Anti-β-actin antibody was from Cytoskeleton (Denver, CO). Anti-SREBP-1, anti-SREBP-2, anti-NFY, anti-Sp1, anti-Lamin B were purchased from Santa Cruz Biotechnology (Santa Cruz, CA). Monoclonal mouse GLUT4 antibody was purchased from Biogenesis (Kingston, NH). Near-infrared IR-dye 800- and 700-conjugated anti-mouse IgG secondary antibodies were purchased from LI-COR Biosciences (Lincoln, NE) or Rockland (Gilbertsville, PA). Amplex Red Cholesterol Assay Kit was purchased from Molecular Probes (Eugene, OR). Rhodamine red-X/FITC-

conjugated donkey anti-rabbit or goat anti-mouse antibodies were from Jackson

Immunoresearch Inc. (West Grove, PA). Fatty acid free BSA was from MP

Biomedicals (Solon, OH). Unless indicated, all other chemicals and used were

from Sigma.

2. Cell culture and treatments

3T3-L1 adipocyte culture and induction of insulin resistance.

Preadipocytes were cultured and differentiated as described previously [56]. All

studies were performed on cells which were between 8 and 12 days post-

differentiation. Insulin resistance was induced by incubating cells with 5 nM

insulin for 12 h or DMEM containing 10% FBS and 2 mM GlcN for 12 h, in the

absence of glucose, glutamine, and insulin (hereafter referred to as 12 h GlcN).

Acute insulin stimulation was achieved by spiking the cells with 100 nM insulin

during the last 30 min of incubation. βCD was used to remove (2.5 mM βCD) or

add (1 mM-5 mM βCD loaded with cholesterol) cholesterol as previously

described [56] for 30 min prior to insulin stimulation. Adipocytes were also

cultured in DMEM/10% fetal bovine serum growth medium containing either 5.5

or 25 mM glucose for 48 h before the experimental treatment. Cells were treated

with serum-free DMEM with or without 10 nM CrPic (Nutrition 21, Purchase, NY)

for 16 hours.

L6-GLUT4myc culture and induction of insulin resistance. Rat L6-

GLUT4myc (generously obtained from Dr. Amira Klip, The Hospital for Sick

Children, Toronto, Canada) were cultured as previously described [1]. Myoblasts

were maintained in α-Minimum essential medium (α-MEM) containing 5 mM glucose and 10% fetal bovine serum (FBS; HyClone Laboratories, Grand Island, NY), and differentiated into multinucleated myotubes with 2% FBS. All studies used myotubes between 4 and 6 days post-initiation of differentiation. Hyperinsulinemia induction of insulin resistance was performed by treating cells with 5 nM insulin for 12 hr in DMEM supplemented with 1%FBS.

3. Plasma membrane sheet assay

Preparation of plasma membrane sheets from the adipocytes was performed as previously described [56]. After the isolation of plasma membrane sheets, these purified membranes were used for immunofluorescence. The sheets were fixed for 20 min at 25°C in a solution containing 2% paraformaldehyde, 70 mM KCl, 30 mM HEPES, pH 7.5, 5 mM $MgCl_2$ and 3 mM EGTA. The sheets were then blocked in 5% milk or Odyssey Blocking Buffer (LI-COR, Lincoln NE) for 60 min at 25°C and incubated overnight at 4°C with a 1:1000 dilution of monoclonal GLUT4 antibody, followed by incubation with a 1:100 dilution of IR-dye-800-conjugated anti-mouse IgG secondary antibody for 60 min at 25°C. The amount of glucose transporter on the plasma membrane was quantitated by digital image processing as described previously [142, 175].

4. Subcellular fractionation

3T3-L1 Adipocyte Fractionation. Adipocyte subcellular fractions were obtained using the differential centrifugation method previously described [176]

with slight modification. Briefly, control and experimentally-treated 3T3-L1 adipocytes were washed and resuspended in HES buffer (20 mM HEPES, pH 7.4, 1 mM EDTA and 255 mM sucrose containing 1 mM PMSF, 10 µg/ml pepstatin, 10 µg/ml aprotinin, and 5 µg/ml leupeptin). Cell lysates were prepared by shearing the cells through a 22-gauge needle 10 times. Lysates were then centrifuged at 19,000 x g for 20 min at 4°C. The intracellular membrane pellet was obtained by centrifugation of the resulting supernatant at 180,000 x g for 75 min at 4°C. The plasma membrane pellet was obtained by resuspending the pellet from the initial 19,000 x g centrifugation in HES buffer followed by layering onto a 1.12 M sucrose cushion for centrifugation at 100,000 x g for 60 min. The plasma membrane layer was removed from the sucrose cushion and centrifuged at 40,000 x g for 20 min. All pelleted fractions were resuspended in a detergent-containing lysis buffer and assayed for soluble protein content.

L6-GLUT4myc Fractionation. Crude plasma membrane fractions were obtained using a differential centrifugation method as detailed by Khayat *et al.* [177], with slight modifications. Briefly, skeletal muscle or L6-GLUT4myc myotubes were washed, resuspended in HES buffer (20 mM HEPES, pH 7.4, 1 mM EDTA, and 255 mM sucrose containing 1 mM phenylmethylsulfonyl fluoride (PMSF), 10 µg/ml pepstatin, 10 µg/ml aprotinin, and 5 µg/ml leupeptin), and processed by polytron homogenization (15 s) or shearing the sample through a 22-gauge needle 10 times, respectively. Lysates were then centrifuged at 5,000 ×g for 20 min at 4°C. The supernatant was subjected to centrifugation at 100,000

114

×g for 30 min. The pellet was resuspended in HES buffer and assayed for protein (Bradford) and cholesterol (Amplex Red) content as previously described [178]

5. Glucose transport assay

3T3-L1 adipocytes were either untreated or stimulated with 100 nM insulin for 30 min and exposed to 50 μM 2-deoxyglucose containing 0.5 μCi of 2-[^{3}H] deoxyglucose in the absence or presence of 20 μM cytochalasin B. Glucose transport was determined as previously described [41].

6. Preparation of cell lysates and immunoblotting

Cell lysates were prepared from 100-mm plates of 3T3-L1 adipocytes following the appropriate treatments. Cells from each plate were washed two times with ice-cold PBS and scraped into 1 ml of lysis buffer (25 mM Tris, pH 7.4, 50 mM NaF, 10 mM Na$_3$PO$_2$O$_7$, 137 mM NaCl, 10% glycerol, and 1% Nonidet P-40) containing 2 mM phenylmethylsulfonyl fluoride, 2 mM Na$_3$VO$_4$, 5 μg/ml aprotinin, 10 μM leupeptin, and 1 μM pepstatin A, then rotated for 15 min at 4°C. Insoluble material was separated from the soluble extract by microcentrifugation for 15 min at 4°C. To assess whole cell GLUT4 content, crude cellular membrane was prepared as previously described [57]. To ensure equal loading, protein concentrations were determined by the Bradford method and equivalent protein amounts of each sample were loaded onto an acrylamide gel. Samples were subjected directly to SDS-PAGE, as described below.

7. Preparation of nuclear extracts

Nuclear extracts were collected as previously described [179]. Briefly, 3T3-L1 adipocytes were washed with PBS and 2 ml of hypotonic buffer (10 mM HEPES, pH 7.4, 10 mM KCl, 1.5 mM MgCl2, 1 mM DTT containing 20 mM leupeptin, 2 mM pepstatin, 2 mM aprotinin and 0.5 M PMSF). Cell lysates were prepared by shearing the cells through a 22-gauge needle 5 times. Prepared lysates were centrifuged at 800 g for 10 min at 4°C. The pellet was then carefully dried and resuspended in 0.5 ml of buffer C (10 mM HEPES, pH 7.4, 0.42 M NaCl, 25% glycerol (v/v), 1.5 mM MgCl2, 0.5 mM EDTA containing 20 mM leupeptin, 2 mM pepstatin, 2 mM aprotinin and 0.5 M PMSF). Nuclei were then visualized by staining with 0.2% trypan blue. Proteins were allowed to swell out of the nuclei by vortexing for 15 s every 10 min for 40 min. The mixture was then centrifuged at full speed in a microcentrifuge at 4°C for 15 min. Supernatant was collected and assayed for soluble protein content.

8. Electrophoresis and immunoblot analysis

Cell lysate fractions were separated by 10% SDS-PAGE (GLUT4) or 7.5% SDS-PAGE and the resolved fractions were transferred to nitrocellulose membrane (Bio-Rad, Hercules, CA). Proteins were immunoblotted with either a phospho-specific Akt, p-AMPK, p-ACC, SREBP-1, NFY, Sp1, RL-2, or β-actin antibody. Equal protein loading was confirmed by Ponceau staining and by immunoblot analysis for β-actin, Caveolin-1, or Lamin B for nuclear extracts. All immunoblots were analyzed via LI-COR quantification.

9. PM & Actin Analyses

Plasma membrane sheets were prepared as previously described [41, 142]. Briefly, following treatments, cells were fixed by incubation for 20 min in a 2% paraformaldehyde solution containing PBS (GLUT4 analyses) or TBS (PIP$_2$ analyses), and these membranes were used for immunofluorescence. For GLUT4 immunofluorescence, incubation with a 1:1000 dilution of GLUT4 antibody was followed by incubation with a 1:50 dilution of FITC-conjugated secondary antibody, both for 60 min at 25°C. For PIP$_2$ immunofluorescence, incubation with a 1:50 dilution of PIP$_2$ antibody was performed for 30 min at 37°C. Appropriate FITC-conjugated secondary antibody was added for 60 min at 25°C. For labeling of actin after fixation, cells were incubated with 5 mg/ml of FITC-conjugated phalloidin for 2 h at 25°C (Confocal analyses) or blocked in fish serum (1 h at 25°C) and labeled with a 1:100 dilution of F-actin specific primary antibody (overnight at 4°C; LI-COR analyses). All PM sheet and cell images were obtained using the Zeiss LSM 510 NLO Confocal Microscope, and all microscope settings were identical between groups. Images were quantitated with the LI-COR infrared imaging system as previously described [1, 142, 180].

10. Immunofluoresence Quantitation

For GLUT4 quantitation, plasma membrane sheets were prepared and labeled as described above. The amount of glucose transporter on the plasma membrane was quantitated by digital image processing as described previously

[57, 142, 175]. To ensure that quantitation was performed in an unbiased manner, fields of sheets were selected based solely on their staining with rhodamine-conjugated wheat-germ agglutinin (WGA). Additional population-based quantitation of PIP_2 and F-actin was done using the Odyssey infrared imaging system (LI-COR, Lincoln, NE) as previously described [1, 142, 180].

11. RNA isolation and measurement using RT-PCR

L6-GLUT4myc myotubes and 3T3-L1 adipocytes were treated with or without 5 nM insulin for 12 hours, washed twice in ice cold PBS. Cells were lysed using a Qiagen QIAshredder and RNA was isolated using a Qiagen RNeasy mini kit. RNA was reversed transcribed with the High Capacity cDNA Reverse Transcription Kit (Applied Biosystems) for production of a RT-PCR template. Reactions were performed in a 96-well plate format using the ABI Prism 7000 Sequence Detection System (Applied Biosystems). Each reaction contained the following: 12.5 µL of SYBR GREEN (Applied Biosystems), 500 nM of each primer, cDNA, and RNase free water up to a total volume of 25 µL. The ΔΔCt method of relative quantification using real-time quantitative PCR was used. Data are expressed as the ratio of *Hmgr* to *36B4* for 3T3-L1 adipocytes using primers specific for the mouse *Hmgr* gene (forward 5'-TGT GGG AAC GGT GAC ACT TA-3'; reverse 5'-CTT CAA ATT TTG GGC ACT CA-3') and mouse *36B4* gene (forward 5'-AAG CGC GTC CTG GCA TTG TCT-3'; reverse 5'-CCG CAG GGG CAG CAG TGG T-3') with an annealing temperature of 60°C. Data are expressed as the ratio of *Hmgr* to *Gapdh* for L6 myotubes using primers specific

118

for the rat *Hmgr* gene (forward 5'-TGT GGG AAC GGT GAC ACT TA-3'; reverse

5'-CTT CAA ATT TTG GGC ACT CA-3') and rat *Gapdh* gene (forward 5'-ATG

GCC AGC CTC GTC CCG TAG ACC AAA ATG-3'; reverse 5'-AAG TGG GCC

CCG GCC TTC TCC AT-3') with an annealing temperature of 60°C.

12. ATP measurement.

Intracellular ATP content was measured using a luminescence ATP

detection assay system (ATPlite^{TM}, PerkinElmer Inc.) as we have previously

described [181]. Briefly, following experimental treatments, 3T3-L1 adipocytes

were lysed using a mammalian cell lysis buffer which inactivates endogenous

ATPase. Subsequently whole cell lysate was incubated with substrate buffer and

luminescence was detected using the SpectraMax M2 (Molecular Devices).

Luminescence was converted to actual ATP content (nM) by use of an ATP

standard curve. ATP concentrations were normalized for protein concentration

determined by the Bradford method.

13. siRNA design and transfection.

Three independent oligonuceotide sequences, designed and purchased

from Ambion (Austin, TX), were tested for OGT. The oligonucleotides with the

highest knockdown efficiency for OGT was CAU UUA UGA CAA UCG AAU Att

(siRNA ID#: s130675). Only one oligo was necessary for OGT knockdown

studies. Ambion's Negative Control #1 siRNA (Cat #:4635) was used as a control

in all experiments. For all knockdown experiments cells were seeded as

described before. Cells were first transfected at approximately 48 hr post seeding (or ~60% confluency). Calcium phosphate transfection protocol was utilized as follows, 60 pmol of siRNA was added to siRNA mix: 15 µl ddH$_2$O, 15 µl Buffer A (0.5 M CaCl$_2$, 0.1 M HEPES (pH 7.0)), and 30 µl Buffer B (0.28 M NaCl, 0.75 mM NaH$_2$PO$_4$, 0.75 mM Na$_2$HPO$_4$, 0.05 M HEPES (pH 7.0)) and after 10 min at room temperature, the siRNA mix was added to each well of a 12 well plate containing 600 µl DMEM + 5% FBS and incubated 12-16 hr. Following 12-16 hr incubation, media was aspirated and replaced with DMEM+2% FBS. Additional transfection was repeated 72 hr after initial transfection. Cells were treated and assayed 72 hr after final transfection.

14. Statistics

Values are presented as means ±SE. The significance of differences between means was evaluated by analysis of variance. Where differences among groups were indicated, the Neumann-Keuls test was used for post hoc comparison between groups. GraphPad Prism 4 software was used for all analyses. $P < 0.05$ was considered significant.

Chapter V

References

1. McCarthy, A.M., et al., *Loss of cortical actin filaments in insulin-resistant skeletal muscle cells impairs GLUT4 vesicle trafficking and glucose transport.* Am J Physiol Cell Physiol, 2006. **291**(5): p. C860-8.

2. Kandror, K.V. and P.F. Pilch, *The insulin-like growth factor II/mannose 6-phosphate receptor utilizes the same membrane compartments as GLUT4 for insulin-dependent trafficking to and from the rat adipocyte cell surface.* J Biol Chem, 1996. **271**(36): p. 21703-8.

3. Kandror, K.V. and P.F. Pilch, *Compartmentalization of protein traffic in insulin-sensitive cells.* Am J Physiol, 1996. **271**(1 Pt 1): p. E1-14.

4. Rea, S. and D.E. James, *Moving GLUT4: the biogenesis and trafficking of GLUT4 storage vesicles.* Diabetes, 1997. **46**(11): p. 1667-77.

5. Pessin, J.E., et al., *Molecular basis of insulin-stimulated GLUT4 vesicle trafficking. Location! Location! Location!* J Biol Chem, 1999. **274**(5): p. 2593-6.

6. Satoh, S., et al., *Use of bismannose photolabel to elucidate insulin-regulated GLUT4 subcellular trafficking kinetics in rat adipose cells. Evidence that exocytosis is a critical site of hormone action.* J Biol Chem, 1993. **268**(24): p. 17820-9.

7. Jhun, B.H., et al., *Effects of insulin on steady state kinetics of GLUT4 subcellular distribution in rat adipocytes. Evidence of constitutive GLUT4 recycling.* J Biol Chem, 1992. **267**(25): p. 17710-5.

8. Yang, J. and G.D. Holman, *Comparison of GLUT4 and GLUT1 subcellular trafficking in basal and insulin-stimulated 3T3-L1 cells.* J Biol Chem, 1993. **268**(7): p. 4600-3.

9. Puigserver, P., et al., *Insulin-regulated hepatic gluconeogenesis through FOXO1-PGC-1alpha interaction.* Nature, 2003. **423**(6939): p. 550-5.

10. Guo, S., et al., *Insulin suppresses transactivation by CAAT/enhancer-binding proteins beta (C/EBPbeta). Signaling to p300/CREB-binding protein by protein kinase B disrupts interaction with the major activation domain of C/EBPbeta.* J Biol Chem, 2001. **276**(11): p. 8516-23.

11. Bjornholm, M. and J.R. Zierath, *Insulin signal transduction in human skeletal muscle: identifying the defects in Type II diabetes.* Biochem Soc Trans, 2005. **33**(Pt 2): p. 354-7.

12. Luo, R.Z., et al., *Quaternary structure of the insulin-insulin receptor complex.* Science, 1999. **285**(5430): p. 1077-80.

13. Tamemoto, H., et al., *Insulin resistance and growth retardation in mice lacking insulin receptor substrate-1.* Nature, 1994. **372**(6502): p. 182-6.

14. Araki, E., et al., *Alternative pathway of insulin signalling in mice with targeted disruption of the IRS-1 gene.* Nature, 1994. **372**(6502): p. 186-90.

15. Withers, D.J., et al., *Disruption of IRS-2 causes type 2 diabetes in mice.* Nature, 1998. **391**(6670): p. 900-4.

16. Huang, C., et al., *Differential contribution of insulin receptor substrates 1 versus 2 to insulin signaling and glucose uptake in l6 myotubes.* J Biol Chem, 2005. **280**(19): p. 19426-35.

17. Fantin, V.R., et al., *Mice lacking insulin receptor substrate 4 exhibit mild defects in growth, reproduction, and glucose homeostasis.* Am J Physiol Endocrinol Metab, 2000. **278**(1): p. E127-33.

18. Shepherd, P.R., *Mechanisms regulating phosphoinositide 3-kinase signalling in insulin-sensitive tissues.* Acta Physiol Scand, 2005. **183**(1): p. 3-12.

19. Sarbassov, D.D., et al., *Phosphorylation and regulation of Akt/PKB by the rictor-mTOR complex.* Science, 2005. **307**(5712): p. 1098-101.

20. Alessi, D.R., et al., *Characterization of a 3-phosphoinositide-dependent protein kinase which phosphorylates and activates protein kinase Balpha.* Curr Biol, 1997. **7**(4): p. 261-9.

21. Stokoe, D., et al., *Dual role of phosphatidylinositol-3,4,5-trisphosphate in the activation of protein kinase B.* Science, 1997. **277**(5325): p. 567-70.

22. Cho, H., et al., *Akt1/PKBalpha is required for normal growth but dispensable for maintenance of glucose homeostasis in mice.* J Biol Chem, 2001. **276**(42): p. 38349-52.

23. Cho, H., et al., *Insulin resistance and a diabetes mellitus-like syndrome in mice lacking the protein kinase Akt2 (PKB beta).* Science, 2001. **292**(5522): p. 1728-31.

24. Jiang, Z.Y., et al., *Insulin signaling through Akt/protein kinase B analyzed by small interfering RNA-mediated gene silencing.* Proc Natl Acad Sci U S A, 2003. **100**(13): p. 7569-74.

25. Katome, T., et al., *Use of RNA interference-mediated gene silencing and adenoviral overexpression to elucidate the roles of AKT/protein kinase B isoforms in insulin actions.* J Biol Chem, 2003. **278**(30): p. 28312-23.

26. Calera, M.R., et al., *Insulin increases the association of Akt-2 with Glut4-containing vesicles.* J Biol Chem, 1998. **273**(13): p. 7201-4.

27. Kupriyanova, T.A. and K.V. Kandror, *Akt-2 binds to Glut4-containing vesicles and phosphorylates their component proteins in response to insulin.* J Biol Chem, 1999. **274**(3): p. 1458-64.

28. Kane, S., et al., *A method to identify serine kinase substrates. Akt phosphorylates a novel adipocyte protein with a Rab GTPase-activating protein (GAP) domain.* J Biol Chem, 2002. **277**(25): p. 22115-8.

29. Sakamoto, K. and G.D. Holman, *Emerging role for AS160/TBC1D4 and TBC1D1 in the regulation of GLUT4 traffic.* Am J Physiol Endocrinol Metab, 2008. **295**(1): p. E29-37.

30. Sano, H., et al., *Insulin-stimulated phosphorylation of a Rab GTPase-activating protein regulates GLUT4 translocation.* J Biol Chem, 2003. **278**(17): p. 14599-602.

31. Larance, M., et al., *Characterization of the role of the Rab GTPase-activating protein AS160 in insulin-regulated GLUT4 trafficking.* J Biol Chem, 2005. **280**(45): p. 37803-13.

32. Eguez, L., et al., *Full intracellular retention of GLUT4 requires AS160 Rab GTPase activating protein.* Cell Metab, 2005. **2**(4): p. 263-72.

33. Zeigerer, A., M.K. McBrayer, and T.E. McGraw, *Insulin stimulation of GLUT4 exocytosis, but not its inhibition of endocytosis, is dependent on RabGAP AS160.* Mol Biol Cell, 2004. **15**(10): p. 4406-15.

34. Miinea, C.P., et al., *AS160, the Akt substrate regulating GLUT4 translocation, has a functional Rab GTPase-activating protein domain.* Biochem J, 2005. **391**(Pt 1): p. 87-93.

35. Elmendorf, J.S., D.J. Boeglin, and J.E. Pessin, *Temporal separation of insulin-stimulated GLUT4/IRAP vesicle plasma membrane docking and fusion in 3T3L1 adipocytes.* J Biol Chem, 1999. **274**(52): p. 37357-61.

36. Sano, H., et al., *Rab10 in insulin-stimulated GLUT4 translocation.* Biochem J, 2008. **411**(1): p. 89-95.

37. Bandyopadhyay, G., et al., *Activation of protein kinase C (alpha, beta, and zeta) by insulin in 3T3/L1 cells. Transfection studies suggest a role for PKC-zeta in glucose transport.* J Biol Chem, 1997. **272**(4): p. 2551-8.

38. Omata, W., et al., *Actin filaments play a critical role in insulin-induced exocytotic recruitment but not in endocytosis of GLUT4 in isolated rat adipocytes.* Biochem J, 2000. **346 Pt 2**: p. 321-8.

39. Tsakiridis, T., et al., *Actin filaments facilitate insulin activation of the src and collagen homologous/mitogen-activated protein kinase pathway leading to DNA synthesis and c-fos expression.* J Biol Chem, 1998. **273**(43): p. 28322-31.

40. Bose, A., et al., *Glucose transporter recycling in response to insulin is facilitated by myosin Myo1c.* Nature, 2002. **420**(6917): p. 821-4.

41. Chen, G., et al., *Protective effect of phosphatidylinositol 4,5-bisphosphate against cortical filamentous actin loss and insulin resistance induced by sustained exposure of 3T3-L1 adipocytes to insulin.* J Biol Chem, 2004. **279**(38): p. 39705-9.

42. Eyster, C.A., Q.S. Duggins, and A.L. Olson, *Expression of constitutively active Akt/protein kinase B signals GLUT4 translocation in the absence of an intact actin cytoskeleton.* J Biol Chem, 2005. **280**(18): p. 17978-85.

43. Kanzaki, M. and J.E. Pessin, *Insulin-stimulated GLUT4 translocation in adipocytes is dependent upon cortical actin remodeling.* J Biol Chem, 2001. **276**(45): p. 42436-44.

44. Tsakiridis, T., M. Vranic, and A. Klip, *Disassembly of the actin network inhibits insulin-dependent stimulation of glucose transport and prevents recruitment of glucose transporters to the plasma membrane.* J Biol Chem, 1994. **269**(47): p. 29934-42.

45. Asahi, Y., et al., *Fluoromicroscopic detection of myc-tagged GLUT4 on the cell surface. Co-localization of the translocated GLUT4 with rearranged actin by insulin treatment in CHO cells and L6 myotubes.* J Med Invest, 1999. **46**(3-4): p. 192-9.

46. Kanzaki, M. and J.E. Pessin, *Caveolin-associated filamentous actin (Cav-actin) defines a novel F-actin structure in adipocytes.* J Biol Chem, 2002. **277**(29): p. 25867-9.

47. Bose, A., et al., *G(alpha)11 signaling through ARF6 regulates F-actin mobilization and GLUT4 glucose transporter translocation to the plasma membrane.* Mol Cell Biol, 2001. **21**(15): p. 5262-75.

48. Brozinick, J.T., Jr., et al., *Disruption of cortical actin in skeletal muscle demonstrates an essential role of the cytoskeleton in glucose transporter 4 translocation in insulin-sensitive tissues.* J Biol Chem, 2004. **279**(39): p. 40699-706.

49. Hilpela, P., M.K. Vartiainen, and P. Lappalainen, *Regulation of the actin cytoskeleton by PI(4,5)P2 and PI(3,4,5)P3.* Curr Top Microbiol Immunol, 2004. **282**: p. 117-63.

50. Cunningham, C.C., et al., *Cell permeant polyphosphoinositide-binding peptides that block cell motility and actin assembly.* J Biol Chem, 2001. **276**(46): p. 43390-9.

51. Kwik, J., et al., *Membrane cholesterol, lateral mobility, and the phosphatidylinositol 4,5-bisphosphate-dependent organization of cell actin.* Proc Natl Acad Sci U S A, 2003. **100**(24): p. 13964-9.

52. Bittner, M.A. and R.W. Holz, *Phosphatidylinositol-4,5-bisphosphate: actin dynamics and the regulation of ATP-dependent and -independent secretion.* Mol Pharmacol, 2005. **67**(4): p. 1089-98.

53. Raucher, D., et al., *Phosphatidylinositol 4,5-bisphosphate functions as a second messenger that regulates cytoskeleton-plasma membrane adhesion.* Cell, 2000. **100**(2): p. 221-8.

54. van Rheenen, J. and K. Jalink, *Agonist-induced PIP(2) hydrolysis inhibits cortical actin dynamics: regulation at a global but not at a micrometer scale.* Mol Biol Cell, 2002. **13**(9): p. 3257-67.

55. Kanzaki, M., et al., *Phosphatidylinositol 4,5-bisphosphate regulates adipocyte actin dynamics and GLUT4 vesicle recycling.* J Biol Chem, 2004. **279**(29): p. 30622-33.

56. Liu, P., et al., *Sphingomyelinase activates GLUT4 translocation via a cholesterol-dependent mechanism.* Am J Physiol Cell Physiol, 2004. **286**(2): p. C317-29.

57. Chen, G., et al., *Chromium activates glucose transporter 4 trafficking and enhances insulin-stimulated glucose transport in 3T3-L1 adipocytes via a cholesterol-dependent mechanism.* Mol Endocrinol, 2006. **20**(4): p. 857-70.

58. Habegger, K.M. and J.S. Elmendorf, *Activation of AMPK Enhances Insulin but Not Basal Regulation of GLUT4 Translocation via Lowering Membrane Cholesterol: Evidence for Divergent AMPK GLUT4 Regulatory Mechanisms.* Endocrinology (submitted), 2009.

59. DeFronzo, R.A. and E. Ferrannini, *Insulin resistance. A multifaceted syndrome responsible for NIDDM, obesity, hypertension, dyslipidemia, and atherosclerotic cardiovascular disease.* Diabetes Care, 1991. **14**(3): p. 173-94.

60. Reaven, G.M., *Banting lecture 1988. Role of insulin resistance in human disease.* Diabetes, 1988. **37**(12): p. 1595-607.

61. McGarry, J.D., *Glucose-fatty acid interactions in health and disease.* Am J Clin Nutr, 1998. **67**(3 Suppl): p. 500S-504S.

62. Ferrannini, E., *Hyperinsulinemia and insulin resistance.* Second ed. 2000, Philadelphia: Lippincott, Williams, and Wilkins.

63. Flores-Riveros, J.R., et al., *Insulin down-regulates expression of the insulin-responsive glucose transporter (GLUT4) gene: effects on transcription and mRNA turnover.* Proc Natl Acad Sci U S A, 1993. **90**(2): p. 512-6.

64. Ricort, J.M., et al., *Alterations in insulin signalling pathway induced by prolonged insulin treatment of 3T3-L1 adipocytes.* Diabetologia, 1995. **38**(10): p. 1148-56.

65. Pryor, P.R., et al., *Chronic insulin effects on insulin signalling and GLUT4 endocytosis are reversed by metformin.* Biochem J, 2000. **348 Pt 1**: p. 83-91.

66. Ross, S.A., et al., *Development and comparison of two 3T3-L1 adipocyte models of insulin resistance: increased glucose flux vs glucosamine treatment.* Biochem Biophys Res Commun, 2000. **273**(3): p. 1033-41.

67. Nelson, B.A., K.A. Robinson, and M.G. Buse, *High glucose and glucosamine induce insulin resistance via different mechanisms in 3T3-L1 adipocytes.* Diabetes, 2000. **49**(6): p. 981-91.

68. Marshall, S., V. Bacote, and R.R. Traxinger, *Discovery of a metabolic pathway mediating glucose-induced desensitization of the glucose transport system. Role of hexosamine biosynthesis in the induction of insulin resistance.* J Biol Chem, 1991. **266**(8): p. 4706-12.

69. Copeland, R.J., J.W. Bullen, and G.W. Hart, *Cross-talk between GlcNAcylation and phosphorylation: roles in insulin resistance and glucose toxicity.* Am J Physiol Endocrinol Metab, 2008. **295**(1): p. E17-28.

70. Kreppel, L.K., M.A. Blomberg, and G.W. Hart, *Dynamic glycosylation of nuclear and cytosolic proteins. Cloning and characterization of a unique O-GlcNAc transferase with multiple tetratricopeptide repeats.* J Biol Chem, 1997. **272**(14): p. 9308-15.

71. Lubas, W.A., et al., *O-Linked GlcNAc transferase is a conserved nucleocytoplasmic protein containing tetratricopeptide repeats.* J Biol Chem, 1997. **272**(14): p. 9316-24.

72. Love, D.C. and J.A. Hanover, *The hexosamine signaling pathway: deciphering the "O-GlcNAc code".* Sci STKE, 2005. **2005**(312): p. re13.

73. Yki-Jarvinen, H., et al., *Increased glutamine:fructose-6-phosphate amidotransferase activity in skeletal muscle of patients with NIDDM.* Diabetes, 1996. **45**(3): p. 302-7.

74. McClain, D.A., *Hexosamines as mediators of nutrient sensing and regulation in diabetes.* J Diabetes Complications, 2002. **16**(1): p. 72-80.

75. McClain, D.A., et al., *Altered glycan-dependent signaling induces insulin resistance and hyperleptinemia.* Proc Natl Acad Sci U S A, 2002. **99**(16): p. 10695-9.

76. Vosseller, K., et al., *Elevated nucleocytoplasmic glycosylation by O-GlcNAc results in insulin resistance associated with defects in Akt activation in 3T3-L1 adipocytes.* Proc Natl Acad Sci U S A, 2002. **99**(8): p. 5313-8.

77. Arias, E.B., J. Kim, and G.D. Cartee, *Prolonged incubation in PUGNAc results in increased protein O-Linked glycosylation and insulin resistance in rat skeletal muscle.* Diabetes, 2004. **53**(4): p. 921-30.

78. Zhang, P., et al., *Hexosamines regulate leptin production in 3T3-L1 adipocytes through transcriptional mechanisms.* Endocrinology, 2002. **143**(1): p. 99-106.

79. Brown, M.S. and J.L. Goldstein, *The SREBP pathway: regulation of cholesterol metabolism by proteolysis of a membrane-bound transcription factor.* Cell, 1997. **89**(3): p. 331-40.

80. Brown, M.S. and J.L. Goldstein, *A proteolytic pathway that controls the cholesterol content of membranes, cells, and blood.* Proc Natl Acad Sci U S A, 1999. **96**(20): p. 11041-8.

81. Soccio, R.E. and J.L. Breslow, *Intracellular cholesterol transport.* Arterioscler Thromb Vasc Biol, 2004. **24**(7): p. 1150-60.

82. Nadeau, K.J., et al., *Insulin regulation of sterol regulatory element-binding protein-1 expression in L-6 muscle cells and 3T3 L1 adipocytes.* J Biol Chem, 2004. **279**(33): p. 34380-7.

83. Han, I. and J.E. Kudlow, *Reduced O glycosylation of Sp1 is associated with increased proteasome susceptibility.* Mol Cell Biol, 1997. **17**(5): p. 2550-8.

84. Zachara, N.E. and G.W. Hart, *The emerging significance of O-GlcNAc in cellular regulation.* Chem Rev, 2002. **102**(2): p. 431-8.

85. Rechsteiner, M. and S.W. Rogers, *PEST sequences and regulation by proteolysis.* Trends Biochem Sci, 1996. **21**(7): p. 267-71.

86. Cagen, L.M., et al., *Insulin activates the rat sterol-regulatory-element-binding protein 1c (SREBP-1c) promoter through the combinatorial actions of SREBP, LXR, Sp-1 and NF-Y cis-acting elements.* Biochem J, 2005. **385**(Pt 1): p. 207-16.

87. Deng, X., et al., *Expression of the rat sterol regulatory element-binding protein-1c gene in response to insulin is mediated by increased transactivating capacity of specificity protein 1 (Sp1).* J Biol Chem, 2007. **282**(24): p. 17517-29.

88. Sekar, N. and J.D. Veldhuis, *Involvement of Sp1 and SREBP-1a in transcriptional activation of the LDL receptor gene by insulin and LH in cultured porcine granulosa-luteal cells.* Am J Physiol Endocrinol Metab, 2004. **287**(1): p. E128-35.

89. Sone, H., et al., *Acetyl-coenzyme A synthetase is a lipogenic enzyme controlled by SREBP-1 and energy status.* Am J Physiol Endocrinol Metab, 2002. **282**(1): p. E222-30.

90.   Raney, M.A. and L.P. Turcotte, *Evidence for the involvement of CaMKII and AMPK in Ca2+-dependent signaling pathways regulating FA uptake and oxidation in contracting rodent muscle.* J Appl Physiol, 2008. **104**(5): p. 1366-73.

91.   Salt, I.P., J.M. Connell, and G.W. Gould, *5-aminoimidazole-4-carboxamide ribonucleoside (AICAR) inhibits insulin-stimulated glucose transport in 3T3-L1 adipocytes.* Diabetes, 2000. **49**(10): p. 1649-56.

92.   Yamaguchi, S., et al., *Activators of AMP-activated protein kinase enhance GLUT4 translocation and its glucose transport activity in 3T3-L1 adipocytes.* Am J Physiol Endocrinol Metab, 2005. **289**(4): p. E643-9.

93.   Yamauchi, T., et al., *Adiponectin stimulates glucose utilization and fatty-acid oxidation by activating AMP-activated protein kinase.* Nat Med, 2002. **8**(11): p. 1288-95.

94.   Minokoshi, Y., et al., *Leptin stimulates fatty-acid oxidation by activating AMP-activated protein kinase.* Nature, 2002. **415**(6869): p. 339-43.

95.   Ju, J.S., et al., *Creatine feeding increases GLUT4 expression in rat skeletal muscle.* Am J Physiol Endocrinol Metab, 2005. **288**(2): p. E347-52.

96.   Fryer, L.G., A. Parbu-Patel, and D. Carling, *The Anti-diabetic drugs rosiglitazone and metformin stimulate AMP-activated protein kinase through distinct signaling pathways.* J Biol Chem, 2002. **277**(28): p. 25226-32.

97.   Konrad, D., et al., *Troglitazone causes acute mitochondrial membrane depolarisation and an AMPK-mediated increase in glucose phosphorylation in muscle cells.* Diabetologia, 2005. **48**(5): p. 954-66.

98.   Lee, W.J., et al., *Alpha-lipoic acid increases insulin sensitivity by activating AMPK in skeletal muscle.* Biochem Biophys Res Commun, 2005. **332**(3): p. 885-91.

99.   Mu, J., et al., *A role for AMP-activated protein kinase in contraction- and hypoxia-regulated glucose transport in skeletal muscle.* Mol Cell, 2001. **7**(5): p. 1085-94.

100.   Lee, Y.S., et al., *Berberine, a natural plant product, activates AMP-activated protein kinase with beneficial metabolic effects in diabetic and insulin-resistant states.* Diabetes, 2006. **55**(8): p. 2256-64.

101.   Zhou, G., et al., *Role of AMP-activated protein kinase in mechanism of metformin action.* J Clin Invest, 2001. **108**(8): p. 1167-74.

102.   Bailey, C.J. and S.L. Turner, *Glucosamine-induced insulin resistance in L6 muscle cells.* Diabetes Obes Metab, 2004. **6**(4): p. 293-8.

103.   Hundal, H.S., et al., *Cellular mechanism of metformin action involves glucose transporter translocation from an intracellular pool to the plasma membrane in L6 muscle cells.* Endocrinology, 1992. **131**(3): p. 1165-73.

104.   Klip, A., et al., *Stimulation of hexose transport by metformin in L6 muscle cells in culture.* Endocrinology, 1992. **130**(5): p. 2535-44.

105. Vinson, J.A., *So many choices, so what's a consumer to do?: A commentary on "Effect of chromium niacinate and chromium picolinate supplementation on lipid peroxidation, TNF-alpha, IL-6, CRP, glycated hemoglobin, triglycerides, and cholesterol levels in blood of streptozotocin-treated diabetic rats".* Free Radic Biol Med, 2007. **43**(8): p. 1121-3.

106. ODS. *Dietary Supplement Fact Sheet: Chromium.* 8/5/2005 [cited 2009; http://ods.od.nih.gov/factsheets/Chromium_pf.asp].

107. Schwarz, K. and W. Mertz, *A glucose tolerance factor and its differentiation from factor 3.* Arch Biochem Biophys, 1957. **72**(2): p. 515-8.

108. Jeejeebhoy, K.N., et al., *Chromium deficiency, glucose intolerance, and neuropathy reversed by chromium supplementation, in a patient receiving long-term total parenteral nutrition.* Am J Clin Nutr, 1977. **30**(4): p. 531-8.

109. Freund, H., S. Atamian, and J.E. Fischer, *Chromium deficiency during total parenteral nutrition.* JAMA, 1979. **241**(5): p. 496-8.

110. Brown, R.O., et al., *Chromium deficiency after long-term total parenteral nutrition.* Dig Dis Sci, 1986. **31**(6): p. 661-4.

111. Lamson, D.S. and S.M. Plaza, *The safety and efficacy of high-dose chromium.* Altern Med Rev, 2002. **7**(3): p. 218-35.

112. Riales, R. and M.J. Albrink, *Effect of chromium chloride supplementation on glucose tolerance and serum lipids including high-density lipoprotein of adult men.* Am J Clin Nutr, 1981. **34**(12): p. 2670-8.

113. Striffler, J.S., et al., *Chromium improves insulin response to glucose in rats.* Metabolism, 1995. **44**(10): p. 1314-20.

114. Morris, B.W., T.A. Gray, and S. Macneil, *Glucose-dependent uptake of chromium in human and rat insulin-sensitive tissues.* Clin Sci (Lond), 1993. **84**(4): p. 477-82.

115. Cefalu, W.T., et al., *Oral chromium picolinate improves carbohydrate and lipid metabolism and enhances skeletal muscle Glut-4 translocation in obese, hyperinsulinemic (JCR-LA corpulent) rats.* J Nutr, 2002. **132**(6): p. 1107-14.

116. Striffler, J.S., M.M. Polansky, and R.A. Anderson, *Overproduction of insulin in the chromium-deficient rat.* Metabolism, 1999. **48**(8): p. 1063-8.

117. Striffler, J.S., M.M. Polansky, and R.A. Anderson, *Dietary chromium decreases insulin resistance in rats fed a high-fat, mineral-imbalanced diet.* Metabolism, 1998. **47**(4): p. 396-400.

118. Fulop, T., Jr., et al., *Glucose intolerance and insulin resistance with aging--studies on insulin receptors and post-receptor events.* Arch Gerontol Geriatr, 1987. **6**(2): p. 107-15.

119. Mertz, W., *Chromium occurrence and function in biological systems.* Physiol Rev, 1969. **49**(2): p. 163-239.

120. Anderson, R.A., et al., *Effects of supplemental chromium on patients with symptoms of reactive hypoglycemia.* Metabolism, 1987. **36**(4): p. 351-5.

121. Vincent, J.B., *Mechanisms of chromium action: low-molecular-weight chromium-binding substance.* J Am Coll Nutr, 1999. **18**(1): p. 6-12.

122. Davis, C.M. and J.B. Vincent, *Chromium oligopeptide activates insulin receptor tyrosine kinase activity.* Biochemistry, 1997. **36**(15): p. 4382-5.

123. Evans, G.W. and T.D. Bowman, *Chromium picolinate increases membrane fluidity and rate of insulin internalization.* J Inorg Biochem, 1992. **46**(4): p. 243-50.

124. Kao, A.W., et al., *Expression of a dominant interfering dynamin mutant in 3T3L1 adipocytes inhibits GLUT4 endocytosis without affecting insulin signaling.* J Biol Chem, 1998. **273**(39): p. 25450-7.

125. Kublaoui, B., J. Lee, and P.F. Pilch, *Dynamics of signaling during insulin-stimulated endocytosis of its receptor in adipocytes.* J Biol Chem, 1995. **270**(1): p. 59-65.

126. Wang, B., Y. Balba, and V.P. Knutson, *Insulin-induced in situ phosphorylation of the insulin receptor located in the plasma membrane versus endosomes.* Biochem Biophys Res Commun, 1996. **227**(1): p. 27-34.

127. Dombrowski, L., R. Faure, and A. Marette, *Sustained activation of insulin receptors internalized in GLUT4 vesicles of insulin-stimulated skeletal muscle.* Diabetes, 2000. **49**(11): p. 1772-82.

128. Czech, M.P., *Insulin action and the regulation of hexose transport.* Diabetes, 1980. **29**(5): p. 399-409.

129. Pilch, P.F., P.A. Thompson, and M.P. Czech, *Coordinate modulation of D-glucose transport activity and bilayer fluidity in plasma membranes derived from control and insulin-treated adipocytes.* Proc Natl Acad Sci U S A, 1980. **77**(2): p. 915-8.

130. Muller, S., et al., *Action of metformin on erythrocyte membrane fluidity in vitro and in vivo.* Eur J Pharmacol, 1997. **337**(1): p. 103-10.

131. Wiernsperger, N.F., *Membrane physiology as a basis for the cellular effects of metformin in insulin resistance and diabetes.* Diabetes Metab, 1999. **25**(2): p. 110-27.

132. Fischer, Y., et al., *Action of metformin on glucose transport and glucose transporter GLUT1 and GLUT4 in heart muscle cells from healthy and diabetic rats.* Endocrinology, 1995. **136**(2): p. 412-20.

133. Garvey, W.T., et al., *Glucose and insulin co-regulate the glucose transport system in primary cultured adipocytes. A new mechanism of insulin resistance.* J Biol Chem, 1987. **262**(1): p. 189-97.

134. Kralik, S.F., et al., *Ceramide and glucosamine antagonism of alternate signaling pathways regulating insulin- and osmotic shock-induced glucose transporter 4 translocation.* Endocrinology, 2002. **143**(1): p. 37-46.

135. Ross, S.A., et al., *Development and Comparison of Two 3T3-L1 Adipocyte Models of Insulin Resistance: Increased Glucose Flux vs Glucosamine Treatment.* Biochem Biophys Res Commun, 2000. **273**(3): p. 1033-1041.

136. Yin, H.L. and P.A. Janmey, *Phosphoinositide regulation of the actin cytoskeleton.* Annu Rev Physiol, 2003. **65**: p. 761-89.

137. Janez, A., D.S. Worrall, and J.M. Olefsky, *Insulin-mediated cellular insulin resistance decreases osmotic shock-induced glucose transport in 3T3-L1 adipocytes.* Endocrinology, 2000. **141**(12): p. 4657-63.

138. Morris, B., T. Gray, and S. MacNeil, *Evidence for chromium acting as an essential trace element in insulin-dependent glucose uptake in cultured mouse myotubes.* J Endocrinol, 1995. **144**(1): p. 135-41.

139. Joost, H.G. and A. Schurmann, *Subcellular fractionation of adipocytes and 3T3-L1 cells.* Methods Mol Biol, 2001. **155**: p. 77-82.

140. Vincent, J.B., *The biochemistry of chromium.* J Nutr, 2000. **130**(4): p. 715-8.

141. Liu, P., et al., *Sphingomyelinase Activates GLUT4 Translocation via a Cholesterol-Dependent Mechanism.* Am J Physiol Cell Physiol, 2003: p. 00073.2003.

142. Strawbridge, A.B. and J.S. Elmendorf, *Phosphatidylinositol 4,5-Bisphosphate Reverses Endothelin-1-Induced Insulin Resistance via an Actin-Dependent Mechanism.* Diabetes, 2005. **54**(6): p. 1698-705.

143. Niswender, K.D., et al., *Insulin activation of phosphatidylinositol 3-kinase in the hypothalamic arcuate nucleus: a key mediator of insulin-induced anorexia.* Diabetes, 2003. **52**(2): p. 227-31.

144. Chen, R., et al., *A monoclonal antibody to visualize PtdIns(3,4,5)P(3) in cells.* J Histochem Cytochem, 2002. **50**(5): p. 697-708.

145. Tanaka, K., et al., *Evidence that a phosphatidylinositol 3,4,5-trisphosphate-binding protein can function in nucleus.* J Biol Chem, 1999. **274**(7): p. 3919-22.

146. Evans, G.W. and T.D. Bowman, *Chromium picolinate increases membrane fluidity and rate of insulin internalization.* J Inorg Biochem, 1992. **46**(4): p. 243-50.

147. Hresko, R.C., et al., *Glucosamine-induced insulin resistance in 3T3-L1 adipocytes is caused by depletion of intracellular ATP.* J Biol Chem, 1998. **273**(32): p. 20658-68.

148. Strawbridge, A.B. and J.S. Elmendorf, *Endothelin-1 impairs glucose transporter trafficking via a membrane-based mechanism.* J Cell Biochem, 2006. **97**(4): p. 849-56.

149. Lin, Y., et al., *The hyperglycemia-induced inflammatory response in adipocytes: the role of reactive oxygen species.* J Biol Chem, 2005. **280**(6): p. 4617-26.

150. Habegger, K.M., et al., *Fat-Induced Membrane Cholesterol Accrual and Glucose Transport Dysfunction.* Diabetologia (in revision), 2009.

151. Weigert, C., et al., *Palmitate-induced activation of the hexosamine pathway in human myotubes: increased expression of glutamine:fructose-6-phosphate aminotransferase.* Diabetes, 2003. **52**(3): p. 650-6.

152. Musi, N., et al., *Metformin increases AMP-activated protein kinase activity in skeletal muscle of subjects with type 2 diabetes.* Diabetes, 2002. **51**(7): p. 2074-81.

153. Hardie, D.G., *Minireview: the AMP-activated protein kinase cascade: the key sensor of cellular energy status.* Endocrinology, 2003. **144**(12): p. 5179-83.

154. Advani, A., S.M. Marshall, and T.H. Thomas, *Impaired neutrophil actin assembly causes persistent CD11b expression and reduced primary granule exocytosis in Type II diabetes.* Diabetologia, 2002. **45**(5): p. 719-27.

155. Advani, A., S.M. Marshall, and T.H. Thomas, *Increasing neutrophil F-actin corrects CD11b exposure in Type 2 diabetes.* Eur J Clin Invest, 2004. **34**(5): p. 358-64.

156. Yu, P.K., et al., *Endothelial F-actin cytoskeleton in the retinal vasculature of normal and diabetic rats.* Curr Eye Res, 2005. **30**(4): p. 279-90.

157. Zhou, X., et al., *High glucose alters actin assembly in glomerular mesangial and epithelial cells.* Lab Invest, 1995. **73**(3): p. 372-83.

158. Cortes, P., et al., *F-actin fiber distribution in glomerular cells: structural and functional implications.* Kidney Int, 2000. **58**(6): p. 2452-61.

159. Candiloros, H., et al., *Hyperinsulinemia is related to erythrocyte phospholipid composition and membrane fluidity changes in obese nondiabetic women.* J Clin Endocrinol Metab, 1996. **81**(8): p. 2912-8.

160. Younsi, M., et al., *Erythrocyte membrane phospholipid composition is related to hyperinsulinemia in obese nondiabetic women: effects of weight loss.* Metabolism, 2002. **51**(10): p. 1261-8.

161. Yang, X., et al., *Phosphoinositide signalling links O-GlcNAc transferase to insulin resistance.* Nature, 2008. **451**(7181): p. 964-9.

162. Dentin, R., et al., *Hepatic glucose sensing via the CREB coactivator CRTC2.* Science, 2008. **319**(5868): p. 1402-5.

163. Robinson, K.A., et al., *Effects of diabetes and hyperglycemia on the hexosamine synthesis pathway in rat muscle and liver.* Diabetes, 1995. **44**(12): p. 1438-46.

164. Buse, M.G., et al., *Increased activity of the hexosamine synthesis pathway in muscles of insulin-resistant ob/ob mice.* Am J Physiol, 1997. **272**(6 Pt 1): p. E1080-8.

165. McClain, D.A., et al., *Adipocytes with increased hexosamine flux exhibit insulin resistance, increased glucose uptake, and increased synthesis and storage of lipid.* Am J Physiol Endocrinol Metab, 2005. **288**(5): p. E973-9.

166. Fujita, T., et al., *Glucosamine induces lipid accumulation and adipogenic change in C2C12 myoblasts.* Biochem Biophys Res Commun, 2005. **328**(2): p. 369-74.

167. Rabinovitz, H., et al., *Effect of chromium supplementation on blood glucose and lipid levels in type 2 diabetes mellitus elderly patients.* Int J Vitam Nutr Res, 2004. **74**(3): p. 178-82.

168. Press, R.I., J. Geller, and G.W. Evans, *The effect of chromium picolinate on serum cholesterol and apolipoprotein fractions in human subjects.* West J Med, 1990. **152**(1): p. 41-5.

169. Anderson, R.A., et al., *Elevated intakes of supplemental chromium improve glucose and insulin variables in individuals with type 2 diabetes.* Diabetes, 1997. **46**(11): p. 1786-91.

170. Savage, D.B., K.F. Petersen, and G.I. Shulman, *Disordered lipid metabolism and the pathogenesis of insulin resistance.* Physiol Rev, 2007. **87**(2): p. 507-20.

171. Hirosumi, J., et al., *A central role for JNK in obesity and insulin resistance.* Nature, 2002. **420**(6913): p. 333-6.

172. Yuan, M., et al., *Reversal of obesity- and diet-induced insulin resistance with salicylates or targeted disruption of Ikkbeta.* Science, 2001. **293**(5535): p. 1673-7.

173. Zhao, P., et al., *A newly synthetic chromium complex-Chromium (d-phenylalanine)(3) activates AMP-activated protein kinase and stimulates glucose transport.* Biochem Pharmacol, 2009. **77**(6): p. 1002-10.

174. Wang, Y.Q., Y. Dong, and M.H. Yao, *Chromium picolinate inhibits resistin secretion in insulin-resistant 3T3-L1 adipocytes through the activation of AMP activated protein kinase.* Clin Exp Pharmacol Physiol, 2009.

175. Hausdorff, S.F., J.V. Frangioni, and M.J. Birnbaum, *Role of p21ras in insulin-stimulated glucose transport in 3T3-L1 adipocytes.* J Biol Chem, 1994. **269**(34): p. 21391-4.

176. Elmendorf, J.S., *Fractionation analysis of the subcellular distribution of GLUT-4 in 3T3-L1 adipocytes.* Methods Mol Med, 2003. **83**: p. 105-11.

177. Khayat, Z.A., et al., *Rapid stimulation of glucose transport by mitochondrial uncoupling depends in part on cytosolic Ca2+ and cPKC.* Am J Physiol, 1998. **275**(6 Pt 1): p. C1487-97.

178. Pattar, G.R., et al., *Chromium picolinate positively influences the glucose transporter system via affecting cholesterol homeostasis in adipocytes cultured under hyperglycemic diabetic conditions.* Mutat Res, 2006. **610**(1-2): p. 93-100.

179. Dugail, I., *Transfection of adipocytes and preparation of nuclear extracts.* Methods Mol Biol, 2001. **155**: p. 141-6.

180. Razidlo, G.L., et al., *Phosphorylation regulates KSR1 stability, ERK activation, and cell proliferation.* J Biol Chem, 2004. **279**(46): p. 47808-14.

181. Bhonagiri, P., et al., *Hexosamine biosynthesis pathway flux contributes to insulin resistance via altering membrane phosphatidylinositol 4,5-bisphosphate and cortical filamentous actin.* Endocrinology, 2009. **150**(4): p. 1636-45.

Curriculum Vitae

Guruprasad R. Pattar

Education

2005-2014
Indiana University
Indianapolis, Indiana
Ph.D. Cellular & Integrative Physiology
   Concentration: Life Sciences
   Thesis: *A Nutrient Network Regulating Cellular*
      Cholesterol and Glucose Metabolism

2005-2011
Indiana University School of Medicine
Indianapolis, Indiana
M.D.

2004-2006
Indiana University
Indianapolis, Indiana
M.S. Cellular & Integrative Physiology

1999-2003
Creighton University
Omaha, Nebraska
B.A. Political Science

*Positions/Work
Experience*

2002-2003
Creighton Students Union - Student-elected voting
member, Creighton University, Omaha NE

2003-2004
Research Technician, Elmendorf Laboratory,
Cellular & Integrative Physiology, Indiana
University School of Medicine

2003-2004
Wishard Health Services - Medical volunteer
primarily assisting in aid of postoperative patients
in the recovery room, Indianapolis IN

2004-2006, 2010
American Diabetes Association - Step Out: A Walk

to Fight Diabetes, Fundraising and Participant, Indianapolis IN

2004-2006
Timmy Foundation - Member, Medical Service Mission Trip to Quito Ecuador and fundraising, collecting donations and organizing the supplies warehouse, and participation in events in/around Indianapolis

2007-2008
Adolescent Substance Abuse Prevention Program - Co chair and participated in educating 6th grade school children about substance abuse from the perspective of medicine, Office of Medical Service Learning, Indiana University School of Medicine

Honors and Awards

2006
American College of Physicians Medical Student Abstract Competition Research Poster Finalist

2006
1st place Sigma Xi Graduate Research Competition – Indiana University Medical Center Chapter

2008
3rd place Sigma Xi Graduate Research Competition – Indiana University Medical Center Chapter

2008
Department of Cellular & Integrative Physiology Moenkhaus Award

Professional Society Memberships

American College of Physicians
The American Physiological Society
Sigma Xi-The Scientific Research Society

Publications

Chen G, Raman P, Bhonagiri P, Strawbridge AB, **Pattar GR**, Elmendorf JS. Protective effect of phosphatidylinositol 4,5-bisphosphate against cortical filamentous actin loss and insulin

resistance induced by sustained exposure of 3T3-L1 adipocytes to insulin. J Biol Chem. 2004 Sept 17; 279(38): 39705-9.

Chen G, Liu P, **Pattar GR**, Tackett L, Bhonagiri P, Strawbridge AB, Elmendorf JS. Chromium activates glucose transporter 4 trafficking and enhances insulin-stimulated glucose transport in 3T3-L1 adipocytes via a cholesterol-dependent mechanism. Mol Endocrinol. 2006 Apr;20(4):857-70.

Pattar GR, Tackett L, Liu P, Elmendorf JS. Chromium picolinate positively influences the glucose transporter system via affecting cholesterol homeostasis in adipocytes cultured under hyperglycemic diabetic conditions. Mutat Res. 2006 Nov 7;610(1-2):93-100.

Pattar GR and Elmendorf JS. Dietary Chromium Supplementation and its Role in Carbohydrate and Lipid Metabolism. Biochemical Aspects of Human Nutrition, 2010: 181-196.

Bhonagiri P*, **Pattar GR***, Habegger KM, McCarthy AM, Tackett L, Elmendorf JS. Evidence coupling increased hexosamine biosynthesis pathway activity to membrane cholesterol toxicity and cortical filamentous actin derangement contributing to cellular insulin resistance. Endocrinology. 2011 Sep;152(9):3373-84. *co-first authorship

Abstracts

Chen G, Liu P, Bhonagiri P, Strawbridge AB, **Pattar GR**, and Elmendorf JS. A novel cholesterol-dependent mechanism for chromium's role in enhancing insulin action and glucose transport. (ADA, 2005).

Pattar GR, Tackett L, Liu P, and Elmendorf JS. Plasma membrane cholesterol reduction induced by chromium picolinate improves insulin action in 3T3-L1 adipocytes cultured under hyperglycemic conditions (ADA, 2006).

Pattar GR, Tackett L, Liu P, and Elmendorf JS.

Chromium positively influences the glucose transporter system via affecting cholesterol homeostasis in adipocytes cultured under hyperglycemic diabetic conditions (Keystone Symposia – Lipid Raft, 2006).

Pattar GR and Elmendorf JS. Chromium positively influences the glucose transporter system via affecting cholesterol homeostasis in adipocytes cultured under hyperglycemic diabetic conditions (American College of Physicians Abstract Competition – Medical Student Research Poster Finalist, 2006).

Pattar GR and Elmendorf JS. 5'-AMP Activated Protein Kinase/3-Hydroxy-3-Methylglutaryl CoA (AMPK/HMG-CoA) Reductase pathway implicated in improved insulin action by chromium picolinate (ADA, 2008).

Pattar GR, Bhonagiri P, and Elmendorf JS. Evidence that increased hexosamine biosynthesis pathway flux generates insulin-resistant, cholesterol-laden plasma membrane via increasing the activity of key cholesterol transcription factors (ADA, 2008).

Pattar GR, Habegger KM, Bhonagiri P, and Elmendorf JS. Plasma Membrane Cholesterol Accrual Elicited by Increased Hexosamine Biosynthesis Promotes Insulin Resistance in Fat and Skeletal Muscle Cells (ADA, 2009).

Arthur SN, **Pattar GR**, WuDunn D, Kaehr M, Cantor LB, Hoop J, and Catoira-Boyle Y. Mid-term Results Of Efficacy, Safety, And Survival Rates Of PGY4 Resident Performed Trabeculectomy With MMC Alone Or With The Ex-PRESS Shunt (American Glaucoma Society Meeting, 2011).

Research Experience

Preparation and analysis of Protein: SDS-PAGE, Western blot analysis, whole-cell immunofluorescence, highly purified plasma membrane sheet preparation, immunoprecipitation, fluorescent and confocal microscopy in cultured

cells and intact tissue, subcellular fractionation, nuclear extract preparation

Preparation and analysis of DNA and RNA:
PCR, RT-PCR, qRT-PCR,

Cell culture:
Growth of adipocyte (3T3-L1) and skeletal muscle (L6) cell lines, transient siRNA knockdown, 2DG uptake

Animal Studies:
Dissection of rodent brain, liver, heart, kidney, skeletal muscle, and fat pads.